AD-A043 462 CALIFORNIA UNIV BERKELEY DEPT OF NAVAL ARCHITECTURE F/G 13/10
SHIP MANEUVERING, INCLUDING THE EFFECTS OF TRANSIENT MOTIONS,(U)
AUG 76 C A SCRAGG N00014-75-C-0275
UNCLASSIFIED UCB-NA-76-1 NL

1 OF 2
AD
A043 462

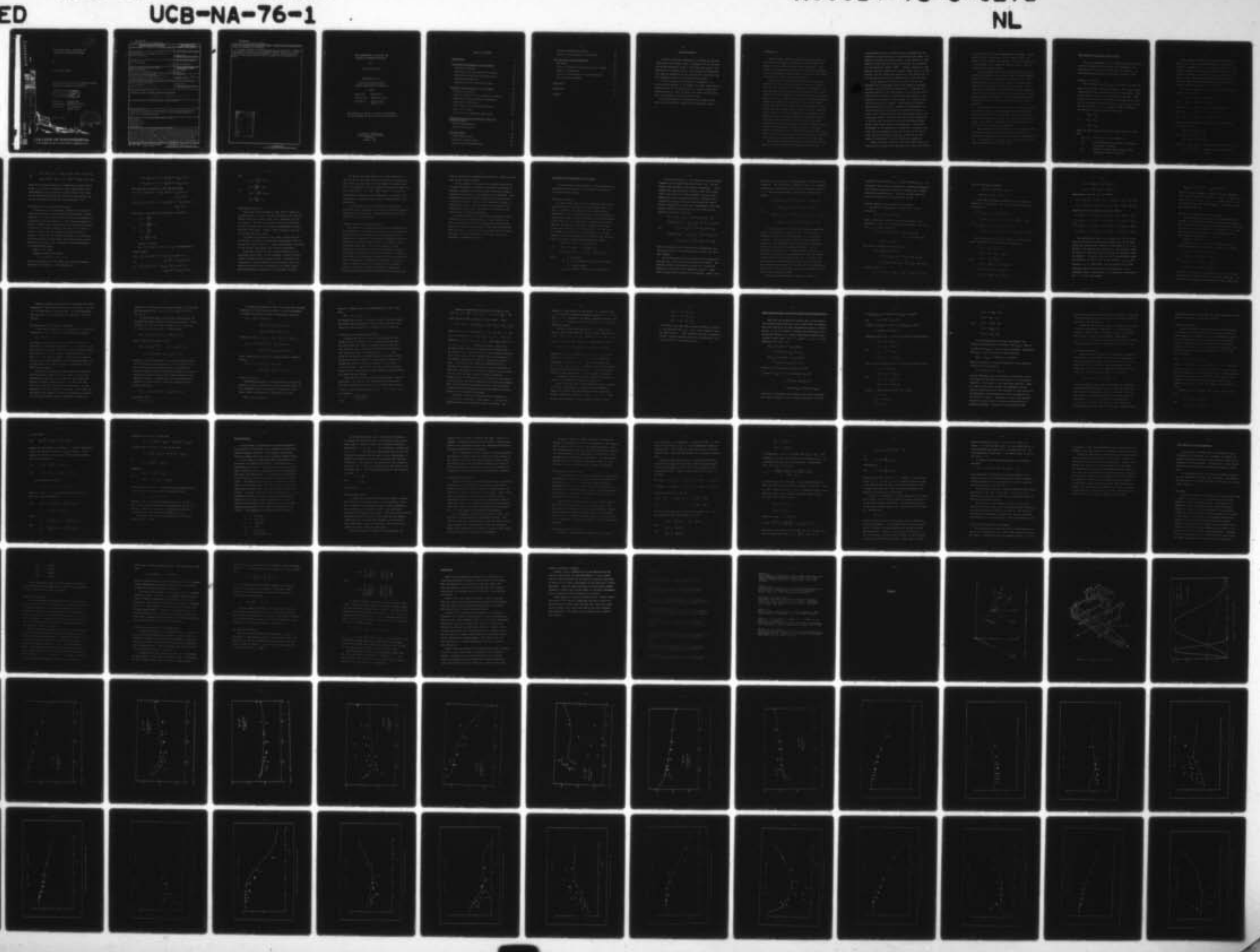

(12)

SHIP MANEUVERING, INCLUDING THE EFFECTS OF TRANSIENT MOTIONS

by

Carl Alden Scragg

Sponsored by the Naval Sea Systems Command
General Hydromechanics Research

Report No. UCB-NA-76-1
Contract No. N00014-75-C-0275
Project No. 61153N R02301
SR023 01 01

August, 1976

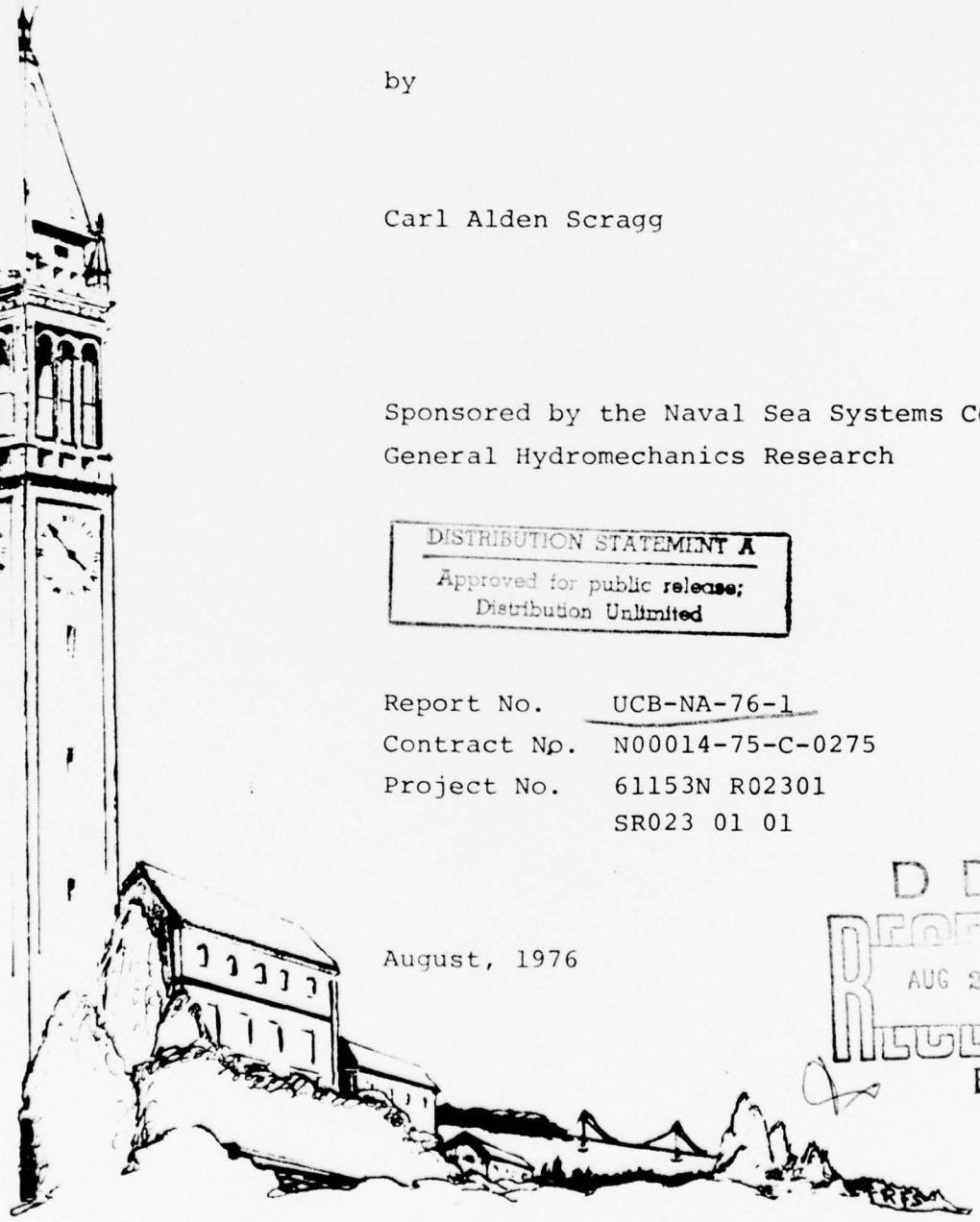

COLLEGE OF ENGINEERING
UNIVERSITY OF CALIFORNIA, BERKELEY

UNCLASSIFIED

SECURITY CLASSIFICATION OF THIS PAGE (When Data Entered)

REPORT DOCUMENTATION PAGE		READ INSTRUCTIONS BEFORE COMPLETING FORM
1. REPORT NUMBER	2. GOVT ACCESSION NO.	3. RECIPIENT'S CATALOG NUMBER
4. TITLE (and Subtitle) (6) Ship Maneuvering, Including the Effects of Transient Motions		5. TYPE OF REPORT & PERIOD COVERED Dissertation
		6. PERFORMING ORG. REPORT NUMBER
7. AUTHOR(s) (10) Carl Alden Scragg		8. CONTRACT OR GRANT NUMBER(s) (15) N00014-75-C-0275
9. PERFORMING ORGANIZATION NAME AND ADDRESS Naval Architecture, Dept of College of Engineering, University of California, Berkeley, Ca 94720		10. PROGRAM ELEMENT, PROJECT, TASK AREA & WORK UNIT NUMBERS 61153N R02301 (16) SR023 01 01
11. CONTROLLING OFFICE NAME AND ADDRESS David W. Taylor Naval Ship Research and Development Center (Code 1505) Bethesda, Maryland 20084 (17) SR023101		12. REPORT DATE 1976
		13. NUMBER OF PAGES 101
14. MONITORING AGENCY NAME & ADDRESS (if different from Controlling Office) Office of Naval Research 800 N. Quincy St Arlington, Va 22217 (11) Aug 76		15. SECURITY CLASS. (of this report) Unclassified
		15a. DECLASSIFICATION/DOWNGRADING SCHEDULE N/A

16. DISTRIBUTION STATEMENT (of this Report)

APPROVED FOR PUBLIC RELEASE: DISTRIBUTION UNLIMITED

(12) 198p. (14) NCB-NA-76-1

17. DISTRIBUTION STATEMENT (of the abstract entered in Block 20, if different from Report)

18. SUPPLEMENTARY NOTES

Sponsored by the Naval Sea Systems Command, General Hydromechanics Reserch (GHR) Program administered by the David W. Taylor Naval Ship R&D Center (Code 1505), Bethesda, Md 20084

19. KEY WORDS (Continue on reverse side if necessary and identify by block number)

GHR Program
Ship Maneuvering
Transient Motions
Added Mass
Ship Stability

20. ABSTRACT (Continue on reverse side if necessary and identify by block number)

In the traditional approach to the problems of ship maneuvering, one uses a set of linearized equations of motion that excludes the possibility that the hydrodynamic forces and moments might be affected by the history of the motion. Using ideas introduced by Cummins, one can obtain another linearized set of the equations of motion which contains a "memory function" as well as the added mass and damping coefficients. These stability coefficients have been evaluated by an impulse-response techniques, a method that is new to ship maneuvering problems and that appears to represent a substantial improvement over the

DD FORM 1 JAN 73 1473 EDITION OF 1 NOV 65 IS OBSOLETE S/N 0102-LF-014-6601

UNCLASSIFIED 406218

SECURITY CLASSIFICATION OF THIS PAGE (When Data Entered)

AB

traditional regular-oscillatory-motion tests. Results from both experimental methods are presented for comparison.

To examine the effect of the memory function upon predictions of standard ship maneuvers, predictions of a few standard maneuvers have been calculated using both sets of the linearized equations of motion. The differences between the predicted motions were found to be small for all the cases we examined.

SHIP MANEUVERING, INCLUDING THE EFFECTS OF TRANSIENT MOTIONS

by

Carl Alden Scragg

Sponsored by the

Naval Sea Systems Command
General Hydromechanics Research

under

Report No. UCB-NA-76-1

Contract No. N00014-75-C-0275

Project No. 61153N R02301
SR023 01 01

College of Engineering
University of California
Berkeley

August, 1976

TABLE OF CONTENTS

ACKNOWLEDGEMENTS

I wish to take this opportunity to express my sincere appreciation to Professor John V. Wehausen for all the time and energy unselfishly given to me during this project and throughout my graduate career. His guidance and encouragement made my experience at the University of California far more rewarding than it might otherwise have been.

I wish to express my gratitude to Professor J. R. Paulling and Professor W. C. Webster for their assistance at various stages of my graduate study. Douglas Loeser, who labored beside me, made the many hours spent at the towing tank more pleasant, as well as productive.

I am also pleased to acknowledge the support of the David Taylor Naval Ship Research and Development Center.

Introduction

Philip Mandel (1967) has defined ship maneuvering as "the controlled change or retention of the direction of motion of a ship and its speed in that direction." The study of ship maneuvering includes the problem of maintaining a fixed heading (course-keeping) as well as the problem of changing the ship's heading (steering).

Traditionally, these problems have been attacked by assuming that all of the hydrodynamic forces and moments that act upon the hull can be expressed as functions of the instantaneous velocities and accelerations of surge, heave, and sway and the instantaneous angular velocities and accelerations of roll, pitch, and yaw. These assumed hydrodynamic forces and moments are then expanded in a Taylor Series about a uniform forward motion and, provided that the deviations from the uniform forward motion are small, only the linear terms of the Taylor expansions are retained. This procedure leads to a set of linearized equations of motion that provide the definitions of the various "stability derivatives" as well as the basis for the traditional experimental techniques used in their evaluation. Once the stability derivatives for a particular ship have been determined, the linearized equations of motion are used to predict the steering and course-keeping capabilities of the ship.

Since this traditional approach to the problem assumes that the forces and moments are functions only of the

instantaneous values of velocities and accelerations, any possibility that the history of the motion might affect the present situation has been excluded. A new approach to the problem, which does not exclude the history of the motion, was introduced by Cummins (1962). Cummins' approach to the problem, which was improved by Ogilvie (1964) and Lin (1966), differs from the traditional approach in the description of the hydrodynamic forces and moments acting upon the ship.

In the approach of Cummins, Ogilvie, and Lin, one expresses the hydrodynamic forces and moments as pressure integrals over the entire wetted surface. Although this approach appears to be much sounder, it is also more difficult since it requires a knowledge of the pressure. Even though one can formulate this problem, it is much too complex to be solved at present. Fortunately, the authors mentioned provide us with a systematic approximation procedure whereby one can express the pressure integral in terms of the same velocities and accelerations used in the traditional method. However, the form of this expression is not the same as that given by the traditional method except under rather special circumstances. The primary difference is the appearance of convolution integrals that allow for the possibility that the history of the motion might affect the present situation, a possibility that cannot be handled by using the traditional approach.

There is reason to believe that this memory effect is often small and that either approach will yield good results

in the prediction of many standard ship maneuvers. Recent papers by Fujino and Motora (1975), Nomoto (1975), and Fujino (1975), support this opinion. One of the objectives of this project is to determine just how large a role is played by this memory effect.

In the present work, after a brief description of the traditional approach, we begin with the linearized expressions for the forces and moments as given by Lin. From these expressions, we develop a method of experimentally determining the necessary stability coefficients. The experimental technique, while new to maneuvering problems, is well known in other areas and is often referred to as an impulse-response technique. It would appear that this new method makes a more efficient use of the planar motion mechanism.

An examination of the special case of regular oscillatory motion leads to relationships between the stability derivatives measured in traditional experiments and the stability coefficients found by the impulse-response technique. Both types of experiments have been performed and the results are presented and compared.

Ship maneuvers that correspond to a few standard rudder commands have been calculated by using the traditional equations of motion as well as the equations recommended by Lin. A comparison of the predictions supports the opinion that the memory effect is often small.

The Traditional Approach to the Problem

To lay the groundwork for the comparisons which follow, a short description of the traditional approach to the determination of stability derivatives is necessary. A more complete description can be found in Mandel (1967).

Equations of Motion

The coordinate system $0_o x_o y_o z_o$ (Figure 1) is fixed in space with z_o taken vertically downward, the (x_o, y_o) plane coinciding with the undisturbed water surface, and x_o taken in the general direction of the motion of the ship. Then the motion of the ship is completely described by the position of the center of gravity $(x_{og}(t), y_{og}(t), z_{og}(t))$ and the heading angle $\psi(t)$. In such a system, we can write the equations of motion from Newton's Laws:

$$
\begin{aligned}
m\ddot{x}_{og} &= X_{oT} \\
m\ddot{y}_{og} &= Y_{oT} \qquad (1) \\
I_{zg}\ddot{\psi} &= N_{og}
\end{aligned}
$$

where the dots indicate derivatives with respect to time and

X_{oT}, Y_{oT} = total force in x,y direction

N_{og} = total moment about vertical axis through the center of gravity

I_{zg} = moment of inertia about vertical axis through the center of gravity

The coordinate system Oxyz is fixed in the ship with the origin on the centerline amidships. The x-axis is forward, z downward, and y to starboard with the (x,y) plane coinciding with the undisturbed water surface. The center of gravity is located at (x_g, y_g, z_g) where y_g is usually zero. The absolute velocity of the origin is $\bar{V} = (u,v)$ and we note that the velocity of the center of gravity is given by $(u_g, v_g) = (u, v + x_g \dot{\psi})$.

In order to convert eqs. (1) into the ship coordinate system, we note that

$$X_{oT} = X_T \cos \psi - Y_T \sin \psi$$

$$Y_{oT} = X_T \sin \psi + Y_T \cos \psi \tag{2}$$

where X_T, Y_T = total forces in x,y directions

and $\dot{x}_{og} = u \cos \psi - (v + x_g \dot{\psi}) \sin \psi$

$$\dot{y}_{og} = u \sin \psi + (v + x_g \dot{\psi}) \cos \psi \tag{3}$$

Taking the time derivatives of eqs.(3) and substituting into eqs.(1) we get

$$m(\dot{u} - v\dot{\psi} - x_g \dot{\psi}^2) = X_T$$

$$m(\dot{v} + u\dot{\psi} + x_g \ddot{\psi}) = Y_T \tag{4}$$

$$I_z \ddot{\psi} + m x_g (\dot{v} + u\dot{\psi}) = N_T$$

where $N_T = N_{og} + x_g Y_T$ = vertical moment about the origin

$I_z = I_{zg} + m x_g^2$ = moment of inertia about the origin.

Equations (4) are nothing more than the Newtonian equations of motion written in the ship coordinate system. The difficulties with which one is faced result from the inability to specify X_T, Y_T, and N_T.

Linearization of the Equations of Motion

The forces and moments of the right-hand side of eqs. (4) are composed of several terms and it is assumed that we can separate these into two parts. The first part consists of all those forces and moments which result from perturbations of the ship's motion about its mean. The second part consists of all other external forces exerted upon the hull: wind, waves, propeller, rudder, etc.

We can write

$$X_T = X + X_E$$

where X = forces created by small motions

X_E = external forces on ship.

It is now assumed that X is function of the variables $u, \dot{u}, v, \dot{v}, \dot{\psi}, \ddot{\psi}$. And since it is assumed that X results from small perturbations about the mean motion, we shall expand X in a Taylor series about $u = u_o$:

$$\begin{aligned} X &= X(u, \dot{u}, v, \dot{v}, \dot{\psi}, \ddot{\psi}) \\ &= X(u_o, o, o, o, o, o) + \Delta u \frac{\partial X}{\partial u} + \dot{u} \frac{\partial X}{\partial \dot{u}} + v \frac{\partial X}{\partial v} + \\ &\quad + \dot{v} \frac{\partial X}{\partial \dot{v}} + \dot{\psi} \frac{\partial X}{\partial \dot{\psi}} + \ddot{\psi} \frac{\partial X}{\partial \ddot{\psi}} + (\text{higher order terms}) \end{aligned}$$

where $\Delta u = u - u_o$.

Noting that X is created by the perturbations, we set $X(u_o,0,0,0,0,0) = 0$. And since the hull is symmetrical about the (x,z) plane, X must be an even function of $v,\dot{v},\dot{\psi},\ddot{\psi}$. Therefore $\frac{\partial X}{\partial v}$, $\frac{\partial X}{\partial \dot{v}}$, $\frac{\partial X}{\partial \dot{\psi}}$, $\frac{\partial X}{\partial \ddot{\psi}}$ must all equal zero.

If we keep only first order terms, then $X = \Delta u \frac{\partial X}{\partial u} + \dot{u} \frac{\partial X}{\partial \dot{u}}$

where all partial derivatives are to be evaluated at $(u = u_o,\ \dot{u} = 0,\ v = 0,\ \dot{v} = 0,\ \dot{\psi} = 0,\ \ddot{\psi} = 0\ )$.

For the lateral force we get

$$Y = v \frac{\partial Y}{\partial v} + \dot{v} \frac{\partial Y}{\partial \dot{v}} + \dot{\psi} \frac{\partial Y}{\partial \dot{\psi}} + \ddot{\psi} \frac{\partial Y}{\partial \ddot{\psi}}$$

where $Y(u_o,0,0,0,0,0) = 0$ and $\frac{\partial Y}{\partial u}$, $\frac{\partial Y}{\partial \dot{u}} = 0$ since a change in forward motion will not produce a lateral force on a symmetrical hull. Similarly

$$N = v \frac{\partial N}{\partial v} + \dot{v} \frac{\partial N}{\partial \dot{v}} + \dot{\psi} \frac{\partial N}{\partial \dot{\psi}} + \ddot{\psi} \frac{\partial N}{\partial \ddot{\psi}}$$

Introducing the yaw rate $r = \dot{\psi}$, we define the stability derivatives $Y_v = \frac{\partial Y}{\partial v}$, $N_v = \frac{\partial N}{\partial v}$, $Y_r = \frac{\partial Y}{\partial r}$, etc.

Since the derivatives are to be evaluated at $(u_o,0,0,0,0,0)$, they are assumed to be constants which may depend upon the Froude number and the shape of the hull but not upon the nature of the motion, so long as the motion remains small.

Rewriting eqs. (4), retaining only linear terms, we obtain $(m - X_{\dot{u}})\dot{u} - X_u \Delta u = X_E$

$$
\begin{aligned}
&(m - Y_{\dot{v}})\dot{v} - Y_v v + (mx_g - Y_{\dot{r}})\dot{r} + (mu_o - Y_r)r = Y_E \\
&(mx_g - N_{\dot{v}})\dot{v} - N_v v + (I_z - N_{\dot{r}})\dot{r} + (mx_g u_o - N_r)r = N_E
\end{aligned} \tag{5}
$$

Note that the surge equation is independent of sway and yaw rates, i.e. to this first-order linear approximation the surge equation is not coupled to either sway or yaw. Since we are concerned here with the effects of sway and yaw, we can now concentrate on the last two equations of (5).

Evaluation of the Stability Derivatives

Although it is, in principle, possible to evaluate the stability derivatives from theoretical hydrodynamic considerations, it is not a simple task and the usual procedure is to evaluate them experimentally, The technique consists of taking a geometrically similar model of the hull and forcing it to move in a known trajectory (so that $v,\dot{v},r,\dot{r}$ are all known) and measuring the externally applied forces and moments. Typically, the imposed trajectory is a sinusoidal oscillation about the mean path, first oscillating in pure sway and then in pure yaw. We refer to these experiments as regular-motion tests.

Case A: Pure Sway

Suppose we impose the motion

$$v = v_o \cos \omega t,\ r = 0,\ u = u_o$$

Then the measured force and moment will also be sinusoidal functions of frequency ω with phase angle ε

$$Y = Y_o \cos(\omega t + \varepsilon_1) = Y_{in} \cos \omega t + Y_{out} \sin \omega t$$

$$N = N_o \cos(\omega t + \varepsilon_2) = N_{in} \cos \omega t + N_{out} \sin \omega t$$

The equations of motion for sway and yaw become

$$(m - Y_{\dot{v}})(-v_o \omega \sin \omega t) - Y_v(v_o \cos \omega t) = Y_{in} \cos \omega t + Y_{out} \sin \omega t \tag{6}$$

$$(mx_g - N_{\dot{v}})(-v_o \omega \sin \omega t) - N_v(v_o \cos \omega t) = N_{in} \cos \omega t + N_{out} \sin \omega t$$

Solving for the stability derivatives, we obtain

$$\begin{aligned} Y_v &= -\frac{Y_{in}}{v_o} \\ Y_{\dot{v}} &= \frac{Y_{out}}{v_o \omega} + m \\ N_v &= -\frac{N_{in}}{v_o} \\ N_{\dot{v}} &= \frac{N_{out}}{v_o \omega} + mx_g \end{aligned} \tag{7}$$

Case B: Pure Yaw

Let $r = r_o \cos \omega t$, $v = o$, $u = u_o$, the equations of motion become

$$(mx_g - Y_{\dot{r}})(-r_o \omega \sin \omega t) + (mu_o - Y_r)(r_o \cos \omega t) = Y_{in} \cos \omega t + Y_{out} \sin \omega t \tag{8}$$

$$(I_z - N_{\dot{r}})(-r_o \omega \sin \omega t) + (mx_g u_o - N_r)(r_o \cos \omega t) = N_{in} \cos \omega t + N_{out} \sin \omega t$$

and

$$
\begin{aligned}
Y_r &= -\frac{Y_{in}}{r_o} + m\, u_o \\
Y_r^{\cdot} &= \frac{Y_{out}}{r_o \omega} + m x_g \\
N_r &= -\frac{N_{in}}{r_o} + m x_g\, u_o \\
N_r^{\cdot} &= \frac{N_{out}}{r_o \omega} + I_z
\end{aligned}
\tag{9}
$$

Experimental Technique

The planar motion mechanism (PMM) used to impose the required motions of pure sway and pure yaw is the same one used by Paulling and Wood (1962) and a schematic is given in Figure 2. The PMM is attached to the towing carriage and two rods which can be oscillated independently connect the PMM to the model. Goodman (1960) provides a more detailed description of a PMM.

The model is attached at two points, forward and aft of midships, by means of strain-gauge dynamometers used to measure the lateral forces. A linear potentiometer connected to the forward rod measures the lateral displacement.

Since the vibration of the carriage produced an unacceptable noise level, it was necessary to pass all three signals through matched low-pass filters. Although this resulted in a greatly improved signal-to-noise ratio, the problem was never totally eliminated. All three signals were simultaneously recorded on a strip-chart recorder.

To impose pure sway motion, it is only necessary to set the PMM so that both rods are oscillating in phase with each other, but pure yaw is not so simple. To produce pure yaw, it is necessary that the forward rod lead the after rod by a phase angle $\alpha = 2 \tan^{-1} \frac{\omega d}{u_o}$, where d is one half the distance between the rods. Therefore, any change of forward speed or frequency necessitates a readjustment of the phase angle.

For the calculation of the stability derivatives, knowledge of the amplitudes of the forces and their relative phase angles are necessary. These quantities can be read directly from the strip-chart.

Problems with the Traditional Method

The results of regular-motion tests are dependent upon the frequency of the oscillatory motion, i.e. the stability derivatives are not constants, as was presumed, but are functions of frequency. This frequency dependence has been observed by Paulling and Wood (1962), van Leeuven (1964), and others since then. For the calculation of ship maneuvers, one generally uses the zero-frequency value of the stability derivatives, but for the study of motions in rough seas, it is necessary to know the extent to which the stability derivatives depend upon frequency. But in any case, it becomes necessary to perform a large number of tests, oscillating the model at different frequencies. Paulling and Wood performed approximately 650 separate test

runs to evaluate the stability derivatives of a Mariner class ship at four Froude numbers.

As one attempts to evaluate the stability derivatives at lower frequencies, it becomes increasingly difficult to accurately measure the forces and one inevitably reaches a frequency below which no good results can be obtained. Some researchers have been further limited by the short length of their towing tank, since a lower frequency requires a longer test section. The zero value of the stability derivatives is found then by attempting to extrapolate the values found at higher frequencies.

Another problem which limits the experimenter is the reflection of the transverse wave. If one tests at too low a forward speed, the wave created by the oscillatory motion can reflect off the sides of the tank and interfere with the model. It has been our experience that this problem makes it almost impossible to get good results for low-speed, shallow-water tests.

Transient-Motion Approach to the Problem

A new approach to the problems of ship maneuvering is presented and this leads to a new method of determining the stability derivatives.

Equations of Motion

We shall again start with the Newtonian equations of motion written in the ship coordinate system, eqs. (4). Then, to simplify the problem, we make the following assumptions: (1) we assume that the ship is sailing in smooth water where the only disturbances are those created by the ship; (2) we assume that if there is any rolling, heaving, or pitching of the ship, the interaction with surge, sway, and yaw is not significant; (3) the fluid is assumed to be inviscid and irrotational. As a consequence of these assumptions, the water can act upon the ship only through normal pressure and we can write

$$
\begin{aligned}
& m(\dot{u} - v\dot{\psi} - x_g \dot{\psi}^2) = \int_S p n_x dS + X_E \\
& m(\dot{v} + u\dot{\psi} + x_g \ddot{\psi}) = \int_S p n_y dS + Y_E \qquad (10) \\
& I_z \ddot{\psi} + m x_g (\dot{v} + u\dot{\psi}) = \int_S p(x n_y - y n_x) dS + N_E
\end{aligned}
$$

where p = pressure

n_x, n_y = x, y components of unit normal vector

S = wetted surface

X_E, Y_E = external forces acting on the hull

The main difficulty is the evaluation of the pressure integrals on the right-hand side of eqs. (10). We now require some systematic approximation procedure. This problem has been attacked by Cummins (1962) and Ogilvie (1964), and later Lin (1966) provided us with a solid foundation within perturbation theory. Assuming only a continuous velocity field and small deviations from a uniform forward motion (and small disturbance of the free surface created by the motions), we can linearize the equations of motion as follows:

$$
\begin{aligned}
m\dot{u} &= -\mu_{xx}\dot{u} - \beta_{xx}\Delta u - \int_0^\infty \Delta u(t-\tau)N_{xx}(\tau)d\tau + X_E \\
m(\dot{v}+u_o\dot{\psi}+x_g\ddot{\psi}) &= -\mu_{yy}\dot{v} - \beta_{yy}v - \int_0^\infty v(t-\tau)\,N_{yy}(\tau)d\tau \\
&\quad - \mu_{y\psi}\ddot{\psi} - \beta_{y\psi}\dot{\psi} - \int_0^\infty \dot{\psi}\,(t-\tau)N_{y\psi}(\tau)d\tau + Y_E \qquad (11) \\
I_z\ddot{\psi}+mx_g(\dot{v}+u_o\dot{\psi}) &= -\mu_{\psi\psi}\ddot{\psi} - \beta_{\psi\psi}\dot{\psi} - \int_0^\infty \dot{\psi}(t-\tau)N_{\psi\psi}(\tau)d\tau \\
&\quad - \mu_{\psi y}\dot{v} - \beta_{\psi y}v - \int_0^\infty v(t-\tau)N_{\psi y}(\tau)d\tau + N_E
\end{aligned}
$$

where, consistent with the small-motion assumption, the non-linear terms on the left-hand side of eqs. (10) have been dropped.

The surge equation is not coupled to the equations of sway and yaw and will not be discussed any further. The external force Y_E and moment N_E contain all forces and moments not contained in the pressure integral. These might include forces caused by the propeller, rudder, wind,

waves and, in the case of our experiments, the planar motion mechanism. The convolution integrals in eqs. (11) represent the effect of the history of the motion. Defining yaw rate $r = \dot{\psi}$, and rearranging terms, the sway and yaw equations become

$$
\begin{aligned}
&(m+\mu_{yy})\dot{v} + \beta_{yy}v + \int_0^\infty v(t-\tau)N_{yy}(\tau)d\tau + (mx_g + \mu_{y\psi})\dot{r} \\
&\quad + (mu_o + \beta_{y\psi})r + \int_0^\infty r(t-\tau)N_{y\psi}(\tau)d\tau = Y_E \\
&(mx_g + \mu_{\psi y})\dot{v} + \beta_{\psi y}v + \int_0^\infty v(t-\tau)N_{\psi y}(\tau)d\tau + (I_z + \mu_{\psi\psi})\dot{r} \\
&\quad + (mx_g u_o + \beta_{\psi\psi})r + \int_0^\infty r(t-\tau)N_{\psi\psi}(\tau)d\tau = N_E
\end{aligned}
\tag{12}
$$

In contrasting eqs. (12) with the linearized equations used in the traditional approach, eqs. (5), the major difference appears to be the presence of the convolution integrals. This means simply that the present approach allows for the possibility that the history of the motion affects in some way the hydrodynamic forces. In the traditional approach, the forces exerted by the water on the hull are presumed to be dependent only upon the instantaneous values of the motion of the ship. It should also be pointed out that we arrived at eqs. (12) via a systematic approximation scheme with its foundation in perturbation theory and in our opinion this approach is sounder than that used in the traditional method.

The problem now consists of finding a method of

evaluating the constants μ_{ij}, β_{ij} and functions $N_{ij}(\tau)$. In principle, these could be found from a theoretical approach, but we shall follow the, hopefully, simpler path of determining them experimentally. For this we shall need the Fourier transform of the equations of motion.

Fourier Transform of the Equations of Motion

The Fourier transform of a function f(t) can be defined as

$$\hat{f}(\omega) = \int_{-\infty}^{\infty} f(t)\, e^{-i\omega t}\, dt$$

where a sufficient condition for the existence of the transform is that f(t) be absolutely integrable. If $f(t) = 0$ for $t \leq o$, then we can write

$$\hat{f}(\omega) = \int_{o}^{\infty} f(t) e^{-i\omega t}\, dt = \int_{o}^{\infty} f(t)\, \cos \omega t\, dt - i \int_{o}^{\infty} f(t)\, \sin \omega t\, dt$$

$$= \hat{f}_c(\omega) - i\, \hat{f}_s(\omega)$$

The Fourier inversion theorem gives us

$$f(t) = \frac{1}{2\pi} \int_{-\infty}^{\infty} \hat{f}(\omega) e^{i\omega t}\, d\omega$$

$$= \frac{1}{\pi} \int_{o}^{\infty} \left[\hat{f}_c(\omega)\, \cos\, \omega t + \hat{f}_s(\omega)\, \sin\, \omega t \right] d\omega$$

$$= \frac{2}{\pi} \int_{o}^{\infty} \hat{f}_c(\omega)\, \cos\, \omega t\, d\omega = \frac{2}{\pi} \int_{o}^{\infty} \hat{f}_s(\omega)\, \sin\, \omega t\, d\omega$$

We shall also use

$$\hat{\dot{f}}(\omega) = i\, \omega\, \hat{f}(\omega) \quad \text{where} \quad \hat{\dot{f}}(\omega) = \int_{-\infty}^{\infty} \dot{f}(t)\, e^{-i\omega t}\, dt$$

and the convolution theorem:

$$\text{if } h(t) = \int_{-\infty}^{\infty} g(t-\tau)\ f(\tau)\ d\tau$$

$$\text{then } \hat{h}(\omega) = \hat{g}(\omega) \cdot \hat{f}(\omega)$$

If we take the Fourier transform of the linearized equations of motion, eqs. (12), we get the following pair of equations:

$$\begin{aligned}
&\left[i\ \omega(m+\mu_{yy}) + \beta_{yy} + \hat{N}_{yy}(\omega)\right]\hat{v}(\omega) + \\
&\quad + \left[i\omega(mx_g + \mu_{y\psi}) + mu_o + \beta_{y\psi} + \hat{N}_{y\psi}(\omega)\right]\hat{r}(\omega) = \hat{Y}_E(\omega) \\
&\left[i\ \omega(mx_g + \mu_{\psi y}) + \beta_{\psi y} + \hat{N}_{\psi y}(\omega)\right]\ \hat{v}(\omega) + \\
&\quad + \left[i\omega(I_z + \mu_{\psi\psi}) + mx_g u_o + \beta_{\psi\psi} + \hat{N}_{\psi\psi}(\omega)\right]\hat{r}(\omega) = \hat{N}_E(\omega)
\end{aligned} \tag{13}$$

We now define the following "stability coefficients" noting that they are all functions of frequency:

$$\begin{aligned}
C_1(\omega) &= \beta_{yy} + \hat{N}_{yyc}(\omega) \\
C_2(\omega) &= \omega(m + \mu_{yy}) - \hat{N}_{yys}(\omega) \\
C_3(\omega) &= \beta_{\psi y} + \hat{N}_{\psi yc}(\omega) \\
C_4(\omega) &= \omega(mx_g + \mu_{\psi y}) - \hat{N}_{\psi ys}(\omega) \\
C_5(\omega) &= mu_o + \beta_{y\psi} + \hat{N}_{y\psi c}(\omega) \\
C_6(\omega) &= \omega(mx_g + \mu_{y\psi}) - \hat{N}_{y\psi s}(\omega)
\end{aligned} \tag{14}$$

$$C_7(\omega) = mx_g u_o + \beta_{\psi\psi} + \hat{N}_{\psi\psi c}(\omega)$$

$$C_8(\omega) = \omega(I_z + \mu_{\psi\psi}) - \hat{N}_{\psi\psi s}(\omega)$$

substituting into eqs. (11), we obtain

$$(C_1 + i\,C_2)(\hat{v}_c - i\,\hat{v}_s) + (C_5 + i\,C_6)(\hat{r}_c - i\,\hat{r}_s) = \hat{Y}_c - i\,\hat{Y}_s$$

$$(C_3 + i\,C_4)(\hat{v}_c - i\,\hat{v}_s) + (C_7 + i\,C_8)(\hat{r}_c - i\,\hat{r}_s) = \hat{N}_c - i\,\hat{N}_s$$

Separating real and imaginary parts, we obtain

$$C_1(\omega)\hat{v}_c(\omega) + C_2(\omega)\hat{v}_s(\omega) + C_5(\omega)\hat{r}_c(\omega) + C_6(\omega)\hat{r}_s(\omega) = \hat{Y}_c(\omega)$$

$$C_1(\omega)\hat{v}_s(\omega) - C_2(\omega)\hat{v}_c(\omega) + C_5(\omega)\hat{r}_s(\omega) - C_6(\omega)\hat{r}_c(\omega) = \hat{Y}_s(\omega)$$

(15)

$$C_3(\omega)\hat{v}_c(\omega) + C_4(\omega)\hat{v}_s(\omega) + C_7(\omega)\hat{r}_c(\omega) + C_8(\omega)\hat{r}_s(\omega) = \hat{N}_c(\omega)$$

$$C_3(\omega)\hat{v}_s(\omega) - C_4(\omega)\hat{v}_c(\omega) + C_7(\omega)\hat{r}_s(\omega) - C_8(\omega)\hat{r}_c(\omega) = \hat{N}_s(\omega)$$

The importance of eqs. (15) is two-fold. First, as we show in the next section, these equations give us the capability of evaluating the stability coefficients $C_1, C_2, ---, C_8$. Secondly, and perhaps more importantly, they provide a means of evaluating the path of the ship given the external forces and moments. Of course, this can also be accomplished using the equations of motion (12) if the constants μ_{ij}, β_{ij} and functions $N_{ij}(\tau)$ are known. But the evaluation of these constants and functions requires a knowledge of (or an assumption about) the behavior of the stability coefficients as $\omega \to \infty$, since, for example

$$N_{yy}(t) = \frac{2}{\pi} \int_0^\infty (C_1(\omega) - \beta_{yy}) \cos \omega t \, d\omega$$

by the inversion theorem. However, for ship maneuvers, $\hat{Y}(\omega)$ and $\hat{N}(\omega)$ will go to zero for $\omega >$ some ω_1; then if we know $C_1, C_2, ---, C_8$ for $0 \leq \omega < \omega_1$, we can find $\hat{v}(\omega)$ and $\hat{r}(\omega)$ by equations (15) and ultimately, $v(t)$ and $r(t)$ by the inversion theorem.

Evaluation of the Stability Coefficients

The experimental evaluation of the stability coefficients is accomplished by taking a geometrically similar model of the hull and giving it an impulsive motion such that $v(t)$ and $r(t)$ are zero before $t = 0$ and after $t = T$. Then the infinite Fourier transform can be replaced by the finite Fourier transform for $0 \leq t \leq T$.

Case A: Pure Sway

Suppose $r(t) = o$, $v(t) = \dot{y}(t)$, where $y(t)$ is the lateral displacement of the model; then eqs. (15) become

$$\begin{aligned}
C_1(\omega)\hat{v}_c(\omega) + C_2(\omega)\hat{v}_s(\omega) &= \hat{Y}_c(\omega) \\
C_1(\omega)\hat{v}_s(\omega) - C_2(\omega)\hat{v}_c(\omega) &= \hat{Y}_s(\omega) \\
C_3(\omega)\hat{v}_c(\omega) + C_4(\omega)\hat{v}_s(\omega) &= \hat{N}_c(\omega) \\
C_3(\omega)\hat{v}_s(\omega) - C_4(\omega)\hat{v}_c(\omega) &= \hat{N}_s(\omega)
\end{aligned} \tag{16}$$

If $y(t)$, $Y(t)$, and $N(t)$ are measured for $o \leq t \leq T$, then their Fourier transforms can be calculated. Then eqs. (16) can be solved, frequency by frequency, as four simultaneous

linear equations in the four unknowns C_1, C_2, C_3, C_4. Note that, in principle, one such test will give us the stability coefficients for all frequencies.

Case B: Combined Sway and Yaw

Once the coefficients C_1, C_2, C_3, C_4 are known, any impulsive motion which combines sway and yaw will enable us to find the remaining coefficients C_5, C_6, C_7, C_8. In practice we set the two supports of the planar motion mechanism to be 180° out of phase. Then if $y_1(t)$ is the position of the forward support and $y_2(t)$ the position of the after support, we obtain the following results: $y_2(t) = -y_1(t)$, and $v(t) = -\frac{u_o}{d} y_1(t)$, and $r(t) = \frac{1}{d}\dot{y}_1(t)$. Measuring $y_1(t)$, $Y(t)$, $N(t)$ we can calculate $\hat{r}(\omega)$, $\hat{v}(\omega)$, $\hat{Y}(\omega)$, $\hat{N}(\omega)$. Rewriting (15) with all known coefficients on the right-hand side, we find

$$
\begin{aligned}
C_5(\omega)\hat{r}_c(\omega) + C_6(\omega)\hat{r}_s(\omega) &= \hat{Y}_c(\omega) - C_1(\omega)\hat{v}_c(\omega) - C_2(\omega)\hat{v}_s(\omega) \\
C_5(\omega)\hat{r}_s(\omega) - C_6(\omega)\hat{r}_c(\omega) &= \hat{Y}_s(\omega) - C_1(\omega)\hat{v}_s(\omega) + C_2(\omega)\hat{v}_c(\omega) \\
C_7(\omega)\hat{r}_c(\omega) + C_8(\omega)\hat{r}_s(\omega) &= \hat{N}_c(\omega) - C_3(\omega)\hat{v}_c(\omega) - C_4(\omega)\hat{v}_s(\omega) \\
C_7(\omega)\hat{r}_s(\omega) - C_8(\omega)\hat{r}_c(\omega) &= \hat{N}_s(\omega) - C_3(\omega)\hat{v}_s(\omega) + C_4(\omega)\hat{v}_c(\omega)
\end{aligned}
\tag{17}
$$

These equations can be solved, frequency by frequency, as four simultaneous equations in the four unknowns C_5, C_6, C_7, C_8. Now we see that, in principle, we need only one sway impulse and one combined sway and yaw impulse to evaluate all eight coefficients over the entire frequency range.

In practice, the situation is not that simple and more tests might be required to achieve sufficient accuracy. This problem will be discussed in a later section.

Experimental Techniques

The model was again attached to the planar motion mechanism, the only alteration being the disconnection of the electric motor so that manual power could be used. The output signals from the strain-gauge dynamometers and the linear potentiometer were filtered and recorded on a 4 channel FM tape recorder and later digitized at 250 samples/second.

Operating the planar motion mechanism manually, the experimenter provided the impetus to initiate the sway or yaw motion and the mechanism was allowed to coast to a smooth stop. The resulting impulses varied considerably between experimental runs, but typically had a duration of about 1 second and maximum energy at 1.25 Hz and a maximum lateral displacement of 1 inch. A second series of experiments was run with a slower pulse of 4 seconds duration and maximum energy at 0.25 Hz. This was the slowest pulse that would yield forces large enough to be accurately measured with our equipment.

Another series of experiments was run, during which we attempted to produce pulses which approximate a step function. As will be explained later, such pulses yield the best results for very low frequencies.

Computer programs were written to calculate the Fourier transforms of the digitized data and to solve eqs. (16) and (17) for the stability coefficients. All data processing was performed on the University of California's CDC 6400 computer.

The Existence of the Fourier Transform

A sufficient condition for the existence of the Fourier transform of f(t) is that f(t) be absolutely integrable:

$$\int_{-\infty}^{\infty} |f(t)|\,dt < \infty .$$

In practice, we require that f(t) be zero for all $t < o$ and return to zero after some time $T > o$. For case A, pure sway, there is no problem since any pulse of finite duration will give us v(t), Y(t), and N(t) equal to zero for $t < o$ and $t > T$. For case B, however, the only way to achieve this is to have the centerline of the model coincident with u_o both before and after the pulse. In practice, this is difficult to achieve.

If we allow the model to come to rest with some non-zero drift angle, then $\hat{v}(\omega)$, $\hat{Y}(\omega)$, and $\hat{N}(\omega)$ will all be non-existent since v(t), Y(t), and N(t) will reach some non-zero constant value for all $t > T$. But note that $\dot{v}(t)$, $\dot{Y}(t)$, and $\dot{N}(t)$ will all go to zero for $t > T$, and therefore $\hat{\dot{v}}(\omega)$, $\hat{\dot{Y}}(\omega)$, and $\hat{\dot{N}}(\omega)$ all exist. If we take the derivative with respect to time of the equations of motion (12) and then take the Fourier transform of these new

equations, we find that we can still use eqs. (17) provided that we replace $\hat{v}(\omega)$, $\hat{r}(\omega)$, $\hat{Y}(\omega)$, $\hat{N}(\omega)$ with $\dot{\hat{v}}(\omega)$, $\dot{\hat{r}}(\omega)$, $\dot{\hat{Y}}(\omega)$, $\dot{\hat{N}}(\omega)$.

It would then appear that we must differentiate the recorded data before taking the Fourier transform. To see that this is not the case, consider $f(t) = f_o$ for all $t \leq o$ and $f(t) = f_T$ for $t \geq T$. Then we find

$$\dot{\hat{f}}(\omega) = \int_{-\infty}^{\infty} \dot{f}(t) e^{-i\omega t}\, dt = \int_{o}^{T} \dot{f}(t) e^{-i\omega t}\, dt$$

upon integrating by parts we find

$$\dot{\hat{f}}(\omega) = \left[f(t) e^{-i\omega t} \right]_{o}^{T} + i\omega \int_{o}^{T} f(t) e^{-i\omega t}\, dt$$

$$= i\omega \int_{o}^{T} f(t) e^{-i\omega t}\, dt + f_T\, e^{-i\omega T} - f_o$$

Since we can then calculate $\dot{\hat{f}}(\omega)$ without differentiating $f(t)$ and since we can rewrite eqs. (17) in terms of $\dot{\hat{v}}(\omega)$, etc., we can use an impulse which has a non-existent Fourier transform without additional complexity or loss of accuracy provided only that the Fourier transform of the derivative exists. Alternatively, we could extend the definition of the Fourier transform to include such a pulse by defining

$$\hat{f}(\omega) = \int_{o}^{T} f(t) e^{-i\omega t}\, dt - \frac{i}{\omega} \left(f_T e^{-i\omega T} - f_o \right)$$

and we see that

$$\dot{\hat{f}}(\omega) = i\omega\, \hat{f}(\omega) \ .$$

It should be pointed out that if one uses this extended definition of the Fourier transform, it will be necessary to extend the Fourier inversion theorem also. We have

$$f(t) - f(o) = \int_o^t \dot{f}(\tau)\,d\tau$$

$$= \int_o^t d\tau\, \frac{2}{\pi} \int_o^\infty \hat{\dot{f}}_c(\omega) \cos \omega\tau\, d\omega$$

$$= \int_o^t d\tau\, \frac{2}{\pi} \int_o^\infty \hat{\dot{f}}_s(\omega) \sin \omega\tau\, d\omega$$

Noting that $\hat{\dot{f}}_c(\omega) = \omega \hat{f}_s(\omega)$ and $\hat{\dot{f}}_s(\omega) = -\omega \hat{f}_c(\omega)$:

$$f(t) - f(o) = \frac{2}{\pi} \int_o^\infty d\omega \int_o^t \omega\, \hat{f}_s(\omega) \cos \omega\tau\, d\tau$$

$$= \frac{2}{\pi} \int_o^\infty d\omega \int_o^t -\omega \hat{f}_c(\omega) \sin \omega\tau\, d\tau$$

After integrating we have the extended Fourier inversion theorem :

$$f(t) - f(o) = \frac{2}{\pi} \int_o^\infty \hat{f}_s(\omega) \sin \omega t\, d\omega$$

$$= \frac{2}{\pi} \int_o^\infty \hat{f}_c(\omega) (\cos \omega t - 1)\, d\omega \,.$$

Effect of a Filter

As mentioned earlier, it was necessary to filter the signals in order to improve the signal-to-noise ratio. If f(t) represents any of the signals, filtering it with a linear filter is equivalent to replacing f(t) with

$$\bar{f}(t) = \int_o^\infty f(t-\tau) W(\tau)\, d\tau$$

where $W(\tau)$ depends upon the characteristics of the filter. Then

$$\hat{\bar{f}}(\omega) = \hat{f}(\omega) \cdot \hat{W}(\omega)$$

An examination of eqs. (15) shows us that if all the signals are passed through identical linear filters, the $\hat{W}(\omega)$ will cancel out and no accuracy is lost due to the filtering.

A Difficulty in Transient Experiments

As mentioned earlier, since a finite pulse has components at all frequencies, it is theoretically possible to run one sway test and one combined sway and yaw test and, from this data, solve for the stability coefficients over the entire range of frequencies $o \leq \omega < \infty$. But, since we are passing the signals through a low-pass filter, we cannot reasonably expect to obtain accurate results for frequencies above the cut-off frequency of the filter, 5 Hz in our case. This is not a severe limitation however, since 5 Hz is a considerably higher frequency than one needs for almost any application.

Unfortunately we face a more serious problem. When one solves eqs. (16) and (17) for the stability coefficients, one finds expressions for $C_1, C_2, ---, C_8$ Which always contain a term in the denominator such as $(\hat{v}_c^2 + \hat{v}_s^2)$ or $(\hat{r}_c^2 + \hat{r}_s^2)$. For example:

$$C_1 = \frac{\hat{v}_c \hat{Y}_c + \hat{v}_s \hat{Y}_s}{\hat{v}_c^2 + \hat{v}_s^2} \tag{18}$$

Suppose we approximate the pulse (for case A: pure sway) by $y(t) = \frac{1}{2}(1 - \cos \omega_o t)$, $o \leq t \leq T = \frac{2\pi}{\omega_o}$. We shall refer to such a pulse as a "full pulse". Then

$$\hat{v}(\omega) = \hat{\dot{y}}(\omega) = -\frac{1}{2} \frac{\omega_o^2}{\omega^2 - \omega_o^2} \left(2 \sin^2 \pi \frac{\omega}{\omega_o} + i \sin 2\pi \frac{\omega}{\omega_o}\right)$$

Notice that $\hat{v}_c(\omega)$ has zeros at $\omega = o, 2\omega_o, 3\omega_o, ---$ and $\hat{v}_s(\omega)$ has zeros at $\omega = o, \frac{1}{2}\omega_o, \frac{3}{2}\omega_o, 2\omega_o, ---$. Then the denominator in eq. (18), $(\hat{v}_c^2 + \hat{v}_s^2)$, has double zeros at $\omega = o, 2\omega_o, 3\omega_o, ---$. There will exist a singularity at these points unless the numerator has matching zeros to cancel it out. The terms in $\hat{v}_s$ in the numerator provide only simple zeros, but one assumes that the transforms of the measured forces will supply the additional matching ones. In practice, this cannot be realized since $\hat{Y}(\omega)$ contains the transform of the signal plus the transform of the noise, and there is no reason to suppose that the transform of the noise goes to zero at these frequencies. However, even if this were so, one is still in the position of dividing two very small quantities at and in the neighborhood of the zeros and consequently one is very vulnerable to small errors in measurement, which may become very large relative to the quantities measured.

With such a pulse, one cannot avoid the problem at $\omega = o$, but one can choose a large enough ω_o so that the remaining zeros are outside the range of interest. For

example, if the duration of the pulse $T = 1$ second, then $\omega_o = 2\pi$ and we can expect reasonable results for $o < \omega < 4\pi$, but if $T = 4$ seconds we can expect reasonable results only for $o < \omega < \pi$. Figure 3 gives the value of $(\hat{v}_c^2 + \hat{v}_s^2)$ for these two pulses.

One way to avoid the problem at $\omega = o$ might be to select a pulse which does not return to zero, such as $y(t) = \frac{1}{2}(1 - \cos \omega_o t)$, $o \leq t \leq \frac{\pi}{\omega_o}$ where $y(t) = 1$ for $t > \frac{\pi}{\omega_o}$. We shall refer to such a pulse as a "step pulse". Then

$$\hat{v}(\omega) = \hat{\dot{y}}(\omega) = -\frac{1}{2}\frac{\omega_o^2}{\omega^2 - \omega_o^2}\left(1 + \cos\frac{\pi\omega}{\omega_o} - i \sin\frac{\pi\omega}{\omega_o}\right)$$

Notice that $\hat{v}_c(\omega)$ has zeros at $\omega = \omega_o, 3\omega_o, 5\omega_o, ---$ and that $\hat{v}_s(\omega)$ has zeros at $\omega = o, 2\omega_o, 3\omega_o, ---$. Then the denominator in eq. (18), $(\hat{v}_c^2 + \hat{v}_s^2)$, has double zeros at $\omega = 3\omega_o, 5\omega_o, 7\omega_o, ---$. Therefore, such a "step pulse" should provide good results for $o \leq \omega < 3\omega_o$. The denominator for a step pulse with $\omega_o = 2\pi$ is shown in Figure 3.

A comparison of the full pulse and the step pulse as used in our experiments is shown in Figure 3a.

There is another way to avoid this difficulty, although it has the disadvantage of requiring more experiments. Suppose we perform the same maneuver several times with slightly different values of ω_o, say $\omega_1 < \omega_2 < \omega_3$. Then we can sum the results of the individual runs to form

$$\hat{v}(\omega) = \hat{v}_1 + \hat{v}_2 + \hat{v}_3$$

$$\hat{Y}(\omega) = \hat{Y}_1 + \hat{Y}_2 + \hat{Y}_3$$

$$\hat{N}(\omega) = \hat{N}_1 + \hat{N}_2 + \hat{N}_3$$

If the three runs have only slightly different values of ω_o, one can show that $(\hat{v}_c^2 + \hat{v}_s^2)$ is not likely to have any zeros near $2\omega_o$. This procedure has been followed and Figure 4 compares results obtained from individual runs and the result of the combined runs.

Relationship Between Traditional Method and Transient Method

Note that the equations of motion used in the impulse test assume nothing about the motion other than the requirement that the motion be small perturbations about a uniform motion. It is of interest to examine the case used in the traditional method, i.e. regular-oscillatory motion about a uniform forward speed. Let $v = v_o \cos\omega t$, $u = u_o$, $r = 0$ and substitute into eqs. (12):

$$(m+\mu_{yy})(-v_o\omega\sin\omega t) + \beta_{yy}(v_o\cos\omega t) + \int_0^\infty v_o\cos\omega(t-\tau)N_{yy}(\tau)d\tau = Y_E$$

$$(mx_g+\mu_{\psi y})(-v_o\omega\sin\omega t) + \beta_{\psi y}(v_o\cos\omega t) + \int_0^\infty v_o\cos\omega(t-\tau)N_{\psi y}(\tau)d\tau = N_E$$

Examining the convolution integral, we find

$$\int_0^\infty v_o\cos\omega(t-\tau)N_{yy}(\tau)d\tau = \int_0^\infty v_o\cos\omega t\cos\omega\tau\, N_{yy}(\tau)d\tau + \int_0^\infty v_o\sin\omega t\,\sin\omega\tau N_{yy}(\tau)d\tau$$

$$= v_o\cos\omega t\,\hat{N}_{yyc}(\omega) + v_o\sin\omega t\,\hat{N}_{yys}(\omega)$$

Using this relationship and separating the force and moment into their in phase and out of phase components, we obtain

$$[\omega(m+\mu_{yy})-\hat{N}_{yys}(\omega)](-v_o\sin\omega t)+[\beta_{yy}+\hat{N}_{yyc}(\omega)]v_o\cos\omega t$$

$$= Y_{in}\cos\omega t + Y_{out}\sin\omega t \tag{19}$$

$$[\omega(mx_g+\mu_{\psi y})-\hat{N}_{\psi ys}(\omega)](-v_o\sin\omega t)+[\beta_{\psi y}+\hat{N}_{\psi yc}(\omega)]v_o\cos\omega t$$

$$= N_{in}\cos\omega t + N_{out}\sin\omega t$$

Comparison with eqs. (6) gives the following relationships:

$$\begin{aligned} Y_v &= -\beta_{yy} - \hat{N}_{yyc}(\omega) \\ Y_{\dot{v}} &= -\mu_{yy} + \omega^{-1}\hat{N}_{yys}(\omega) \\ N_v &= -\beta_{\psi y} - \hat{N}_{\psi yc}(\omega) \\ N_{\dot{v}} &= -\mu_{\psi y} + \omega^{-1}\hat{N}_{\psi ys}(\omega) \end{aligned} \tag{20}$$

and a similar examination of oscillatory yaw motion yields

$$\begin{aligned} Y_r &= -\beta_{y\psi} - \hat{N}_{y\psi c}(\omega) \\ Y_{\dot{r}} &= -\mu_{y\psi} + \omega^{-1}\hat{N}_{y\psi s}(\omega) \\ N_r &= -\beta_{\psi\psi} - \hat{N}_{\psi\psi c}(\omega) \\ N_{\dot{r}} &= -\mu_{\psi\psi} + \omega^{-1}\hat{N}_{\psi\psi s}(\omega) \end{aligned} \tag{21}$$

Finally, a comparison with eqs. (14) yields

$$\begin{aligned} C_1(\omega) &= -Y_v \\ C_2(\omega) &= \omega(m-Y_{\dot{v}}) \\ C_3(\omega) &= -N_v \end{aligned}$$

$$C_4(\omega) = \omega(mx_g - N_{\dot{v}})$$

$$C_5(\omega) = mu_o - Y_r$$

(22) $$C_6(\omega) = \omega(mx_g - Y_{\dot{r}})$$

$$C_7(\omega) = mx_g u_o - N_r$$

$$C_8(\omega) = \omega(I_z - N_{\dot{r}})$$

If, as presumed by the traditional method, the stability derivatives are constants, then $\hat{N}_{yyc}(\omega)$ must be a constant and $\hat{N}_{yys}(\omega)$ must be zero everywhere. This means that $N_{yy}(\tau)$ can be written as a delta function

$$N_{yy}(\tau) = N_{yy}\,\delta(\tau) \text{ where } N_{yy} = \text{constant}$$

Then the convolution integrals appearing in the equations of motion can be written as

$$\int_0^\infty v(t-\tau)N_{yy}\delta(\tau)d\tau = N_{yy}v(t)$$

and any dependence upon the history of the motion is lost and indeed the equations of motion take on a form which is identical to that used in the traditional approach. There is, then an equivalence between the dependency of the stability derivatives upon the frequency of oscillation and the dependency of the instantaneous forces and moments upon the history of motion. Therefore, the fact that previous studies have shown that the stability derivatives are frequency dependent, forces one to conclude that the

traditional equations of motion are not adequate to describe all situations and that the convolution integrals should be included in the equations.

Equations (22) give us a means of comparing the results of the two experimental techniques, i.e. regular-motion tests vs. impulse tests. Therefore, rather than present the results in terms of the stability coefficients C_1, C_2, ---, C_8, we chose to present everything in terms of the more familiar stability derivatives Y_v, $Y_{\dot{v}}$, ---, $N_{\dot{r}}$.

Low-Frequency Behavior

Noting that the Fourier cosine transform is always an even function of frequency and that the sine transform is odd, an inspection of eqs. (20) and (21) leads us to conclude that all the stability derivatives must be even functions. Therefore, if we express the stability derivatives as a Taylor expansion about $\omega = o$, we have

$$Y_v = Y_v(\omega=o) + \frac{1}{2}\,\omega^2\,\frac{\partial^2 Y_v}{\partial \omega^2} + \text{---}$$

It is now apparent that, when one attempts to extrapolate regular-motion test results to $\omega = o$, one may assume that the stability derivatives approach a constant value with zero slope. Furthermore, there must exist some range of frequencies $o \leq \omega < \varepsilon$ over which the approximation $Y_v = Y_v(\omega=o)$ is usable. Obviously, if the forces and moments applied to the hull have frequency components which

are primarily within this range, then there should be little error in using the traditional approach.

Almost Steady Motion

Since it has been shown that the traditional approach to maneuvering problems will yield reasonable results for many standard ship maneuvers, it is of interest to examine the conditions under which the traditional equations of motion (5) become a good approximation to the preferred equations of motion (12). For the sake of simplicity, consider the sway equation for the case where $r = o$. Then eq. (5) becomes

$$(m - Y_{\dot{v}})\dot{v} - Y_v v = Y_E \tag{23}$$

where $Y_{\dot{v}}$ and Y_v are to be evaluated at $\omega = o$. Note that there is nothing in the derivation of eqs. (5) which allows one to assume that the zero-frequency value of the stability derivatives should be used. However, when examining ship maneuvers, one is dealing with very slow motions which suggest a similarity to very low frequency regular-motion tests.

Taking the zero-frequency limit of eqs. (20), we see that

$$\begin{aligned} Y_v &= -\beta_{yy} - \int_o^\infty N_{yy}(\tau)\,d\tau \\ Y_{\dot{v}} &= -\mu_{yy} + \int_o^\infty \tau N_{yy}(\tau)\,d\tau \end{aligned} \tag{24}$$

Substituting eqs. (24) into the traditional sway equation (23), we find

$$(25) \qquad (m + \mu_{yy} - \int_0^\infty \tau N_{yy}(\tau)d\tau)\dot{v} + (\beta_{yy} + \int_0^\infty N_{yy}(\tau)d\tau)v = Y_E$$

The transient-motion sway equation is

$$(26) \qquad (m + \mu_{yy})\dot{v} + \beta_{yy}v + \int_0^\infty v(t-\tau)N_{yy}(\tau)d\tau = Y_E$$

We now ask ourselves, "Under what conditions will the solution of eq. (25) be a good approximation to the solution of eq. (26)?"

Let $v_1(t)$ be the solution of eq. (26) and $v_2(t)$ be the solution of eq. (25), given the same initial conditions and forcing functions for each. Subtracting eq. (25) from eq. (26) and rearranging terms, we find

$$(27) \qquad \begin{aligned}(m + \mu_{yy} - \int_0^\infty \tau N_{yy}(\tau)d\tau)(\dot{v}_1 - \dot{v}_2) \\ + (\beta_{yy} + \int_0^\infty N_{yy}(\tau)d\tau)(v_1 - v_2) = g(t)\end{aligned}$$

where

$$(28) \qquad g(t) = \int_0^\infty \left[\frac{1}{\tau}(v_1(t) - v_1(t-\tau)) - \dot{v}_1(t)\right]\tau N_{yy}d\tau$$

If we assume that $v_1 = v_2$ at $t = o$ and if we define the error $E = v_1 - v_2$, then the solution to eq. (27) is of the form

$$E(t) = \frac{e^{\sigma t} \int_0^t g(\tau) e^{-\sigma \tau} d\tau}{m + \mu_{yy} - \int_0^\infty \tau N_{yy} d\tau}$$

where $$\sigma = - \frac{\beta_{yy} + \int_0^\infty N_{yy} d\tau}{m + \mu_{yy} - \int_0^\infty \tau N_{yy} d\tau} < 0 .$$

From this follows

$$|E| < \max |g(t)| \frac{e^{\sigma t}(-\frac{1}{\sigma})(e^{-\sigma t} - 1)}{m + \mu_{yy} - \int_0^\infty \tau N_{yy} d\tau}$$

or

$$|E| < \max |g(t)| \frac{1 - e^{\sigma t}}{\beta_{yy} + \int_0^\infty N_{yy} d\tau} . \tag{29}$$

Suppose we are willing to accept an error equal to εV, where V is the maximum value of $|v(t)|$ and ε is some small positive constant. Note that it was necessary, in the linearization of the equations of motion, to assume that V is always small relative to u_o. We now define a constant T which has the units of time and is dependent only upon the system. Let

$$T = \frac{\int_0^\infty |\tau N_{yy}(\tau)| d\tau}{\beta_{yy} + \int_0^\infty N_{yy} d\tau} \tag{30}$$

Since the memory function $N_{yy}(\tau)$ must approach zero for large values of τ, it is possible to define a critical time

t_c, such that

$$(31) \qquad \frac{1}{2}\varepsilon \int_0^{t_c} |\tau\, N_{yy}|\,d\tau = \int_{t_c}^{\infty} |\tau\, N_{yy}|\,d\tau$$

Apparently, the smaller one chooses ε (smaller acceptable error), the larger the value of t_c will become. Let us examine the result of placing the following restrictions upon the acceleration:

$$(32) \qquad |\dot{v}(t)| < \frac{1}{2}\frac{V}{T} \qquad \text{for all } t$$

$$(33) \qquad |\dot{v}(t) - \dot{v}(t-\tau)| < \frac{1}{2}\varepsilon\frac{V}{T} \qquad \text{for } \tau \leq t_c$$

By the mean-value theorem

$$v_1(t) - v_1(t-\tau) = \tau\, \dot{v}_1(t-\alpha\tau)$$

where $0 < \alpha(t,\tau) < 1$, so that the definition of $g(t)$, eq. (28), can be rewritten as

$$(34) \qquad g(t) = \int_0^{\infty} \left[\dot{v}_1(t-\alpha\tau) - \dot{v}_1(t)\right] \tau\, N_{yy}\, d\tau$$

$$= g_1(t,t_c) + g_2(t,t_c)$$

where

$$g_1 = \int_0^{t_c} \left[\dot{v}_1(t-\alpha\tau) - \dot{v}_1(t)\right] \tau\, N_{yy}\, d\tau$$

and

$$g_2 = \int_{t_c}^{\infty} \left[\dot{v}_1(t-\alpha\tau) - \dot{v}_1(t)\right] \tau\, N_{yy}\, d\tau\ .$$

Making use of eq. (33), we see that

$$|g_1| < \frac{1}{2} \varepsilon \frac{V}{T} \int_0^{t_c} |\tau N_{yy}| d\tau < \frac{1}{2} \varepsilon \frac{V}{T} \int_0^{\infty} |\tau N_{yy}| d\tau$$

and using eqs. (31) and (32), we can see that

$$|g_2| < \frac{V}{T} \int_{t_c}^{\infty} |\tau N_{yy}| d\tau = \frac{1}{2} \varepsilon \frac{V}{T} \int_0^{t_c} |\tau N_{yy}| d\tau$$

or

$$|g_2| < \frac{1}{2} \varepsilon \frac{V}{T} \int_0^{\infty} |\tau N_{yy}| d\tau$$

Therefore

$$|g(t)| < \varepsilon \frac{V}{T} \int_0^{\infty} |\tau N_{yy}| d\tau$$

or

$$|g(t)| < \varepsilon V \left(\beta_{yy} + \int_0^{\infty} N_{yy} d\tau \right)$$

from the definition of T. Substituting the maximum value of $|g(t)|$ into eq. (29) we reach the following result:

$$|E| < \varepsilon V \left(1 - e^{\sigma t}\right) < \varepsilon V .$$

Therefore, if the maximum acceptable error is to be εV, and if the acceleration meets the requirements of eqs. (32) and (33), then one may use the traditional equations of motion with the coefficients evaluated at $\omega = 0$.

A different approach to this problem can be found in Wehausen et al. (1976).

The Experiments

A large number of experiments have been performed at the University of California in an attempt to perfect the impulse-response technique. This section outlines the various attempts which led to the currently favored method.

In all cases, the experiments were performed at the University's Richmond Field Station. The towing-tank is approximately 200 feet in length, 8 feet wide, and 6 feet deep (the water level was maintained at the maximum depth throughout the experiments). The planar-motion mechanism which was used is the same one used by Paulling and Wood (1962). The model that was used is a light-weight wooden model of a high-speed ship (DE type) and in all cases the tests were performed using the model without propeller or rudder. It should be pointed out that the addition of the propeller and rudder in no way affects the experimental technique and in fact another researcher here (Douglas Loeser) has performed impulse tests using a Mariner model equipped with propeller and rudder [see Wehausen et al. (1976)]. The dimensions of the model are as follows:

$L = 5.0$ feet

$B = 0.585$ feet

$T = 0.19$ feet

$C_B = 0.492$

$M = 0.239$ slugs

$I_z = 0.468$ slug $\cdot$ ft^2

As mentioned earlier, eqs. (22) give us the ability to present the results of both regular-motion tests and impulse tests in terms of either the traditional stability derivatives, Y_v, $Y_{\dot{v}}$, N_v,... , or the stability coefficients C_1, C_2, C_3,... In order that the present results might be more easily compared with the work of other researchers, we present all results in terms of the traditional stability derivatives. The stability derivatives are made dimensionless with $\frac{1}{2}\rho$, L, and u_o following the "prime system" used by Mandel (1967). Two dimensionless forms of the frequency are used:

$$\tau = \frac{\omega u_o}{g}$$

and

$$\omega' = \frac{\omega L}{u_o} \quad .$$

We note that $\tau = F_n^2 \, \omega'$.

Regular-Motion Tests

In order that we would have data with which to compare the results of the impulse-tests, it was necessary to perform a number of regular-motion tests. These experiments were performed by Tomas Frank (1974) using traditional planar-motion mechanism techniques. Since each regular-motion experiment yields the value of the added mass and damping coefficients at one particular frequency, the results of these experiments appear as individual data points and no attempt at curve-fitting has been made.

Note that there is a range of low frequencies (see

Figures 5-12) in which no results are given. This is an inherent problem of regular-motion testing. As mentioned earlier, one inevitably reaches some frequency below which accurate measurements are impossible.

Due to limitations on the accuracy of the measurements, the results of these tests are likely to contain errors on the order of 10-15 per cent and therefore, in the comparisons which follow, the differences between the results of the two experimental techniques should not be regarded as a measure of the inaccuracy of the impulse-test procedure.

Full-Pulse Impulse Tests

The first series of experiments from which we received reasonable results employed a full-pulse, as described earlier (Figure 3a), with a duration of approximately one second and a lateral displacement of one inch. Such a pulse has its peak energy at about 1.25 Hz and will yield reasonable results for some range of frequencies centered about this point. In a previous section, it was explained that such a pulse will lead to results which are singular at $\omega = 0$, and indeed this problem was encountered.

In an attempt to obtain better results at lower frequencies, a second series of experiments was run. This time, we used the longest-duration pulse for which we could still measure the forces accurately with our equipment. These pulses averaged four seconds in duration, peak energy at 0.25 Hz, and one inch lateral displacement.

Figures 5 through 12 show the results of these two series of experiments, as well as the results of the regular-motion tests, for $F_n = 0.30$. The graphs show that, though the longer-duration pulses did yield slightly better results for low frequencies, the improvement was limited to a disappointingly narrow range of frequencies. It also becomes evident that, if one desires information about the zero-frequency limit, a different sort of pulse is required.

The Step-Pulse Impulse Tests

As was pointed out in an earlier section, a pulse which approximates a step-function does not have the problem of singularities at $\omega = 0$. Therefore, another series of experiments was run using the step-pulse (see Figure 3a). The results of these experiments (with an inch displacement) are presented in Figures 13 through 20 for $F_n = 0.30$ and Figures 21 through 28 for $F_n = 0.20$.

These graphs indicate that all of the damping coefficients are well behaved at $\omega = 0$. For the case of pure sway, the added masses are similarly well behaved. However, the two added-mass terms Y'_r and N'_r, which are calculated from the case of combined sway and yaw, still "blow-up" for $\omega = 0$. Therefore, a further examination of this case appears necessary.

The Zero-Frequency Correction

In order to understand the behavior of Y'_r and N'_r at

zero frequency, it is necessary to return to eqs. (17) from which we calculated C_6 and C_8, the corresponding stability coefficients. For the sake of simplicity, only C_6 will be examined here, since the examination of C_8 follows a similar path.

Since the step-pulse leads to a non-zero force before and after the pulse, we shall deal with the Fourier transform of the derivative of the force, which exists in the conventional sense. Rewriting the first pair of eqs. (17), we obtain

$$C_5(\omega)\hat{\dot{r}}_c(\omega) + C_6(\omega)\hat{\dot{r}}_s(\omega) = \hat{\dot{Y}}_c(\omega) - C_1(\omega)\hat{\dot{v}}_c(\omega) - C_2(\omega)\hat{\dot{v}}_s(\omega),$$

$$C_5(\omega)\hat{\dot{r}}_s(\omega) - C_6(\omega)\hat{\dot{r}}_c(\omega) = \hat{\dot{Y}}_s(\omega) - C_1(\omega)\hat{\dot{v}}_s(\omega) + C_2(\omega)\hat{\dot{v}}_c(\omega)$$

and solving for $C_6(\omega)$, we find

$$C_6(\hat{\dot{r}}_c^2 + \hat{\dot{r}}_s^2) = \hat{\dot{Y}}_c\hat{\dot{r}}_s - \hat{\dot{Y}}_c\hat{\dot{r}}_c - C_1(\hat{\dot{v}}_c\hat{\dot{r}}_s - \hat{\dot{v}}_s\hat{\dot{r}}_c)$$

$$- C_2(\hat{\dot{v}}_s\hat{\dot{r}}_s + \hat{\dot{v}}_c\hat{\dot{r}}_c) \qquad (35)$$

If $y(t)$ is the position of the forward support and $-y(t)$ the position of the after support, we have

$$v(t) = -\frac{u_o}{d}\,y(t), \quad r(t) = \frac{1}{d}\,\dot{y}(t)$$

and

$$\hat{\dot{v}}_c(\omega) = -\frac{u_o}{d}\,\hat{\dot{y}}_c(\omega)$$

$$\hat{\dot{v}}_s(\omega) = -\frac{u_o}{d}\,\hat{\dot{y}}_s(\omega) \qquad (36)$$

$$\hat{\dot{r}}_c(\omega) = \frac{\omega}{d}\,\hat{\dot{y}}_s(\omega)$$

$$\hat{\dot{r}}_s(\omega) = -\frac{\omega}{d}\,\hat{\dot{y}}_c(\omega)$$

An examination of eqs. (36) shows that $-\hat{\dot{v}}_s\hat{\dot{r}}_s = \hat{\dot{v}}_c\hat{\dot{r}}_c$, and therefore, the last term on the right hand side of eq. (35) is identically zero for all frequencies. Substituting eqs. (36) into (35) we find

$$C_6(\omega) = \frac{d(\hat{\dot{Y}}_s\hat{\dot{y}}_s - \hat{\dot{Y}}_c\hat{\dot{y}}_c) - C_1(\omega)u_o(\hat{\dot{y}}_c^2 + \hat{\dot{y}}_s^2)}{\omega(\hat{\dot{y}}_c^2 + \hat{\dot{y}}_s^2)}$$

For the case of zero frequency, it is a simple matter to show that both $\hat{\dot{Y}}_s$ and $\hat{\dot{y}}_s$ will go linearly to zero as ω goes to zero. However, both $\hat{\dot{Y}}_c$ and $\hat{\dot{y}}_c$ approach non-zero limits which are equal to the difference between their initial and final steady-state values:

$$\hat{\dot{Y}}_c(\omega=0) = Y_T - Y_o$$

$$\hat{\dot{y}}_c(\omega=0) = y_T - y_o$$

Therefore, when $\omega = 0$, we have

$$C_6(\omega=0) = \lim_{\omega\to o}\frac{1}{\omega}\left(-d\,\frac{Y_T - Y_o}{y_T - y_o} - C_1(\omega=0)u_o + 0(\omega^2)\right)$$

Returning to the equations of motion (12), we can see that, for the steady-state case $v_o = -\frac{u_o}{d}y_o$ and $r = 0$,

$$\beta_{yy} v_o + v_o \int_0^\infty N_{yy}(\tau) d\tau = Y_o$$

or

$$(37) \qquad - C_1(\omega=0) \frac{u_o}{d} y_o = Y_o$$

and similarly

$$(38) \qquad - C_1(\omega=0) \frac{u_o}{d} y_T = Y_T \quad .$$

Finally we see that $C_6(\omega=0) = 0$. However, in our calculations Y_T, Y_o, y_T, and y_o are all measured quantities and it is apparent that an error, no matter how small, in any of these quantities will cause the singular behavior observed in the stability coefficients.

Since it is impossible to obtain measurements of infinite accuracy, the following scheme was adopted, referred to as the zero-frequency correction. Let the measured value of the force be designated by Y_m and the value of the noise Y_n. Then we have

$$Y_m = Y_n + Y \quad .$$

During the period prior to the impulse we can measure Y_m and the displacement y (we assume that we have the capability to measure the displacement with greater accuracy than the force). Equation (37) gives us the value of Y_o for this period, so that we can calculate Y_n and subtract it from Y_m at every point in time. We now make a finite

Fourier transform of $Y_m(t) - Y_n$ from $t=0$ until $t=T$, where T is the time when $Y_m(t) - Y_n$ has stabilized at a value approximately equal to Y_T as defined by eq. (38). The assumption is made that Y is exactly equal to Y_T for all time $t > T$.

In terms of the extended definition of the Fourier transform

$$\hat{Y}(\omega) = \int_0^T Y(t)e^{-i\omega t}dt - \frac{i}{\omega}\left(Y_T e^{-i\omega T} - Y_o\right)$$

this assumption is equivalent to the replacement of the measured values of the force before and after the impulse (which necessarily contain some error) by their values as calculated by eqs. (37) and (38).

It should be noted that a similar assumption has already been made for the case of pure sway. In this case the assumption is that the force must be identically zero both before and after the impulse.

The results of the combined sway and yaw runs were calculated a second time using this zero-frequency correction and are presented in Figures 29 through 36. The change in the damping coefficients is slight and, finally, we obtain good results for all coefficients in the zero-frequency limit.

A Test on the Linearity of the System

The linearization scheme which led to the equations of motion (12) requires that the lateral and angular velocities be "small" in comparison with the forward velocity. If this

requirement is met, the experimental results should be independent of the exact nature of the impulse given to the model.

Since both the lateral and the angular velocities depend upon the peak-to-peak amplitude of the pulse, a series of experiments was run using various amplitudes. Manning (1976) presents the results of the entire series of experiments, with amplitudes of 0.40 to 1.00 inches and Froude numbers of 0.20 and 0.30, using both the full-pulse and the step-pulse. Up to one inch amplitude (the maximum possible with our PMM) no systematic variation of the results could be observed. It would appear then, that the one-inch amplitude does not violate the linearization assumption, and since it produces the best signal-to-noise ratio, it is the "preferred" pulse. Figures 37 and 38 are typical results of this test.

The Prediction of Ship Maneuvers

Once one has a complete set of the stability coefficients for a given ship, it is possible to predict the lateral and angular motions of the ship for a given set of external forces and moments. Alternatively, one could predict the forces and moments necessary to produce a given path.

In the present study, the forces and moments produced by the rudder were the only ones considered. The problem then becomes one of finding the path of the ship for a given rudder command.

The Rudder

Since the model which was used is not fitted with either a rudder or a propeller, it was necessary to make some assumptions about the rudder forces. The presence of a rudder has quite a significant effect upon the overall stability of the ship and the selection of a particular rudder can cause a radically different behavior of the ship if the rudder's contribution to the damping coefficients causes the ship to become stable rather than unstable. However, if we consider two rudders, both of which lead to a stable ship, the predicted maneuvers will differ in absolute value but not in their general behavior. Therefore, if we are careful to select a rudder which is large enough to insure the stability of the ship, we will be able to

predict the general behavior of the ship and to compare predictions made by the traditional approach with the transient-motion approach, even though the absolute value of the predictions may differ somewhat from predictions made for the rudder which is actually on the ship.

Therefore, we shall assume that the ship is outfitted with a spade rudder which has an aspect ratio of two and an area equal to 2.2 per cent of the length times the draft. Assuming a taper ratio of 0.45, the dimensions of the rudder (the length of the full-scale ship is 314.5 feet) are:

Area	=	83 ft^2
Span	=	12.9 ft
Section	=	NACA 0015
Sweep Angle	=	0
Max. Chord	=	8.9 ft
Min. Chord	=	4.0 ft

where the maximum chord is measured at the intersection of the rudder and the hull, and the minimum chord is measured at the tip of the rudder.

By following the technique recommended by Taplin (1960) and using the data compiled by Whicker and Fehlner (1958), it is found that for small rudder angles, the lateral force exerted on the hull by this rudder can be approximated by

$$Y_E = 3000 \text{ lb. per degree rudder angle.}$$

Taking the distance between the center of gravity and the

rudder's center of effort to be 144 feet, we approximate the moment by

$$N_E = - 432{,}000 \text{ ft-lb per degree .}$$

Change in Stability Coefficients Due to Rudder

Since our experiments were run using a model without either a rudder or a propeller, and since the rudder can contribute significantly to the added mass and damping coefficients of the ship, it was necessary to add a correction term to the experimentally determined coefficients. Mandel (1967) suggests a method of finding the correction terms. Mandel assumes that the correction terms are not functions of frequency and, of course we would rather not make this assumption since we wish to compare predictions made with frequency-independent coefficients to predictions made with frequency-dependent coefficients. However, we would expect the added mass and damping coefficients of a deeply submerged body to be frequency-independent and therefore the frequency dependence of the rudder correction terms is not likely to be too great. Therefore, we have followed the method outlined by Mandel and have reached the following results:

$$\Delta Y_v' = - .0019$$

$$\Delta Y_{\dot{v}}' = - .00014$$

$$\Delta N_v' = + .00088$$

$$\Delta N_{\dot{v}}' = + .000066$$

$$\Delta Y_r' = + .00088$$

$$\Delta Y_{\dot{r}}' = + .000066$$

$$\Delta N_r' = - .00040$$

$$\Delta N_{\dot{r}}' = - .000030$$

These correction terms have been added to the experimental results and the (dimensional) stability coefficients for the full-scale ship were calculated.

Methods of Prediction

One of the standard techniques used to find the solutions of eqs. (12), i.e. the equations of motion which allow for "memory effects", is the Fourier transformation. The equations of motion are transformed into the frequency domain, and $\hat{v}(\omega)$ and $\hat{r}(\omega)$, the Fourier transforms of $v(t)$ and $r(t)$, are found by a frequency-by-frequency solution of eqs. (15). The inverse Fourier transform then provides us with the ability to find $v(t)$ and $r(t)$.

There are two major sources of error in such a solution. The first source is simply the inaccuracy inherent in the inverse Fourier transformation of a discrete function $\hat{v}(\omega)$. One must be careful, therefore, to choose the distance $\Delta\omega$ between the discrete values of $\hat{v}(\omega)$, to be sufficiently small. The second source of error is more difficult to control. As mentioned earlier, we can evaluate the stability coefficients for $0 \leq \omega \leq \omega_1$ where ω_1 is finite. Therefore, we must replace the infinite integral in the Inversion

Theorem by a finite integral and $\hat{v}(\omega)$ must be of such a form that

$$\int_0^{\infty} \hat{v}(\omega) e^{i\omega t} d\omega \doteq \int_0^{\omega_1} \hat{v}(\omega) e^{i\omega t} d\omega \quad .$$

Since the velocities of a ship are unlikely to contain significant components at high frequencies, this condition was assumed to hold with sufficient accuracy.

The traditional equations of motion, eqs. (5), are much simpler to solve. In fact, if one assumes constant coefficients (stability derivatives evaluated at $\omega=0$) it is possible to find the exact solution to the problem. Furthermore, it is also possible to solve the equations using the Fourier transformation. Therefore, if we solve eqs. (5) by both methods, exact and Fourier transform solutions, we shall have a measure of the accuracy of the computer program that calculates the inverse Fourier transform.

A Check on the Accuracy of the Computations

A computer program has been written that is capable of solving both the traditional equations of motion, eqs. (5), (where the stability derivatives are assumed to be constant and equal to their zero-frequency value) and the transient-motion equations (12). The program uses the Fourier transform to solve both sets of equations.

A comparison of the solutions of eqs. (5), as computed by the program, to the exact solutions of eqs. (5) provides us with a check on the accuracy of the program itself.

Such comparisons were made for two different rudder commands. Letting δ be the rudder angle in degrees, the first command was

$$\delta_1(t) = \begin{cases} 0 & t < 0 \\ 1.5\,t, & 0 < t < 10 \\ 15 & , \quad t > 10 \end{cases}$$

i.e. the rudder angle is increased linearly to a maximum angle of 15 degrees in ten seconds. The second rudder command was an instantaneous increase in rudder angle to the same 15 degree maximum.

$$\delta_2(t) = \begin{cases} 0 & , \quad t < 0 \\ 15 & , \quad t > 0 \end{cases}$$

For both rudder commands, it was found that the error in the computed solution, relative to the exact solution, was less than two per cent. In terms of the overall accuracy of the experimentally determined stability derivatives, the accuracy of the computer program is quite good.

The Predicted Maneuvers

The two rudder commands already defined, δ_1 and δ_2, correspond to the maneuver known as the turning circle. In addition to these two commands, predictions were made for a simple change of course, δ_3 and for the initial phases of a zig-zag maneuver, δ_4. Where

$$\delta_3(t) = \begin{cases} 0 & , \quad t < 0 \\ 1.5t & , \quad 0 < t < 10 \\ 15 & , \quad 10 < t < 20 \\ 45-1.5t & , \quad 20 < t < 30 \\ 0 & , \quad t > 30 \end{cases}$$

and

$$\delta_4(t) = \begin{cases} 0 & , \quad t < 0 \\ 1.5t & , \quad 0 < t < 10 \\ 15 & , \quad 10 < t < 20 \\ 45-1.5t & , \quad 20 < t < 40 \\ -15 & , \quad 40 < t < 60 \\ -105+1.5t & , \quad 60 < t < 70 \\ 0 & , \quad t > 70 \end{cases}$$

In order to examine the effect of the frequency dependence, predictions were made for each rudder command, based upon the traditional equations of motion (5) as well as the transient-motion equations of motion (12). Let $v_5(t)$ be a computed solution of eqs. (5), $v_{12}(t)$ a computed solution of eqs. (12), and $v_e(t)$ an exact solution of eqs. (5); then we found the remarkable result:

$$|v_5(t) - v_{12}(t)| < |v_5(t) - v_e(t)|$$

for all t and for each rudder command. In other words, the differences between predictions based upon the different equations of motion were always less than the error inherent in the computational technique, which is quite small.

The predictions for the various maneuvers, based upon eqs. (12) are shown in Figures 39 through 42 . Predictions based upon eqs. (5) are not shown since the differences are too small to be seen graphically.

Conclusions

Even if we set aside the question as to which set of linearized equations of motion is the correct one and under what circumstances it is correct to use the simpler traditional approach, we are of the opinion that the impulse-test method is a superior means of evaluating the stability derivatives.

First of all, the impulse technique, even if repeated runs are made to avoid the previously mentioned difficulties, requires substantially fewer experiments than the regular-motion technique to obtain the same results.

Secondly, the regular-motion technique is incapable of evaluating the stability derivatives at very low frequencies, and since this same frequency range is of paramount importance, static-sway tests and rotating-arm tests (if one has the facilities) are used to supplement the data. However, even if these additional tests are performed, they assist only in the evaluation of damping coefficients and contribute little to the evaluations of added masses. The impulse test has the capability of accurate measurement all the way down to zero frequency.

Third, since the impulse test requires measurement of data for only a very limited time, it becomes a more versatile method. Problems such as wave reflection can be avoided simply by recording the data before the reflected wave has time to encounter the ship. Similarly, a short towing tank

ceases to present a problem.

However, once a complete set of the added masses and damping coefficients has been determined, it would appear that the choice between the two sets of linearized equations of motion is of little significance in the prediction of ship maneuvers. Even the idealized case of instantaneous rudder response, a severe test of the effect of frequency dependence, led to predictions which differed only slightly.

Recent papers by Fujino and Motora (1975), Nomoto (1975), and Fujino (1975) have all expressed the opinion that the memory effect is often small and that the traditional equations of motion will yield good results for many standard ship maneuvers. The results of the present study support this opinion.

References

Cummins, W. E.
The impulse response function and ship motions.
Schiffstechnik, Vol. 9, 1962, 101-109.

Frank, T.
New method for determining stability derivatives.
Master's Thesis, Univ. of Calif., Berkeley, 1974,
42 pp. + 32 figs.

Fujino, M.
The effect of frequency dependence of the stability
derivatives on maneuvering motions. International Ship-
building Progress, Vol. 22, 1975, pp. 416-432.

Fujino, M.; Motora, S.
On the effect of frequency dependency of the stability
derivatives upon steering motions. Proc. 14th Internat.
Towing Tank Conf., Ottawa, 1975, Vol. 2, pp. 621-630.

van Leeuven, G.
The lateral damping and added mass of a horizontally
oscillating shipmodel. Studiecentrum T.N.O. voor
Scheepsbouw en Navigatie, Rep. No. 65 S, December 1964,
26 pp.

Lin, W. C.
An initial-value problem for the motion of a ship moving
with constant mean velocity in an arbitrary seaway.
Dissertation, Univ. of Calif., Berkeley, 1966, iii +
86 pp.

Mandel, P.
Ship maneuvering and control. Chap. 8, pp. 463-606,
Principles of Naval Architecture, J. P. Comstock, ed.
Soc. of Naval Arch. Mar. Engrs., New York, 1967.

Manning, M.
Are the stability derivatives linear? Master's Thesis,
Univ. of Calif., Berkeley, 1976, 41 pp. + 42 figs.

Nomoto, K.
Ship response in directional control taking account of frequency dependent hydrodynamic derivatives. Proc. 14th Internat. Towing Tank Conf., Ottawa, 1975, Vol. 2, pp. 703-709.

Ogilvie, T. F.
Recent progress toward the understanding and prediction of ship motions. 5th Symposium on Naval Hydrodynamics, Bergen, 1964, pp. 3-80; discussion, pp. 80-128.

Paulling, J. R.; Wood, L. W.
The dynamic problem of two ships operating on parallel courses in close proximity. Univ. of Calif., Berkeley, Inst. Engrg. Res., Rep. Series 189, Issue 1, July 1962, iii + 26 pp. + 15 figs.

Taplin, A.
Notes on rudder design practice. First Symposium on Ship Maneuverability, DTMB Report 1461, Oct. 1960, 127-149.

Wehausen, J. V.; Frank, T.; Loeser, D. J.; Scragg, C. A.; Sibul, O. J.; Webster, W. C.
Transient-maneuver testing and the equations of maneuvering. 11th. Symposium on Naval Hydrodynamics, London 1976, 20 pp.

Whicker, L. F.; Fehlner, L. F.
Free-stream characteristics of a family of low-aspect-ratio, all-movable control surfaces for application to ship design. DTMB Report 933, Dec. 1958, 121 pp.

Figures

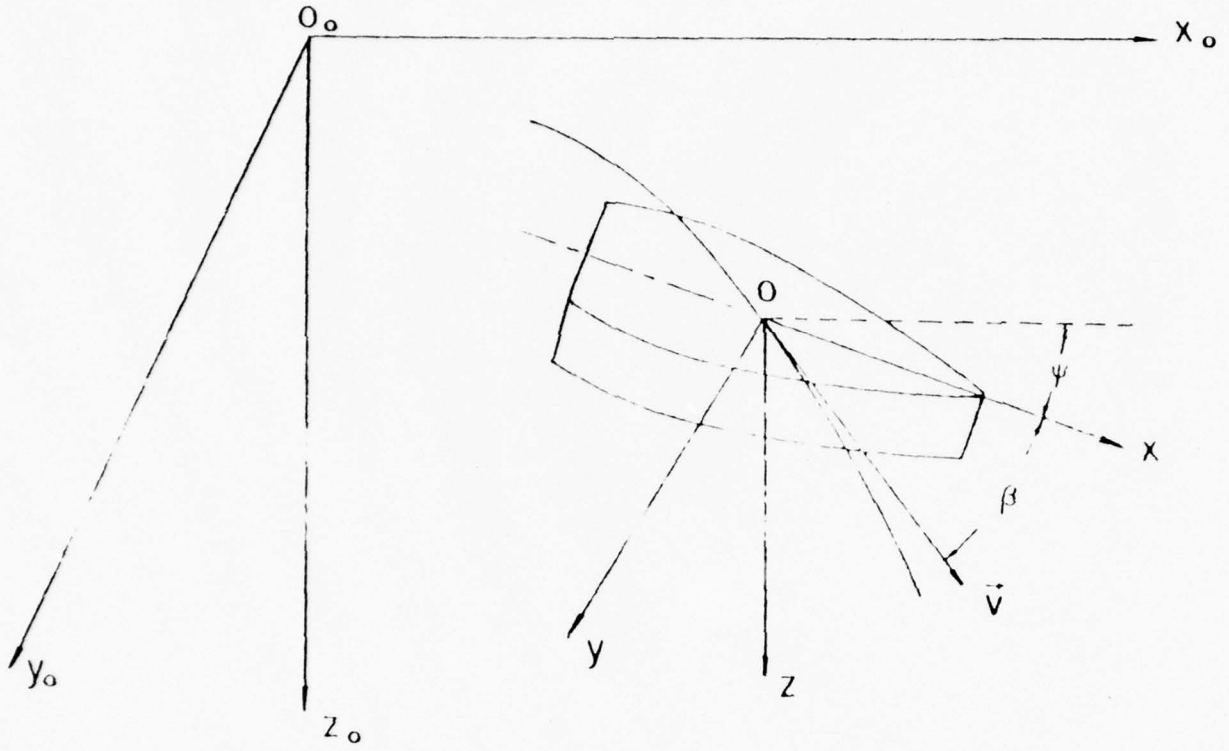

Figure 1: Coordinate systems, heading angle = ψ, drift angle = β.

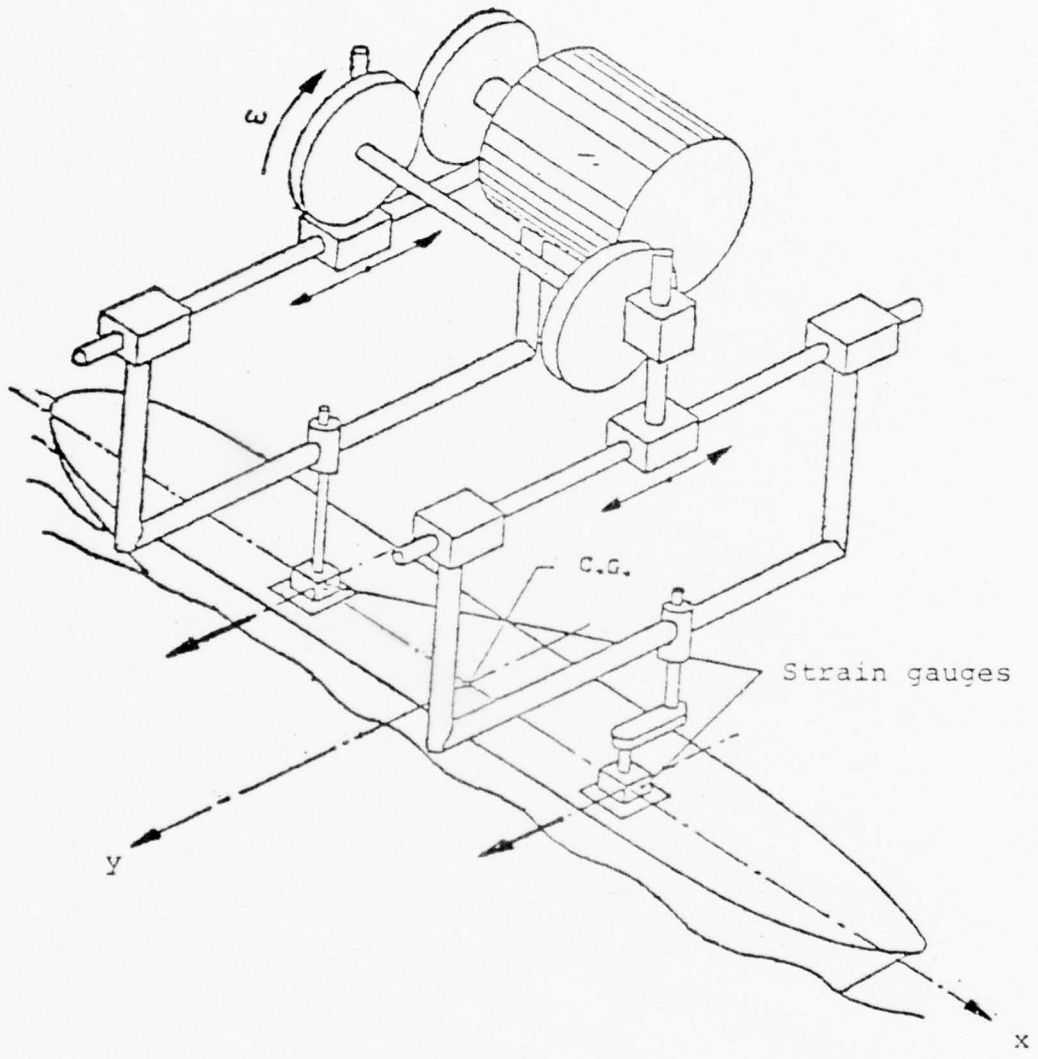

Figure 2: Planar motion mechanism.

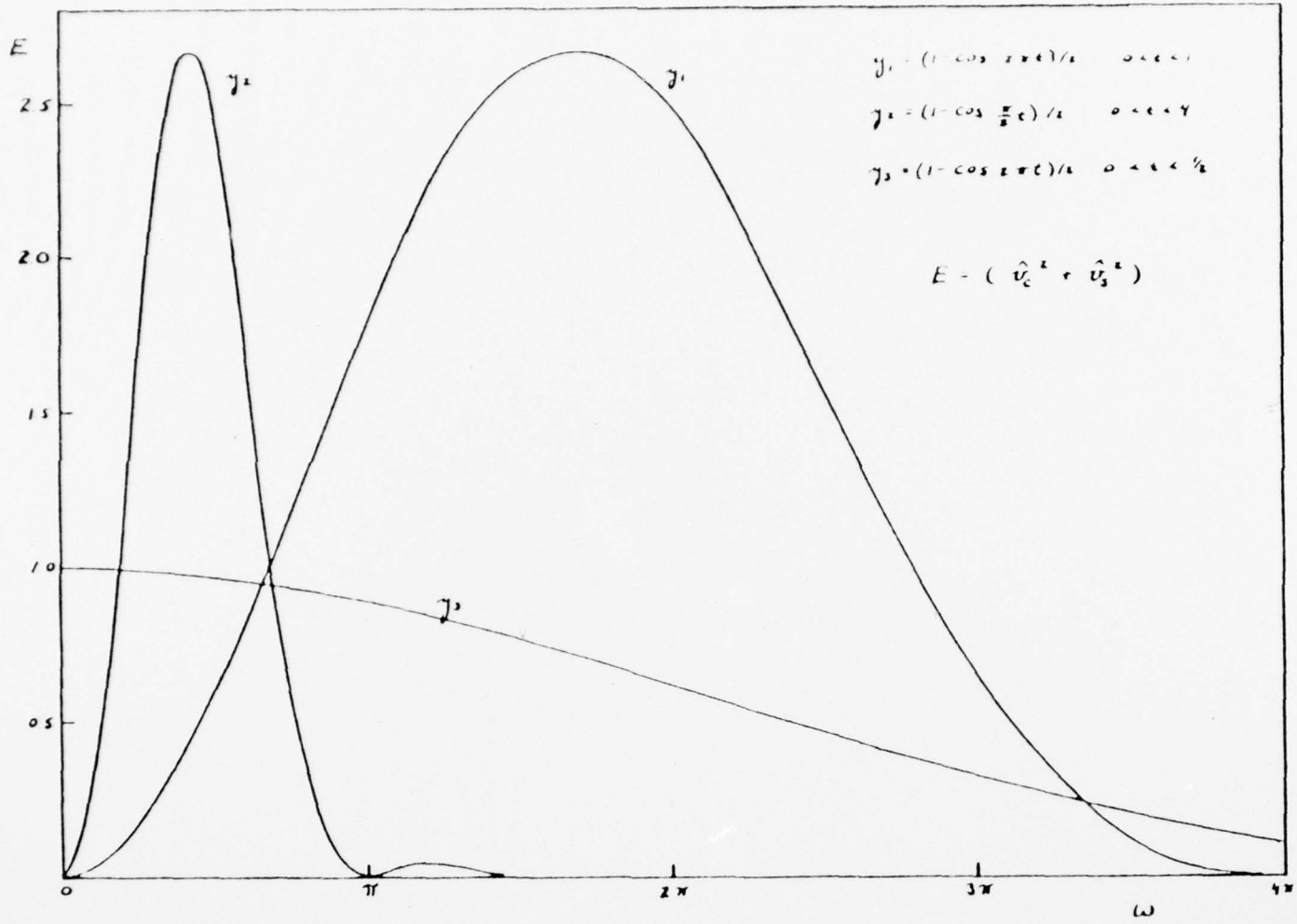

Figure 3: Energy of various pulses.

FULL-PULSE PURE SWAY

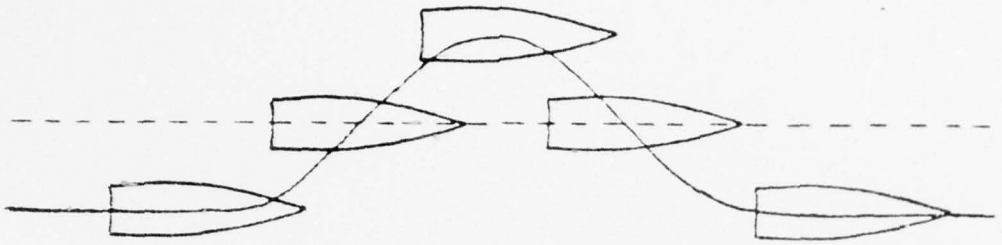

STEP-PULSE PURE SWAY

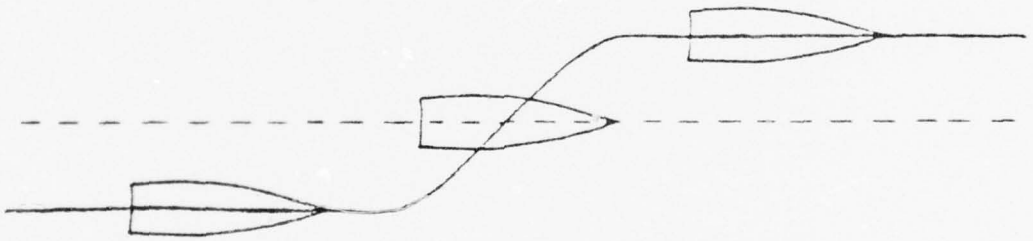

STEP-PULSE SWAY AND YAW

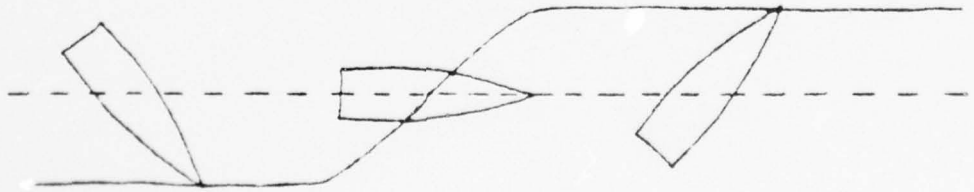

Figure 3a: The full-pulse and the step-pulse.

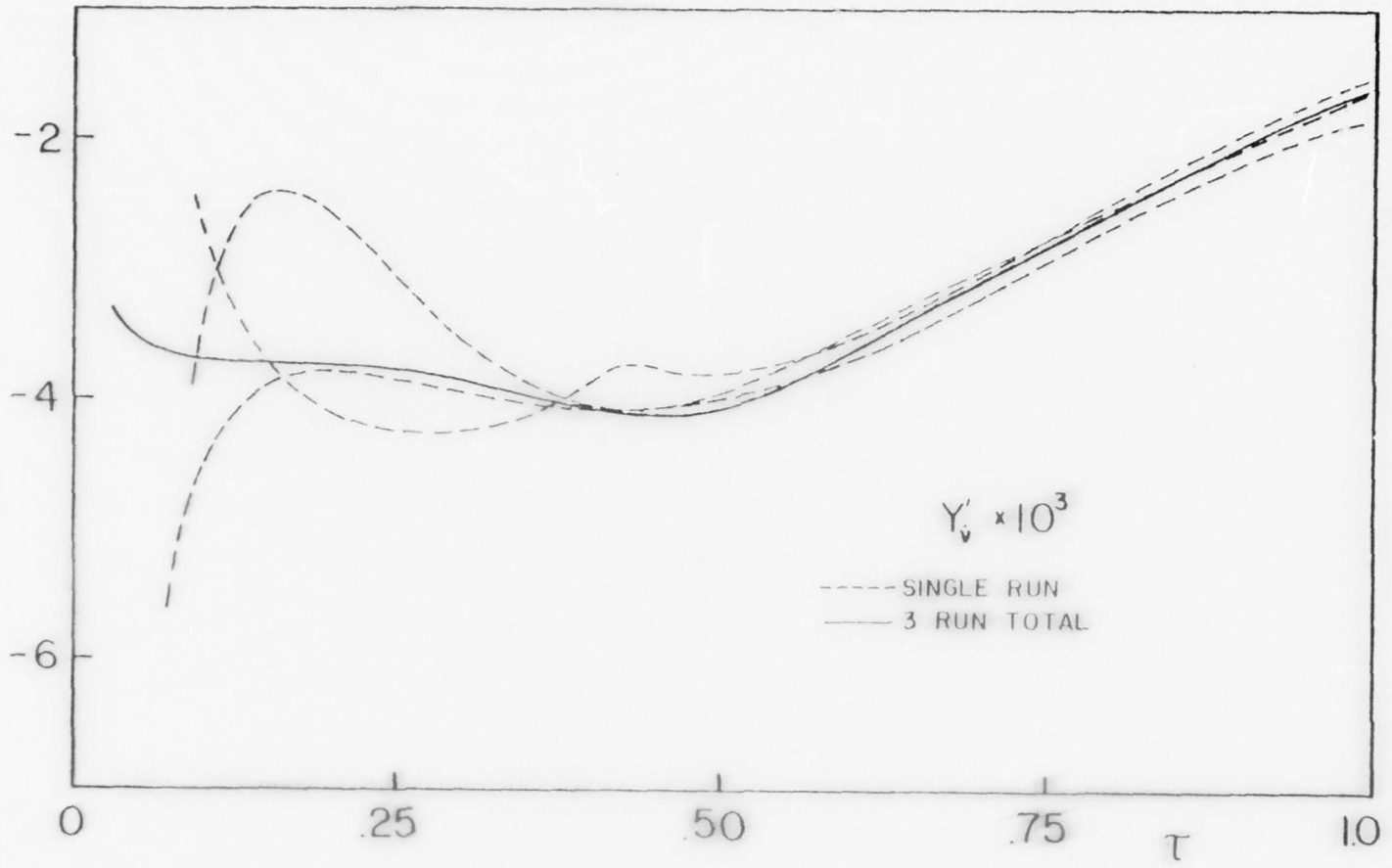

Figure 4: Comparison of results obtained from individual runs and added runs.

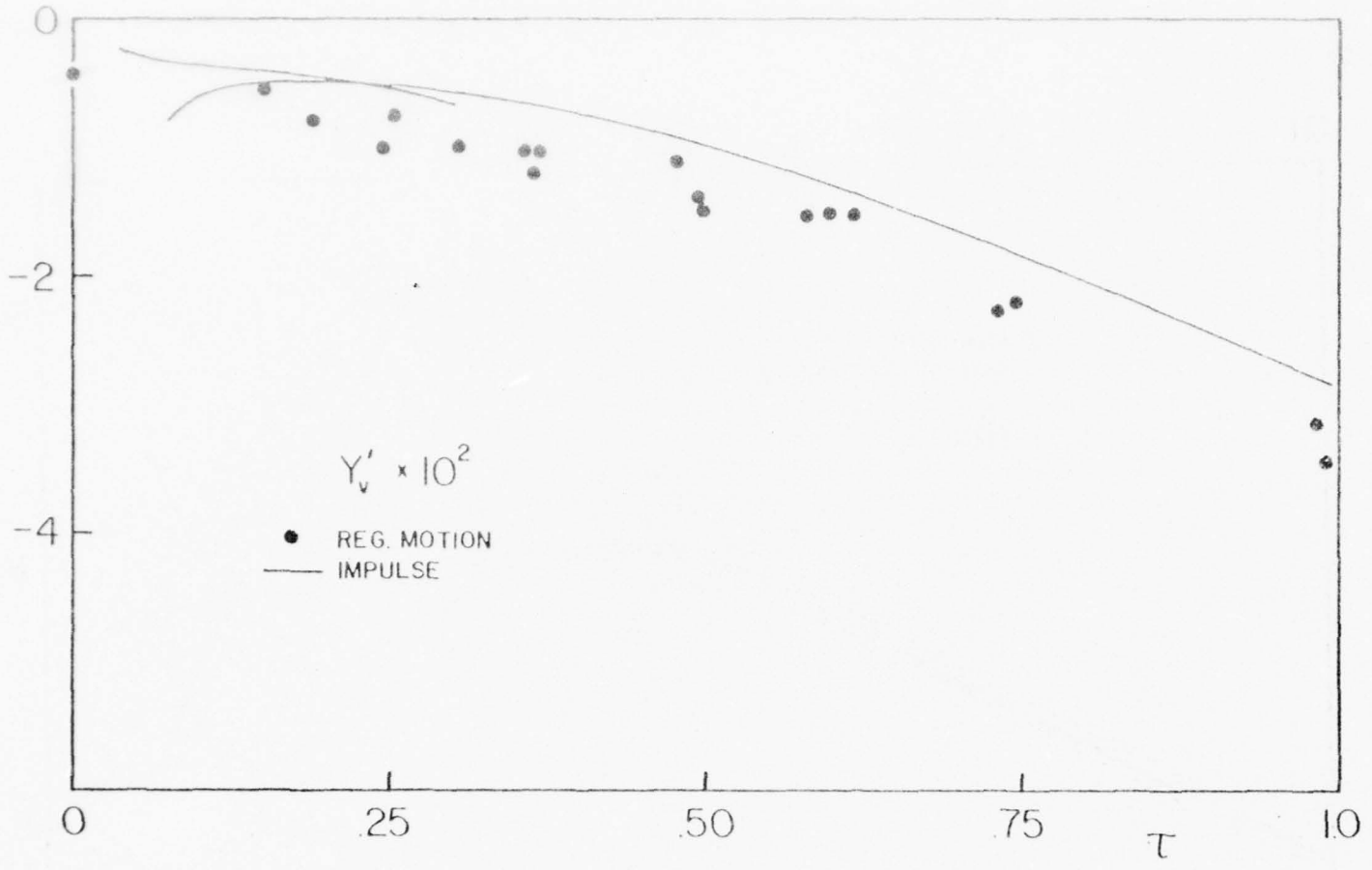

Figure 5: Results of regular-motion tests and full-pulse tests for Fn = 0.30.

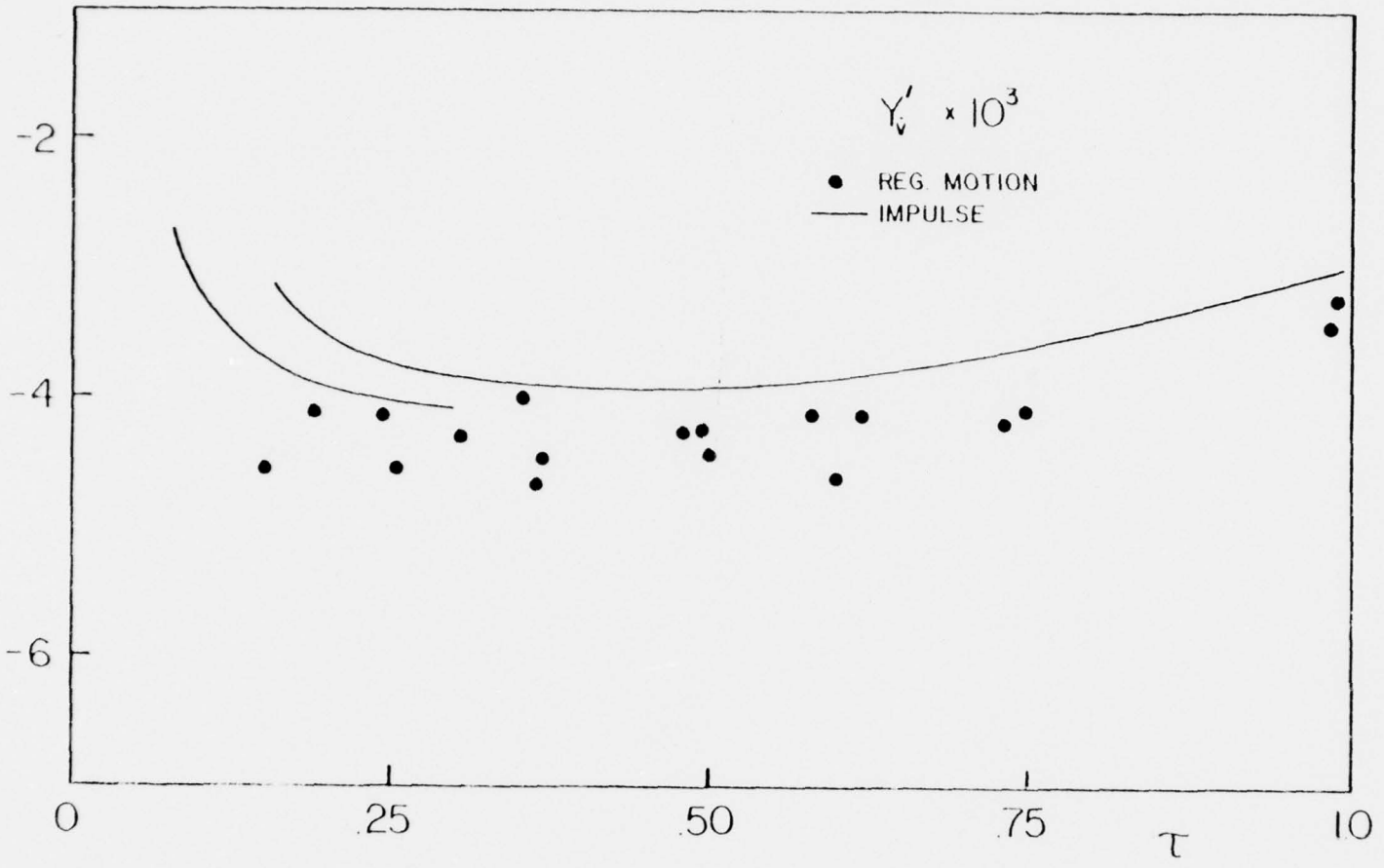

Figure 6: Results of regular-motion tests and full-pulse tests for Fn = 0.30.

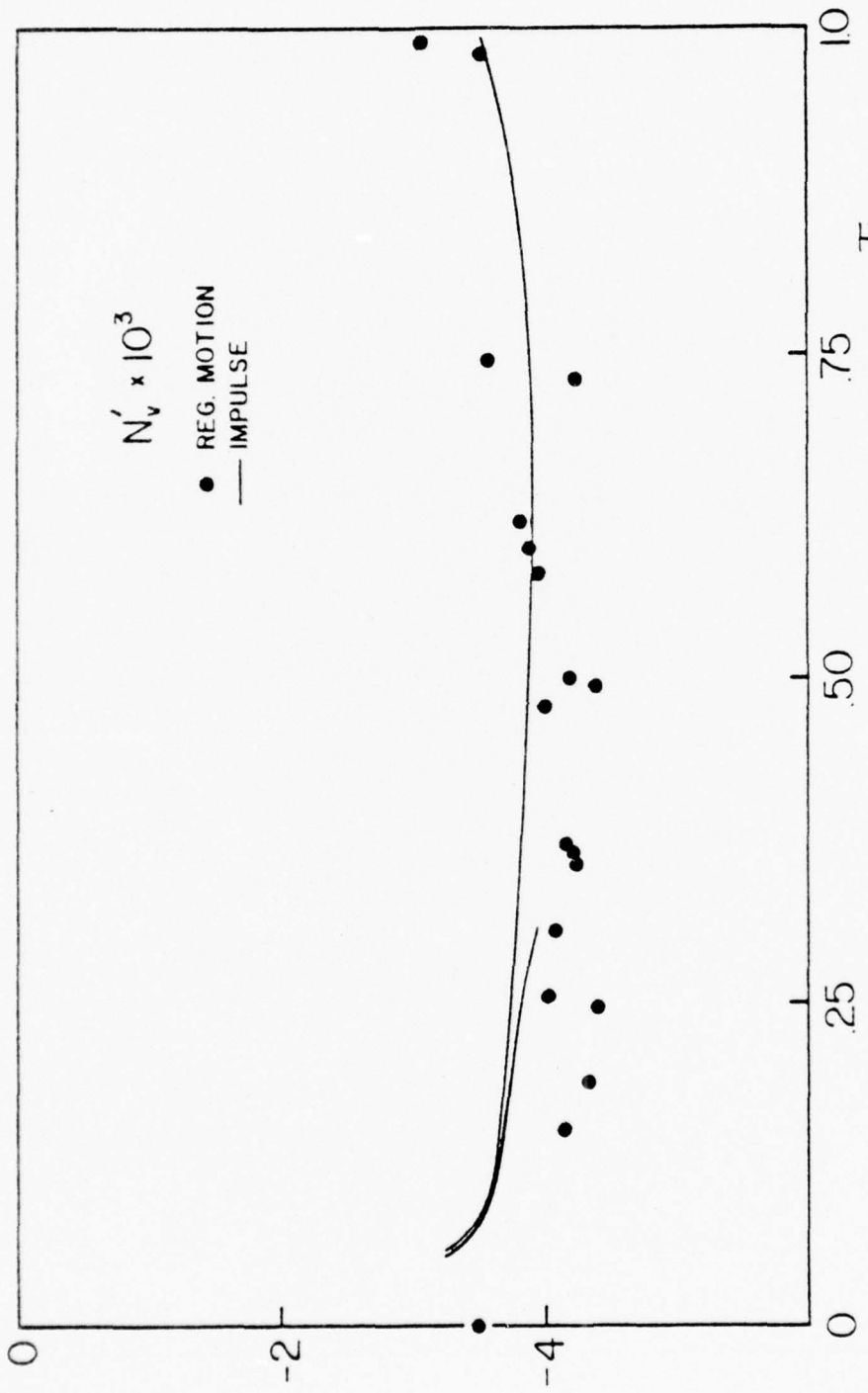

Figure 7: Results of regular-motion tests and full-pulse tests for Fn = 0.30.

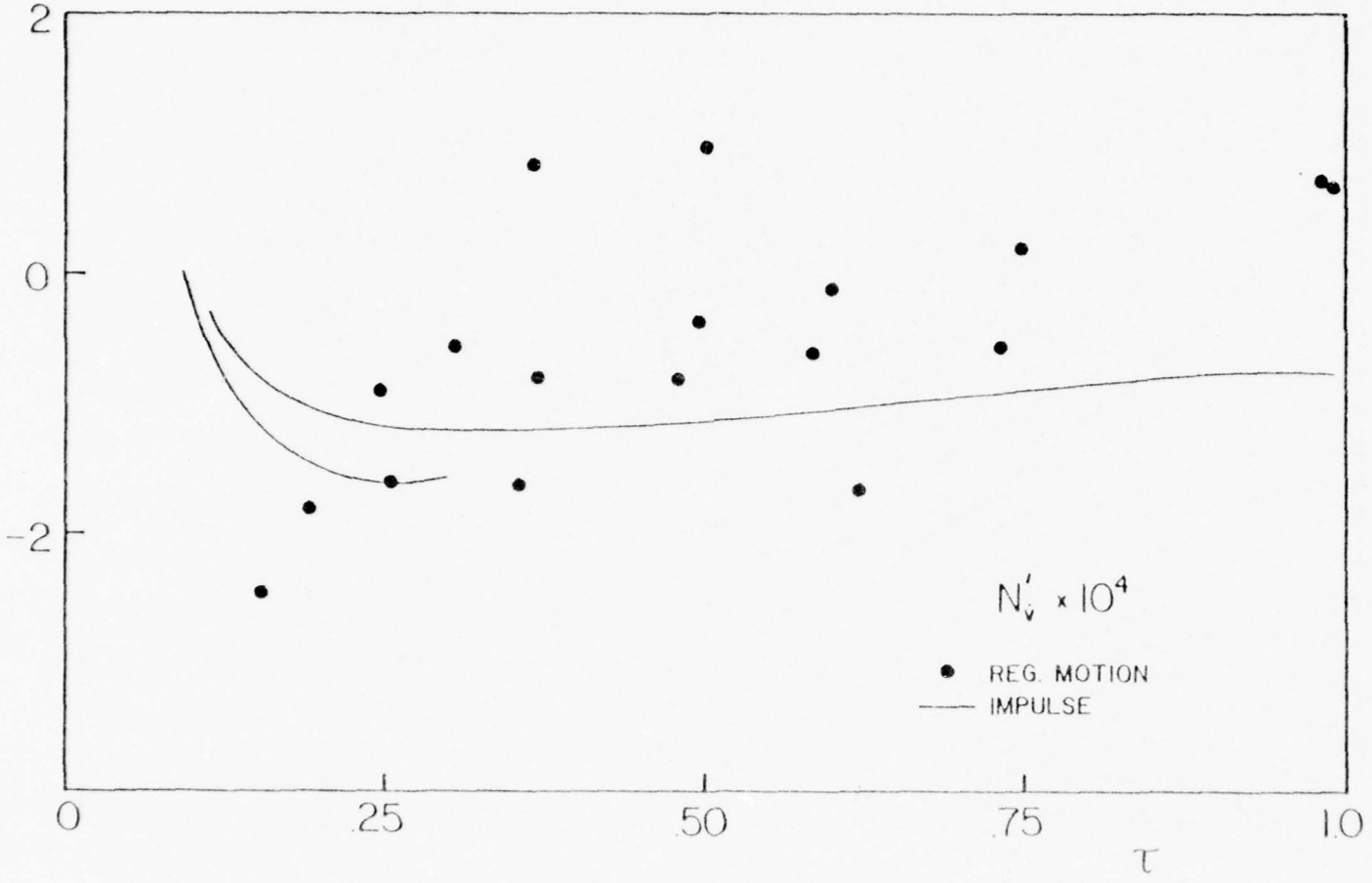

Figure 8: Results of regular-motion tests and full-pulse tests for Fn = 0.30.

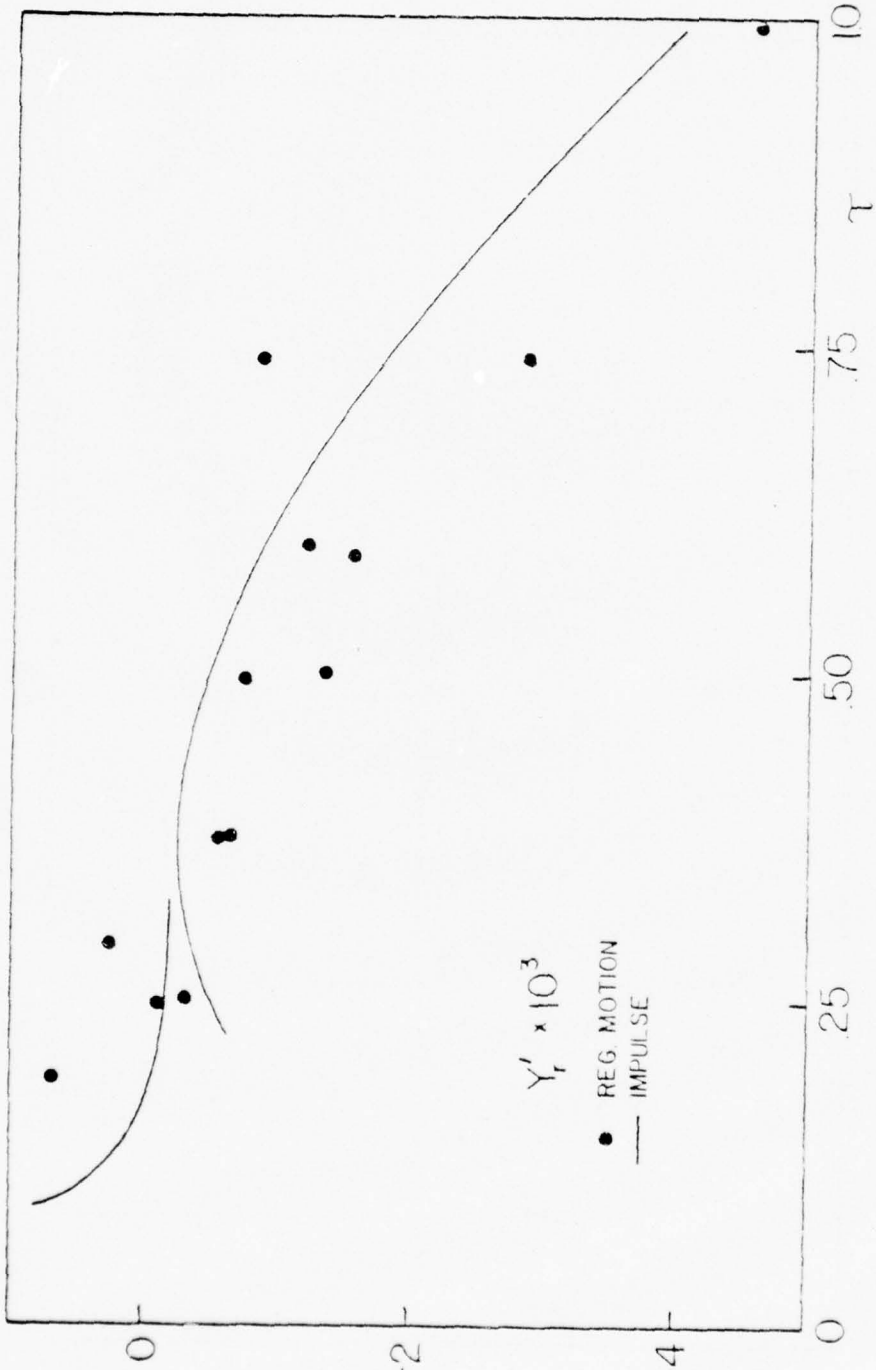

Figure 9: Results of regular-motion tests and full-pulse tests for Fn = 0.30.

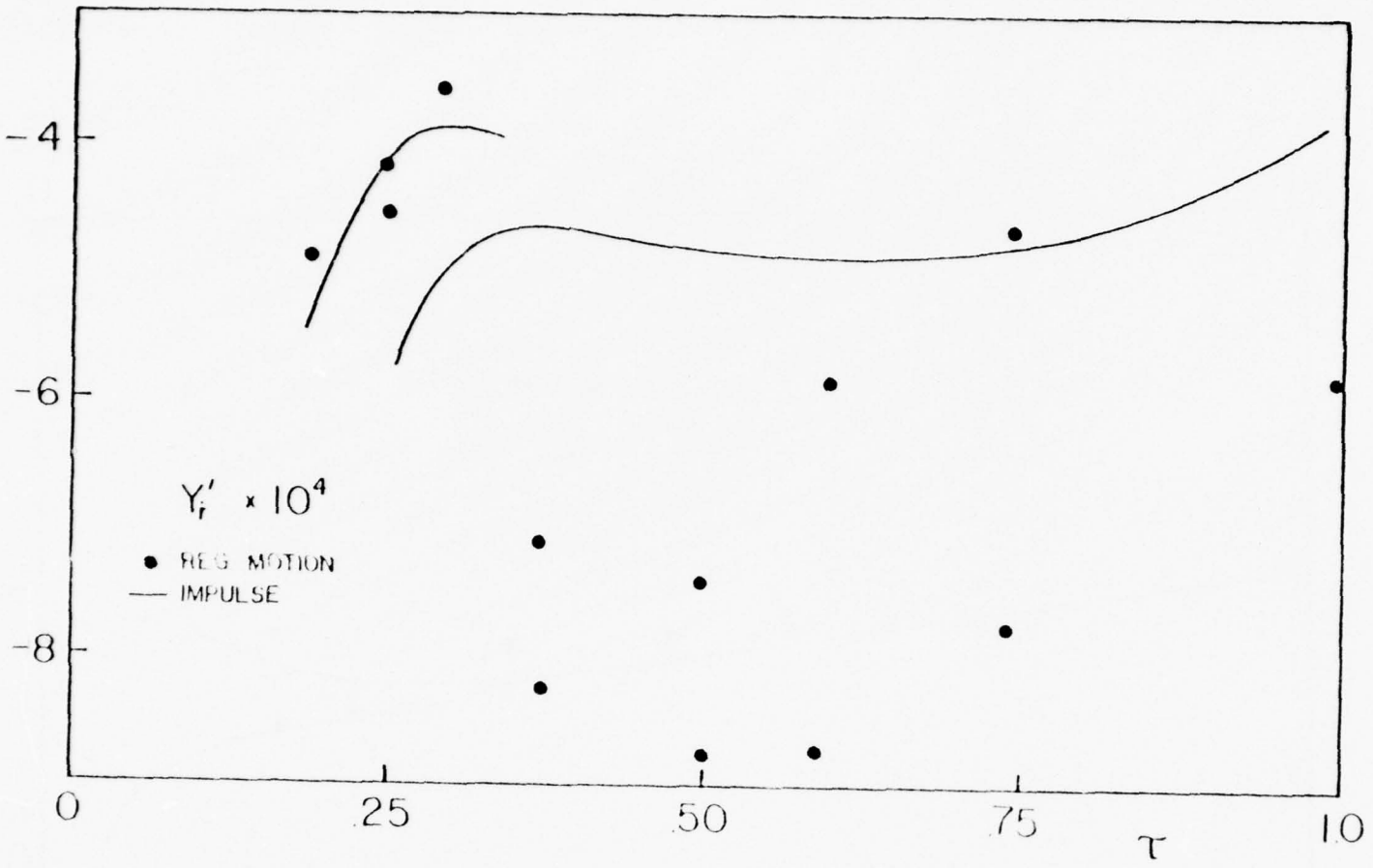

Figure 10: Results of regular-motion tests and full-pulse tests for Fn = 0.30.

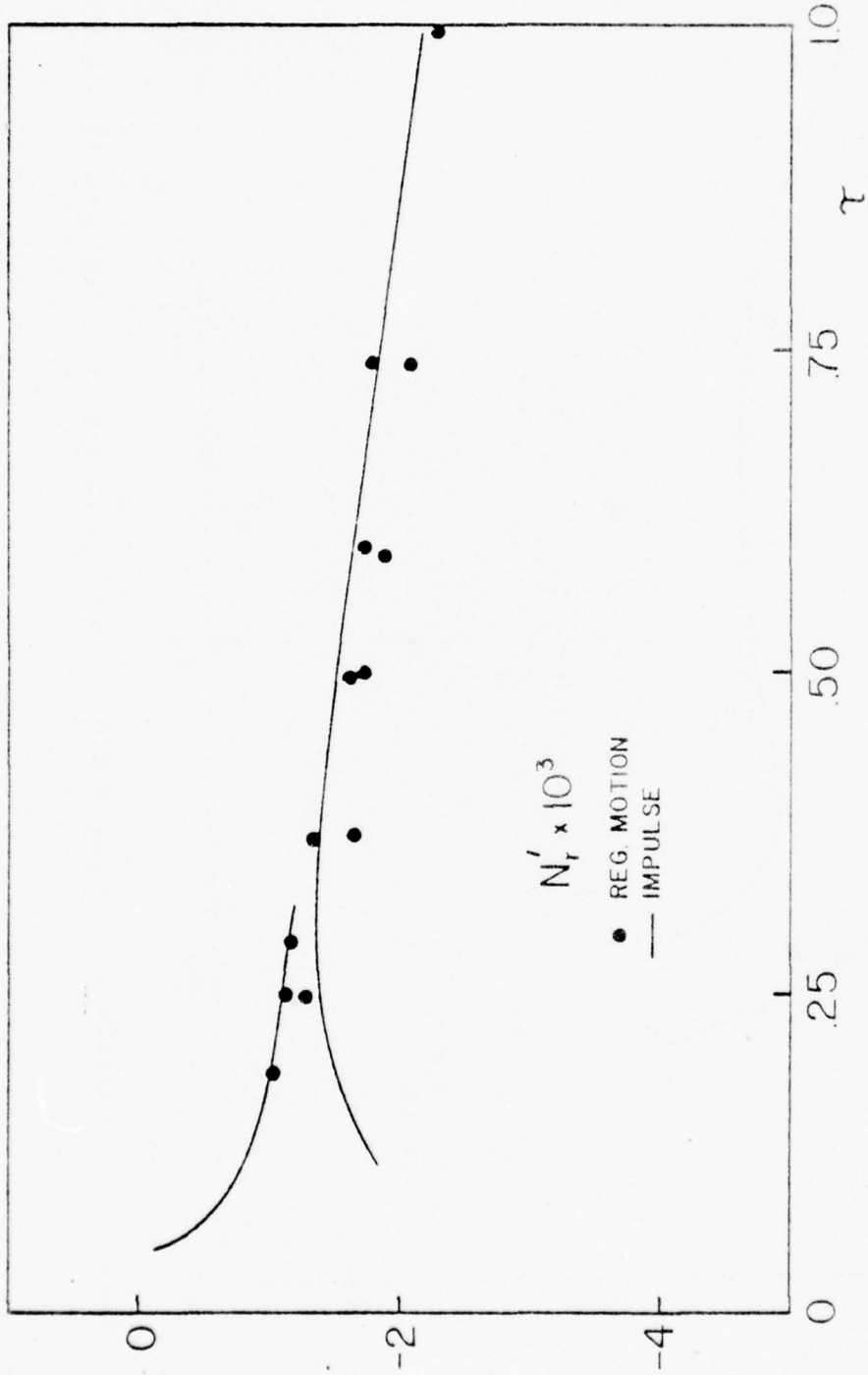

Figure 11: Results of regular-motion tests and full-pulse tests for Fn = 0.30.

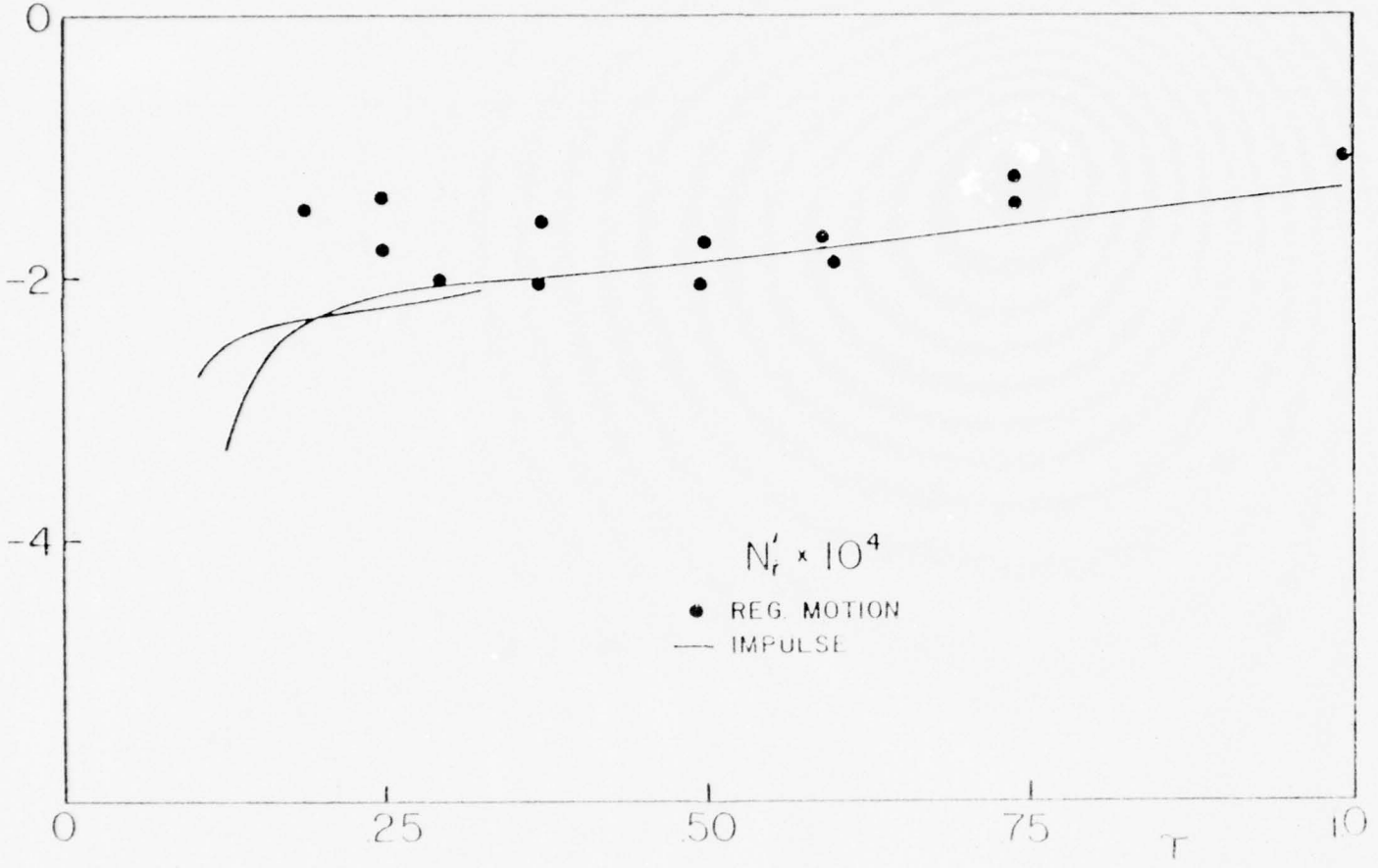

Figure 12: Results of regular-motion tests and full-pulse tests for Fn = 0.30.

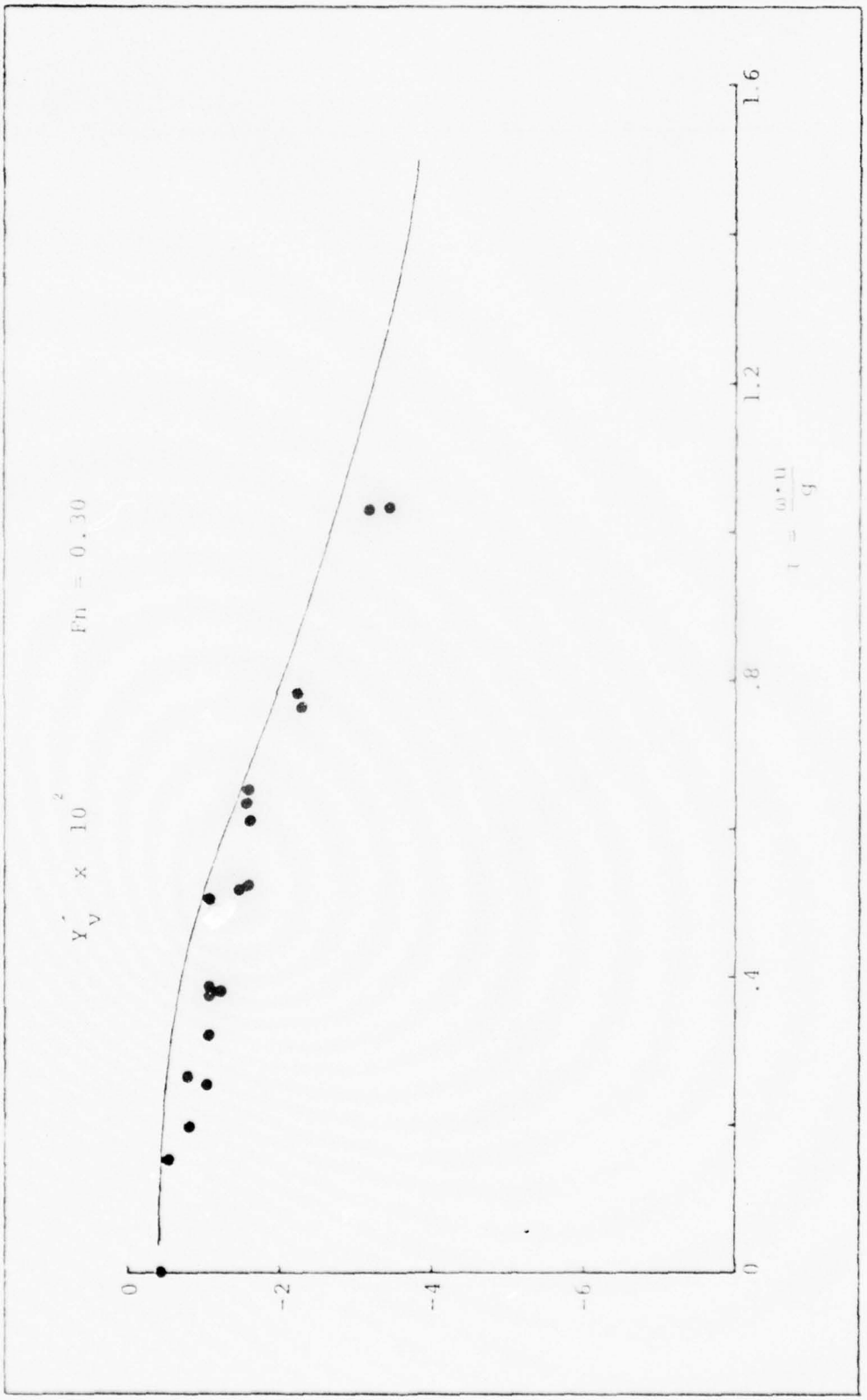

Figure 13: Results from 4 step-pulse runs.

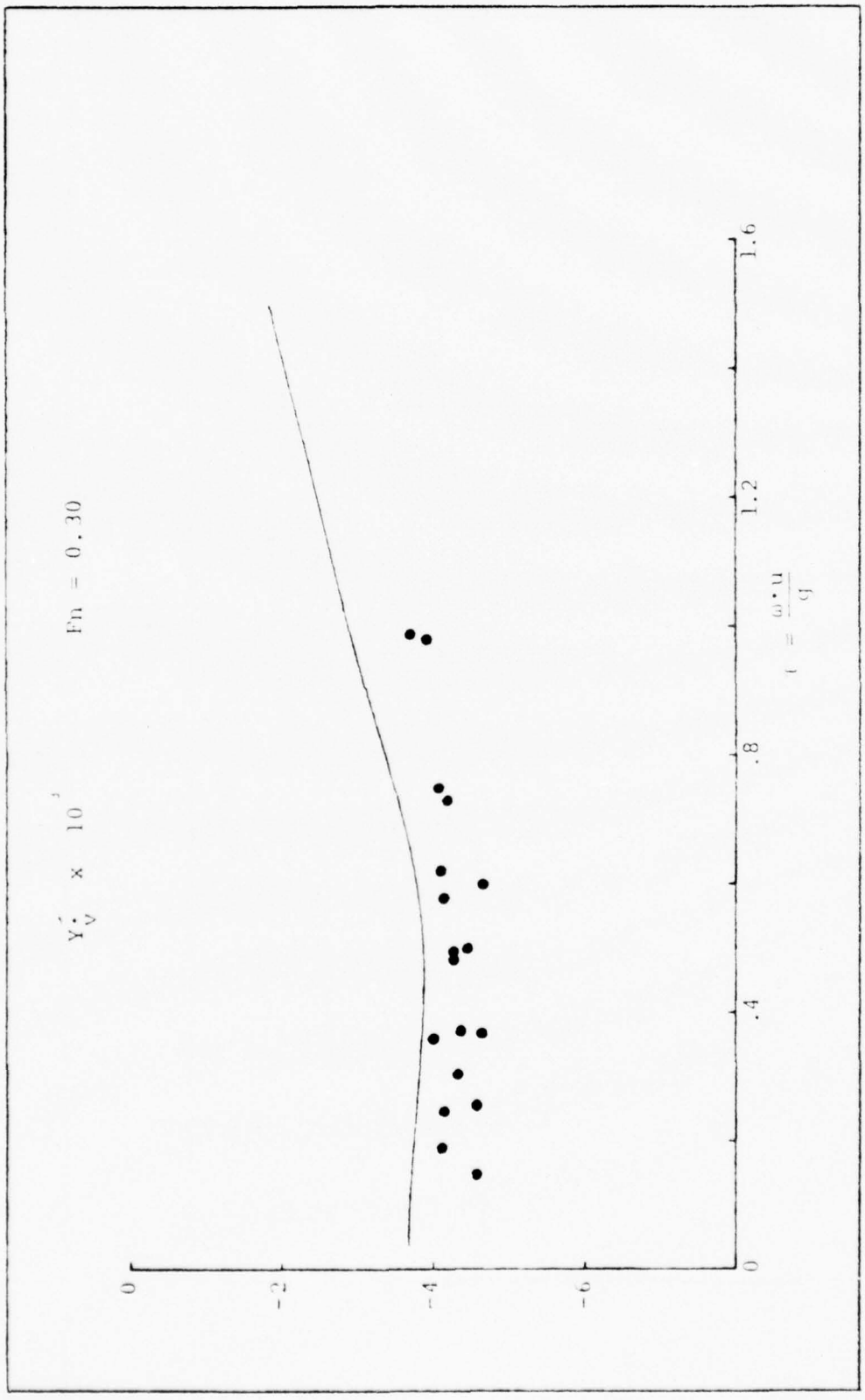

Figure 14: Results from 4 step-pulse runs.

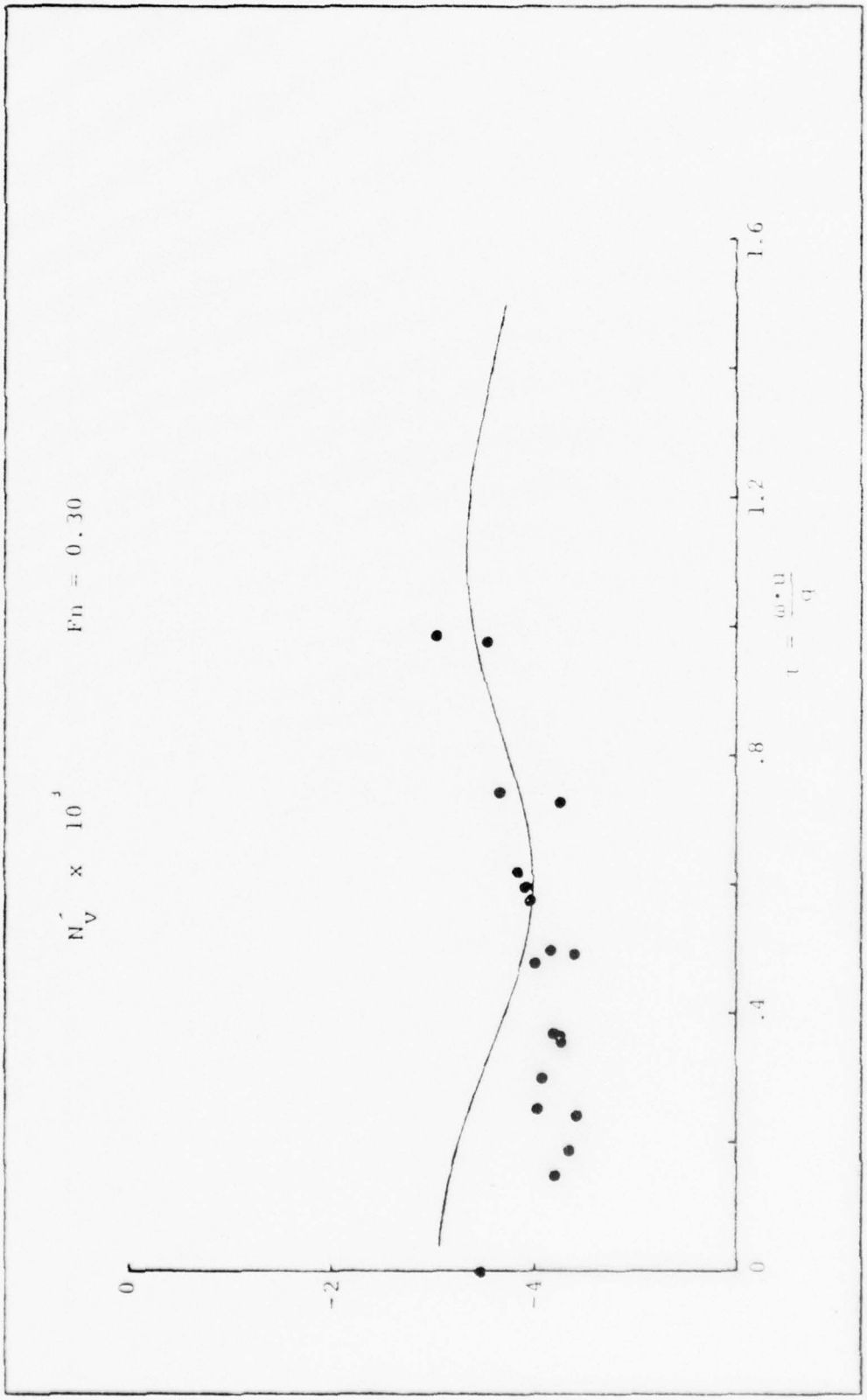

Figure 15: Results from 4 step-pulse runs.

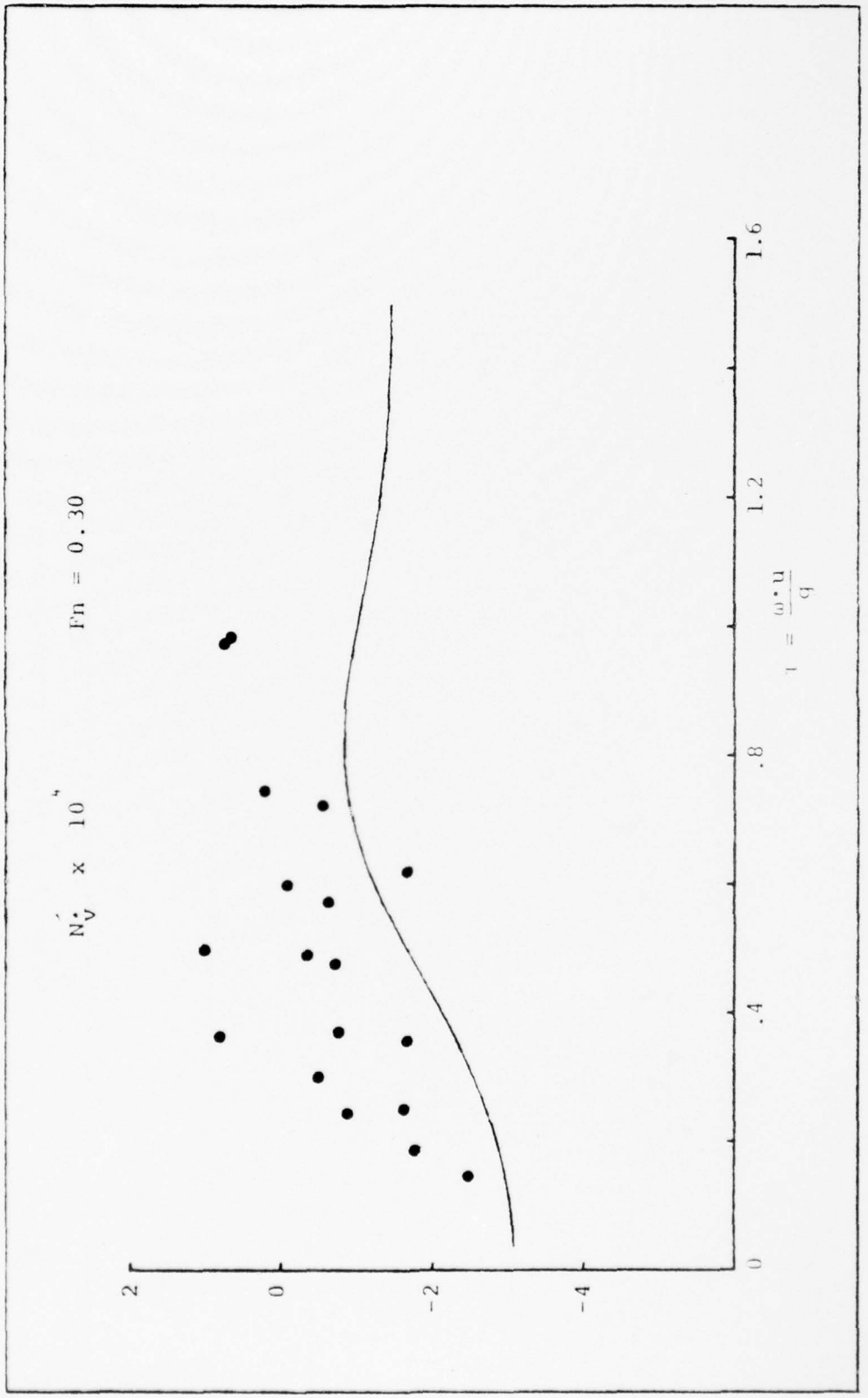

Figure 16: Results from 4 step-pulse runs.

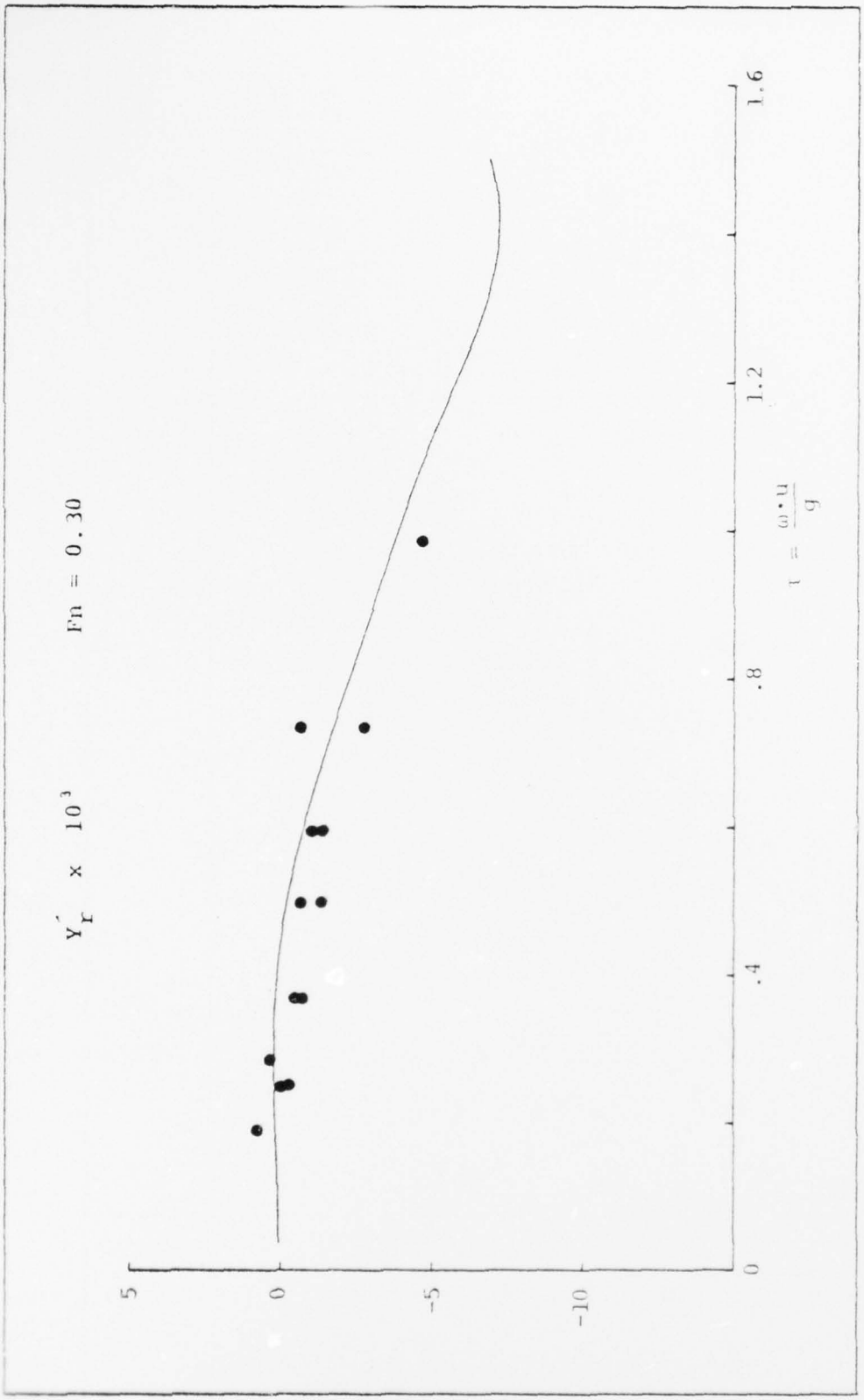

Figure 17: Results from 5 step-pulse runs.

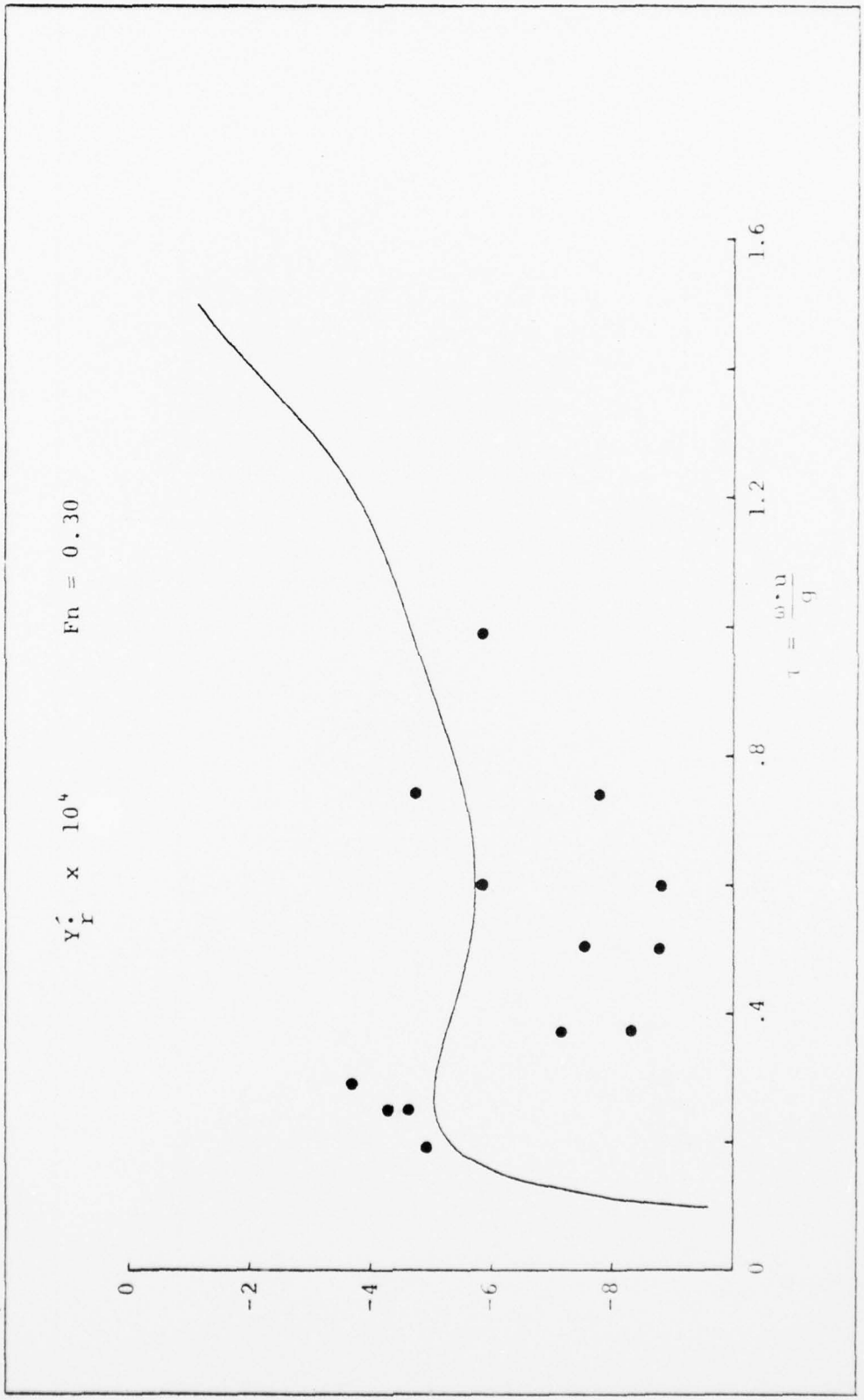

Figure 18: Results from 5 step-pulse runs.

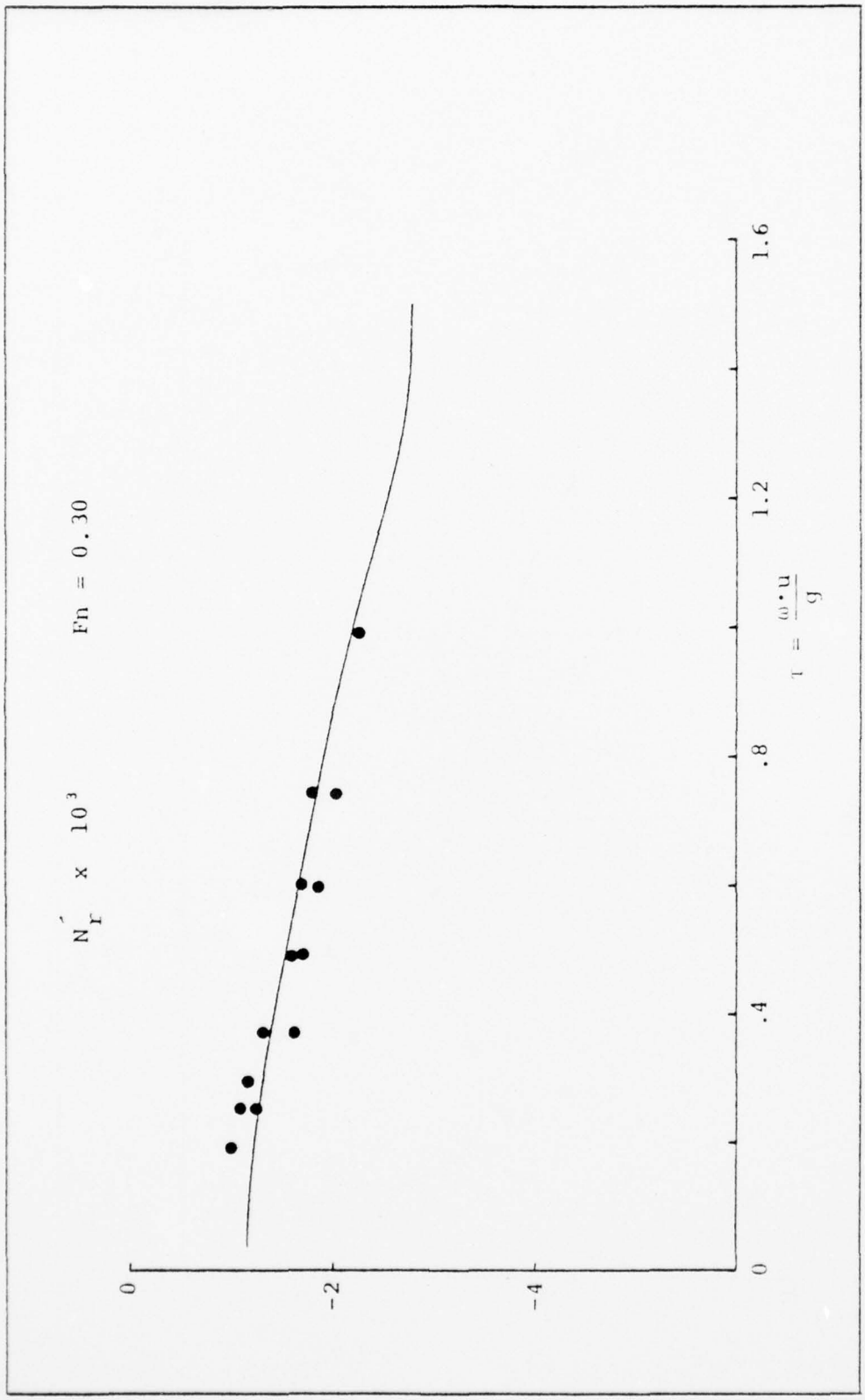

Figure 19: Results from 5 step-pulse runs.

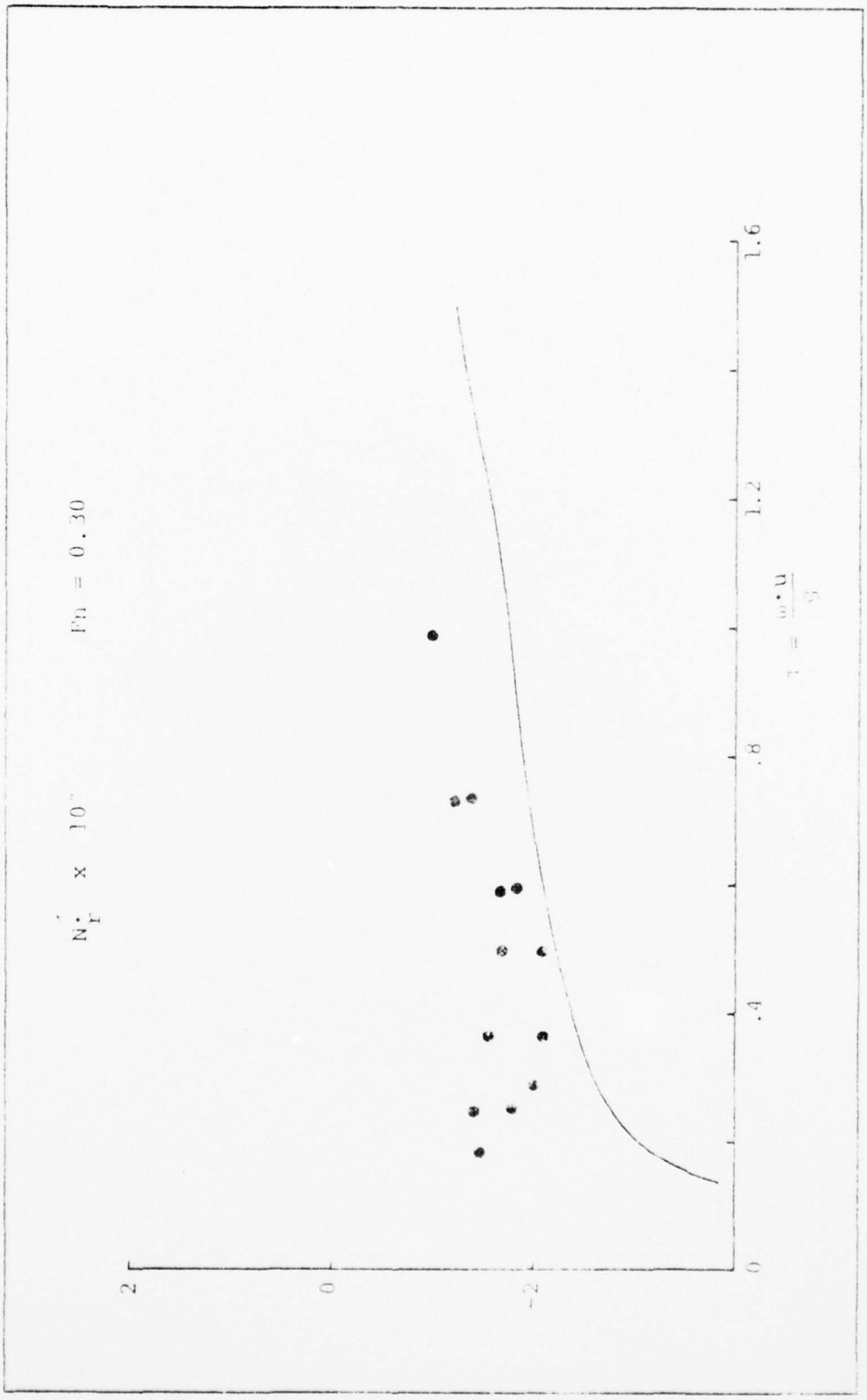

Figure 20: Results from 5 step-pulse runs.

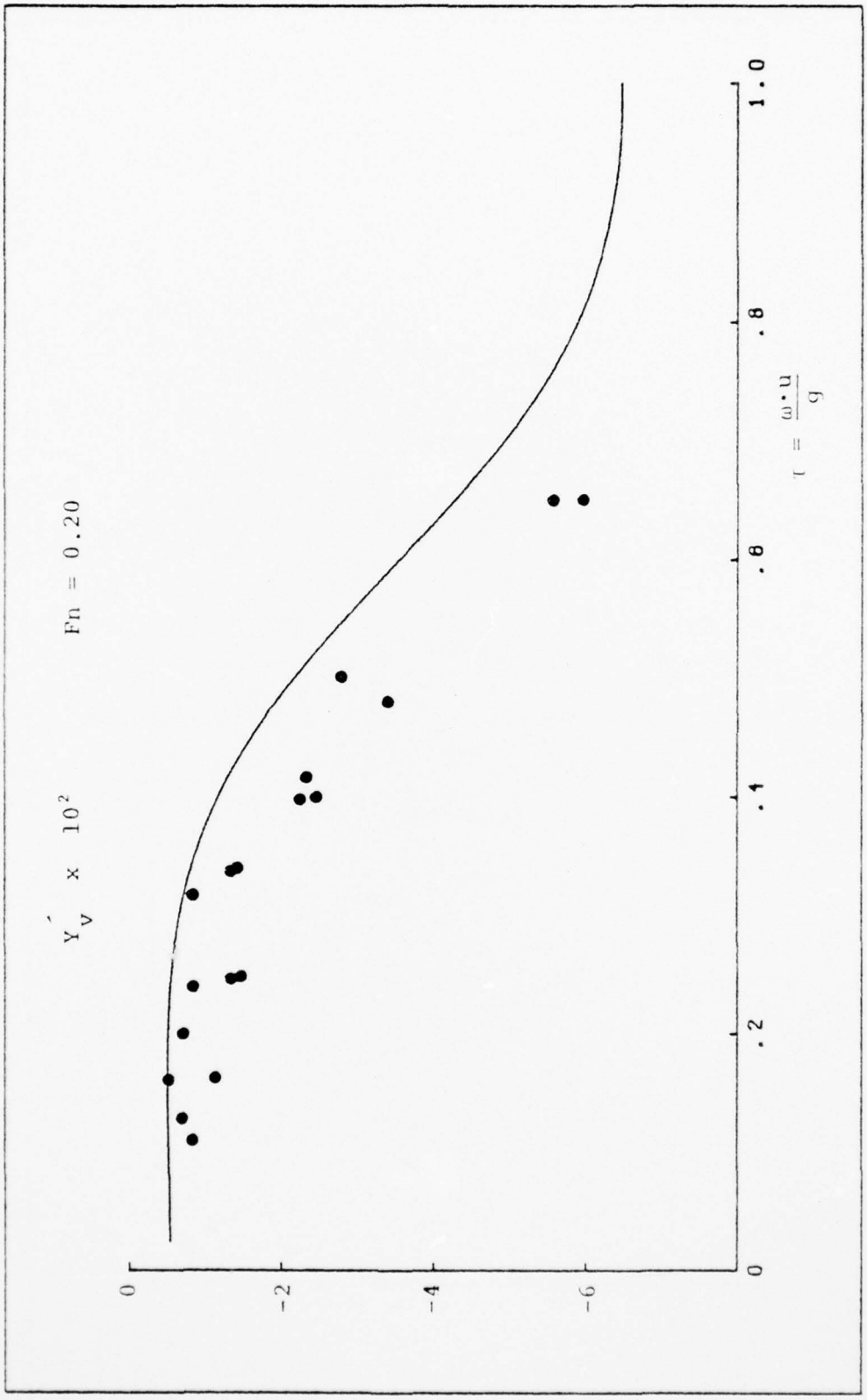

Figure 21: Results from 5 step-pulse runs.

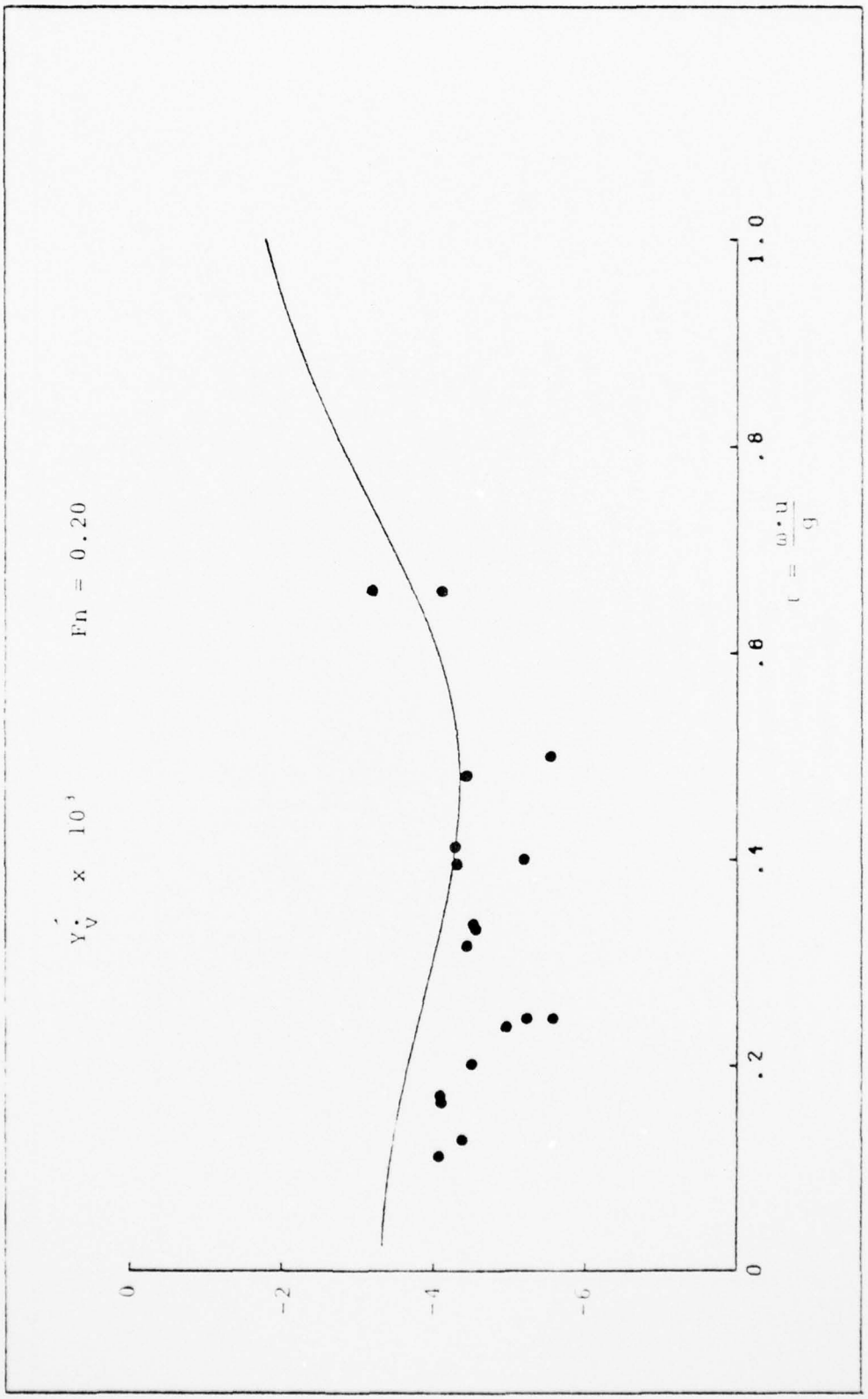

Figure 22: Results from 5 step-pulse runs.

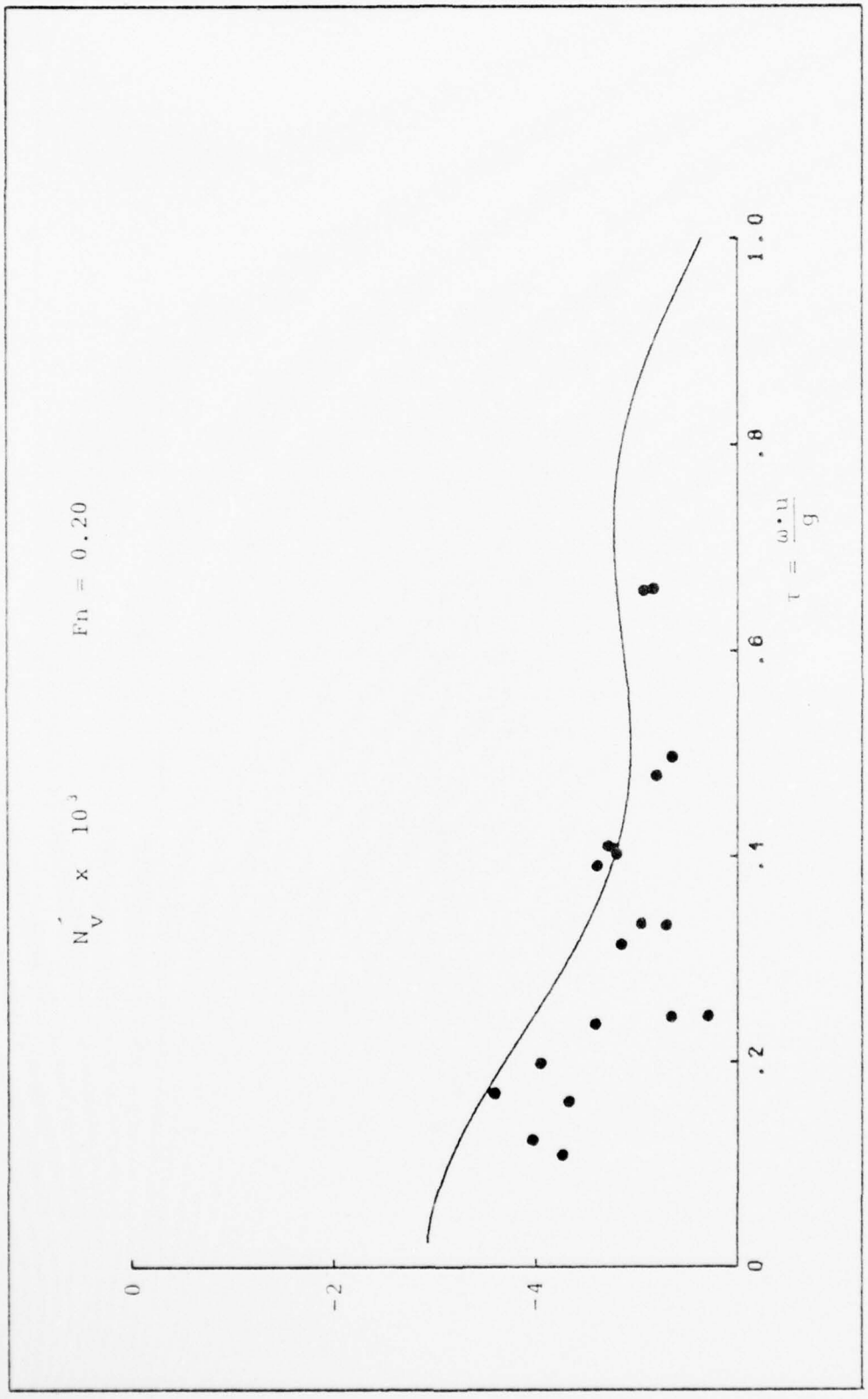

Figure 23: Results from 5 step-pulse runs.

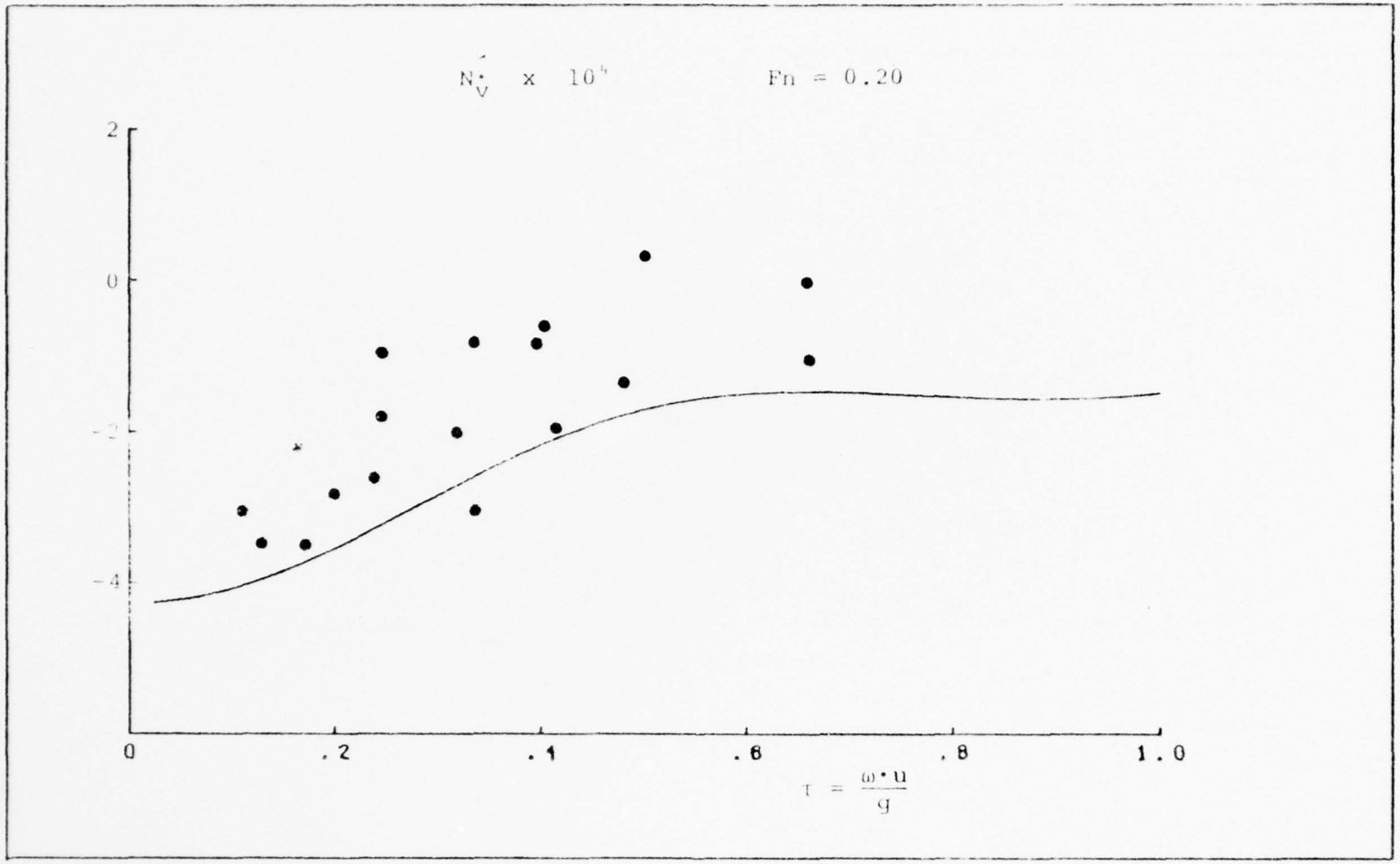

Figure 24: Results from 5 step-pulse runs.

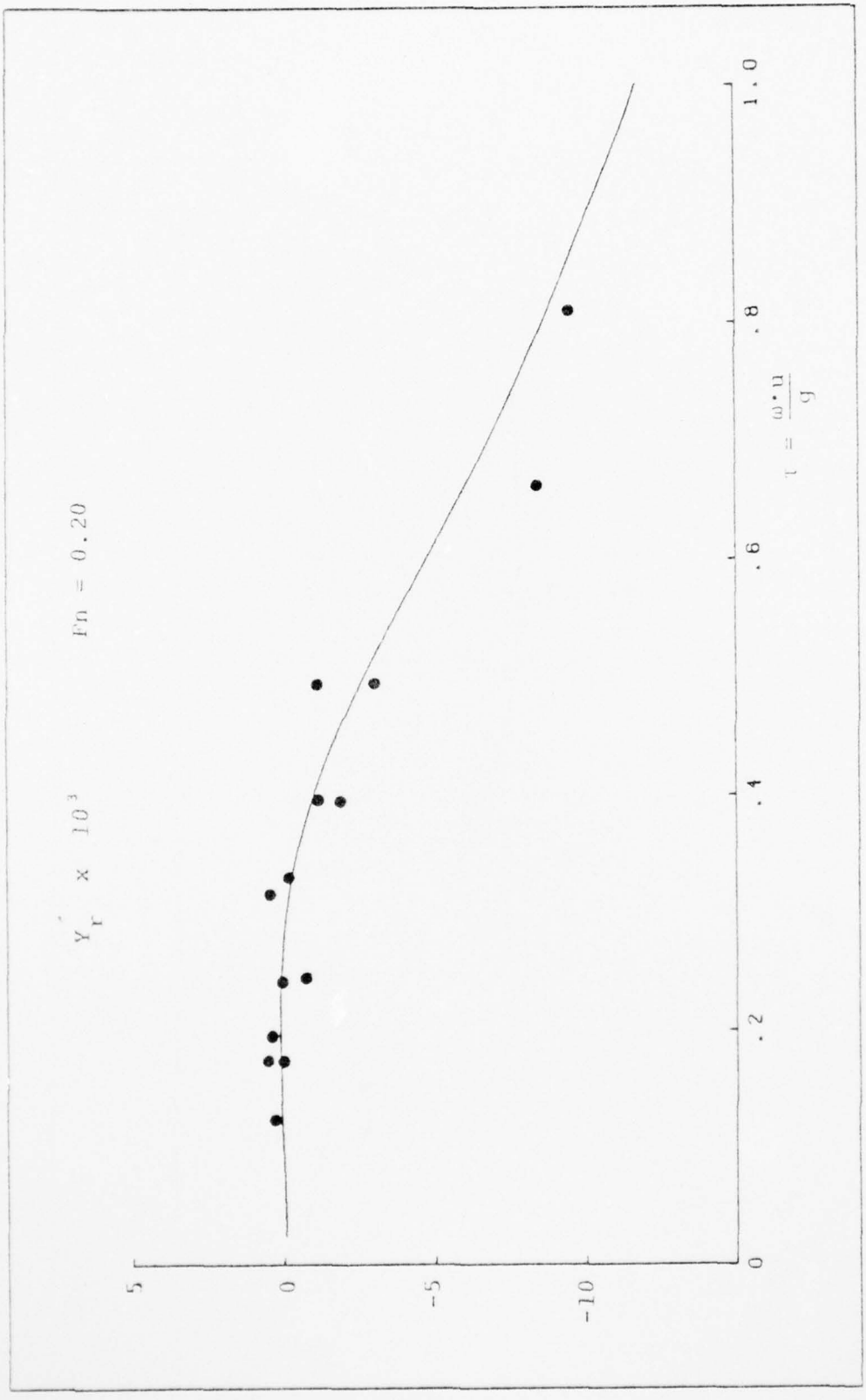

Figure 25: Results from 5 step-pulse runs.

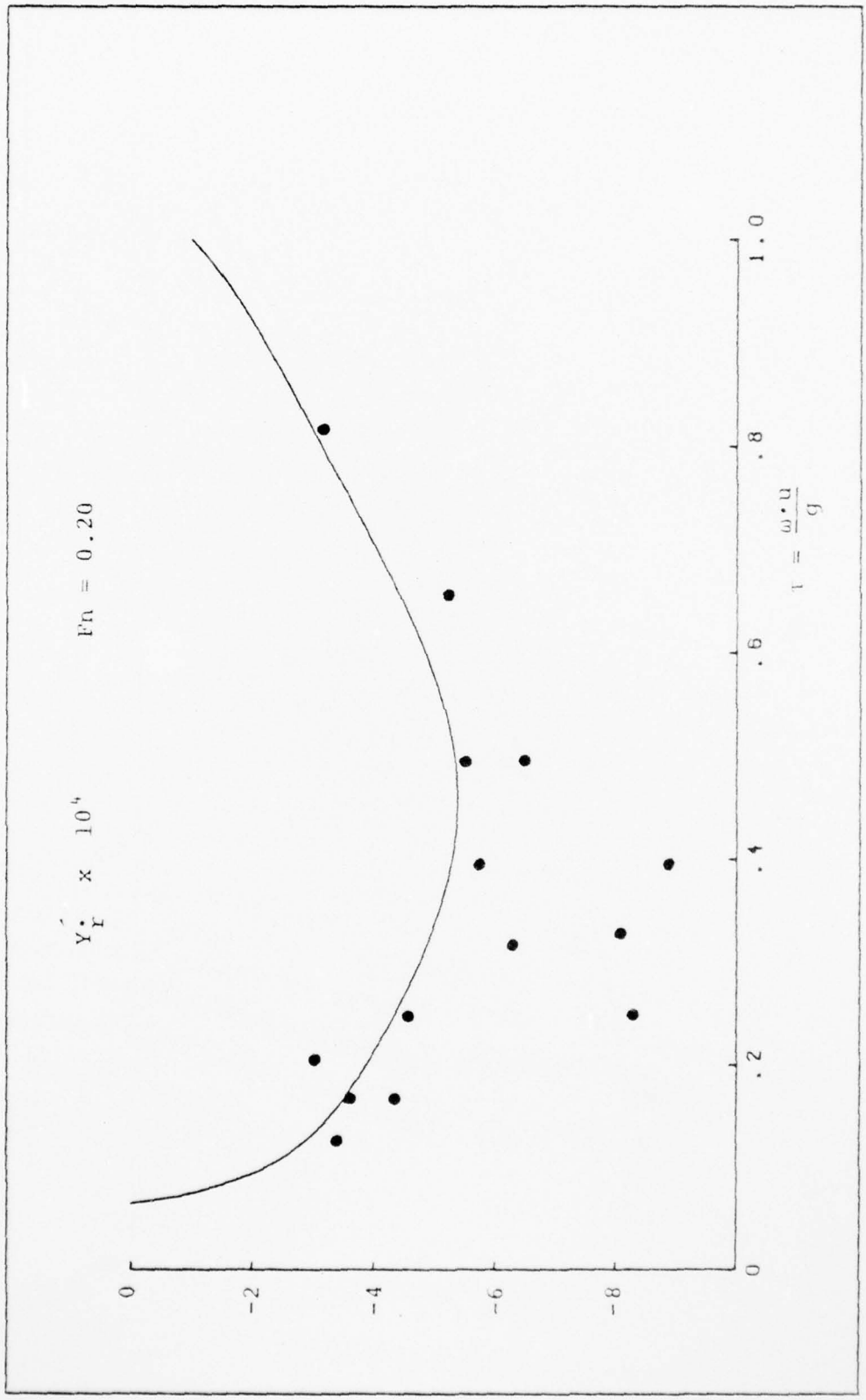

Figure 26: Results from 5 step-pulse runs.

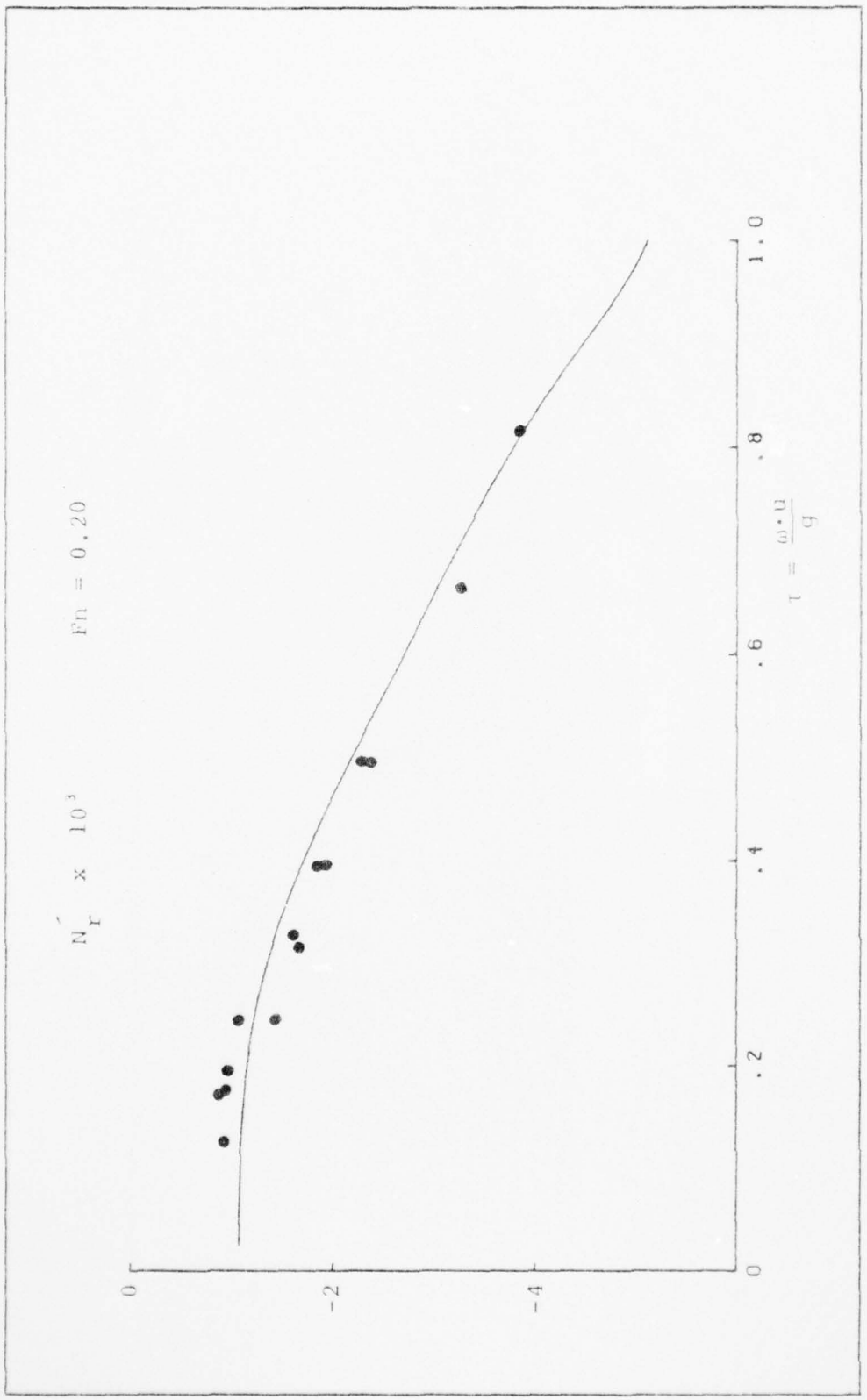

Figure 27: Results from 5 step-pulse runs.

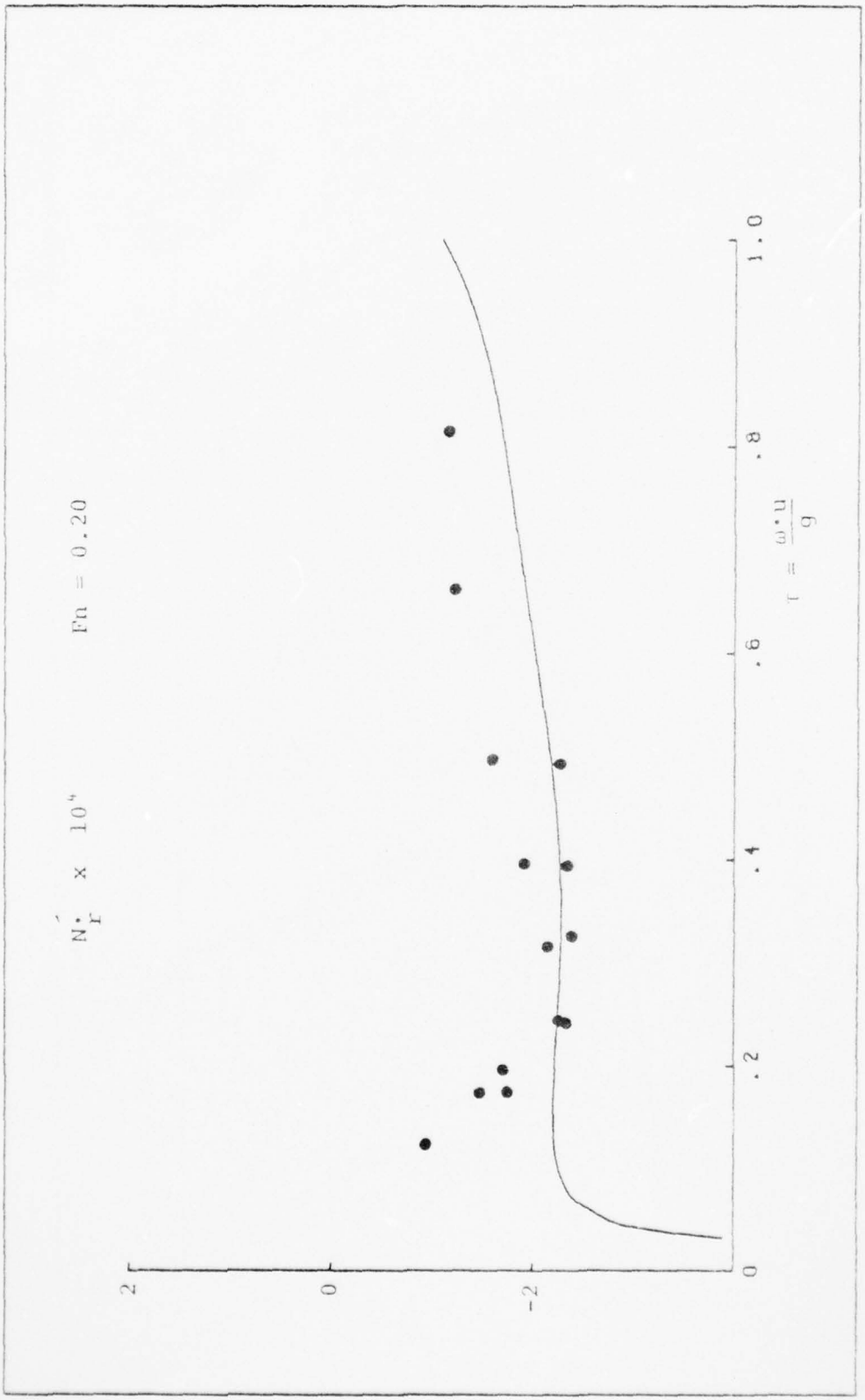

Figure 28: Results from 5 step-pulse runs.

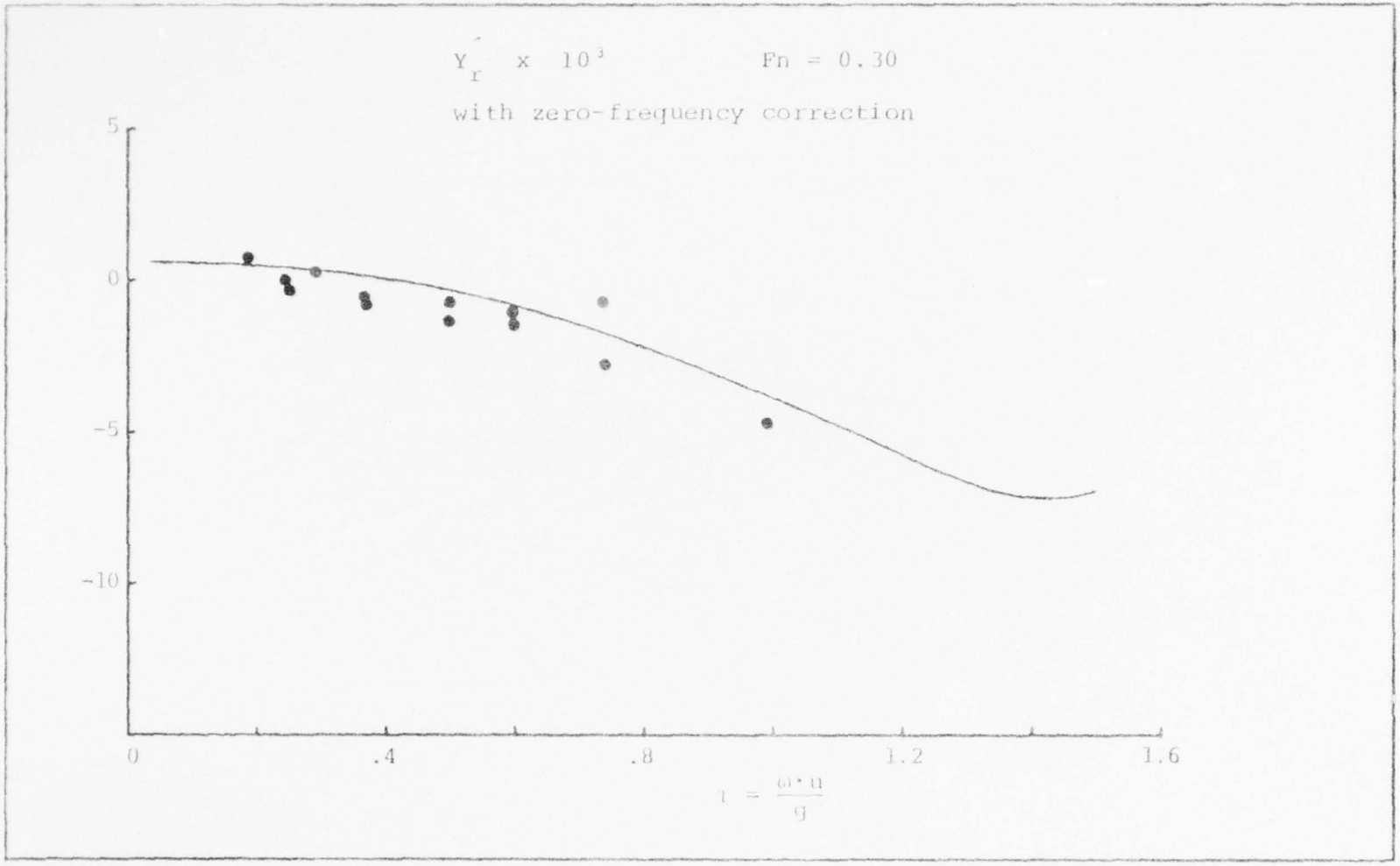

Figure 29: Zero-corrected results from 5 step-pulse runs.

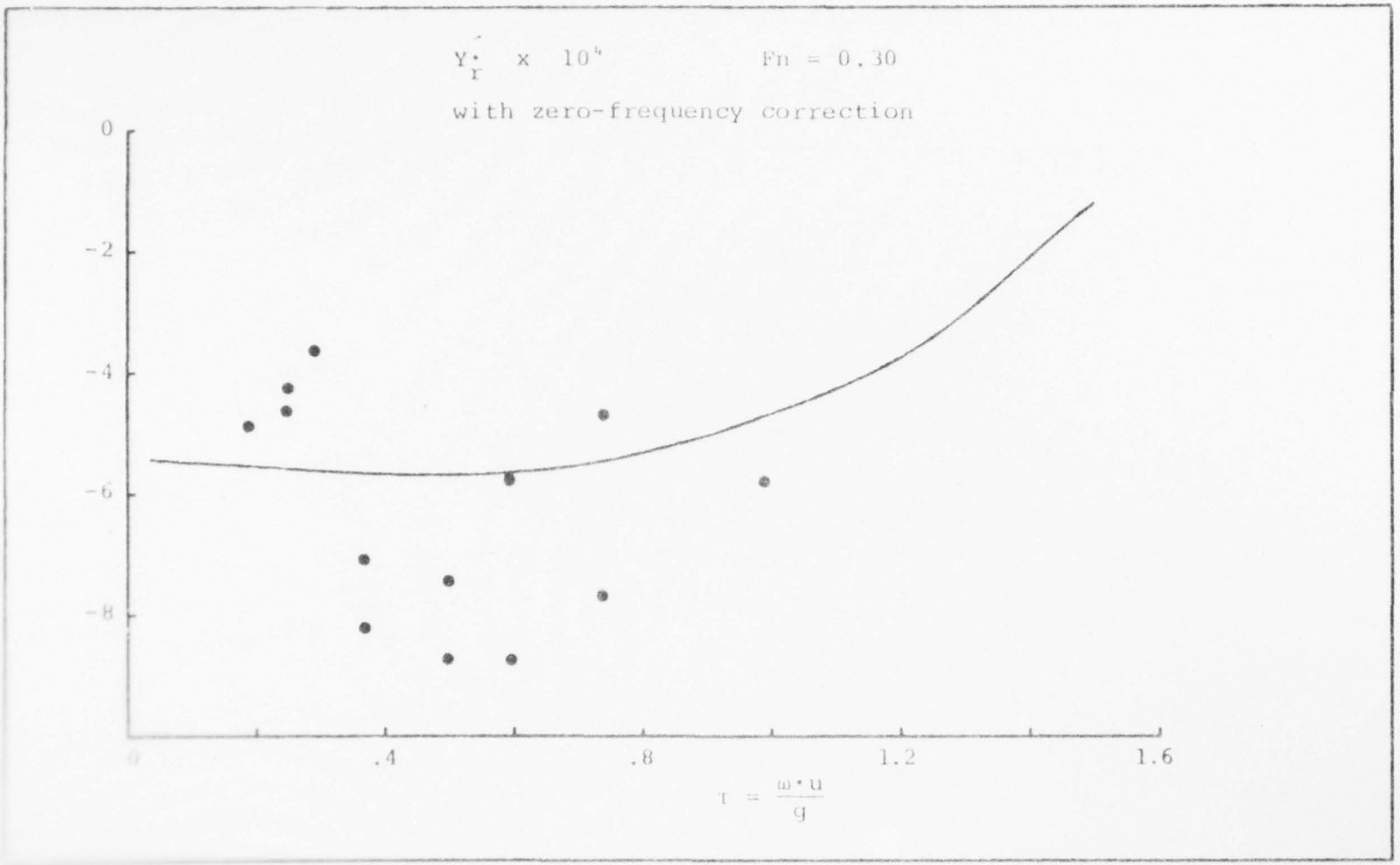

Figure 30: Zero-corrected results from 5 step-pulse runs.

AD-A043 462 CALIFORNIA UNIV BERKELEY DEPT OF NAVAL ARCHITECTURE F/G 13/10
SHIP MANEUVERING, INCLUDING THE EFFECTS OF TRANSIENT MOTIONS,(U)
AUG 76 C A SCRAGG N00014-75-C-0275
UNCLASSIFIED UCB-NA-76-1 NL

2 OF 2
AD
A043 462

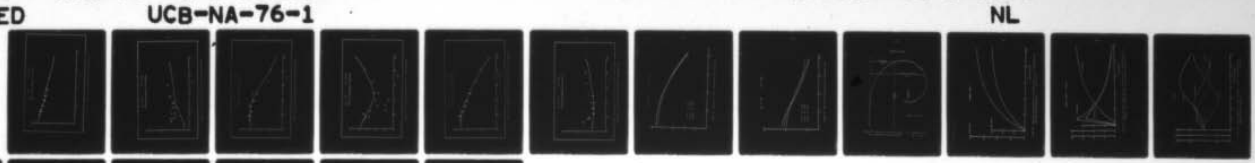

END
DATE
FILMED
9-77
DDC

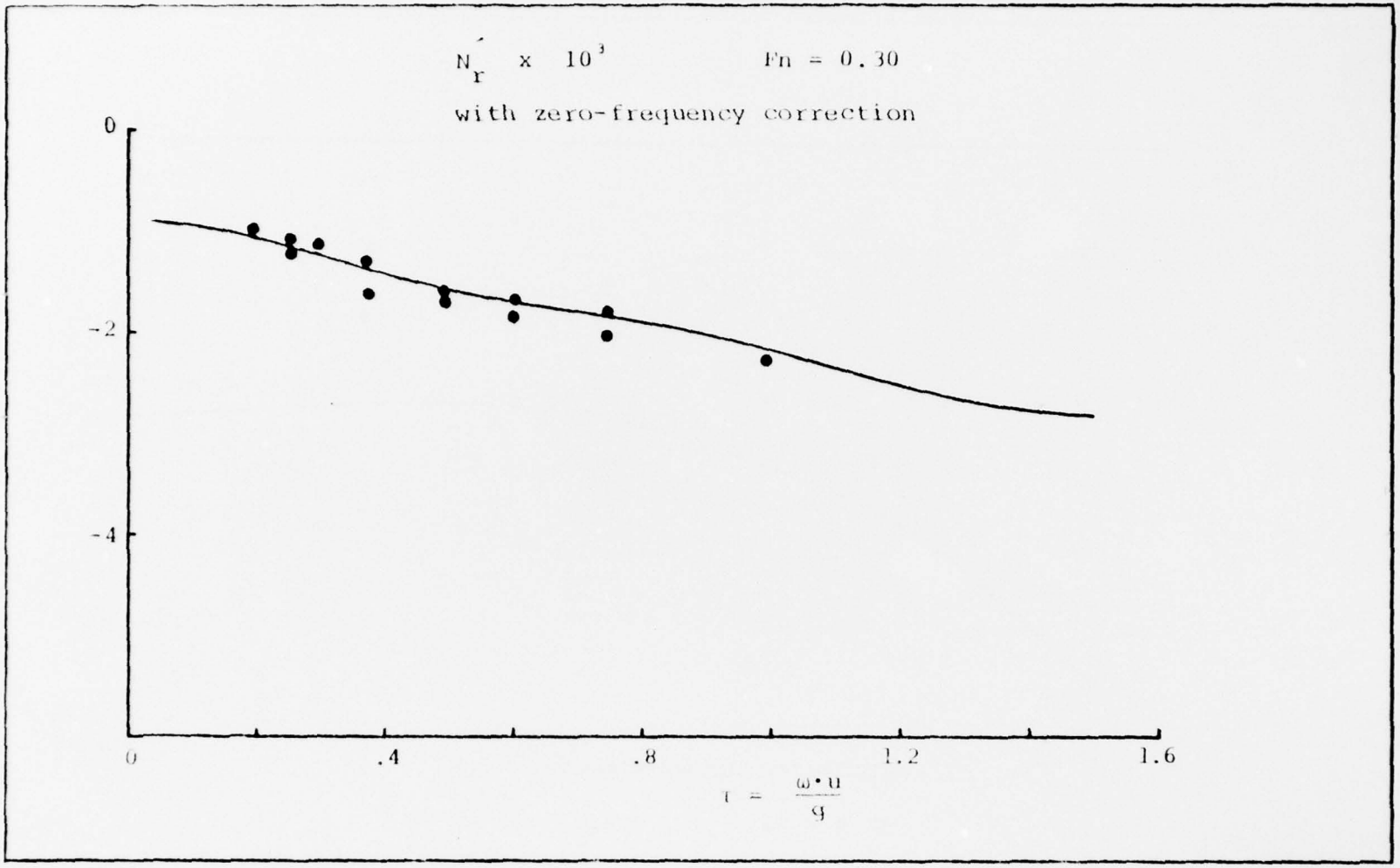

Figure 31: Zero-corrected results from 5 step-pulse runs.

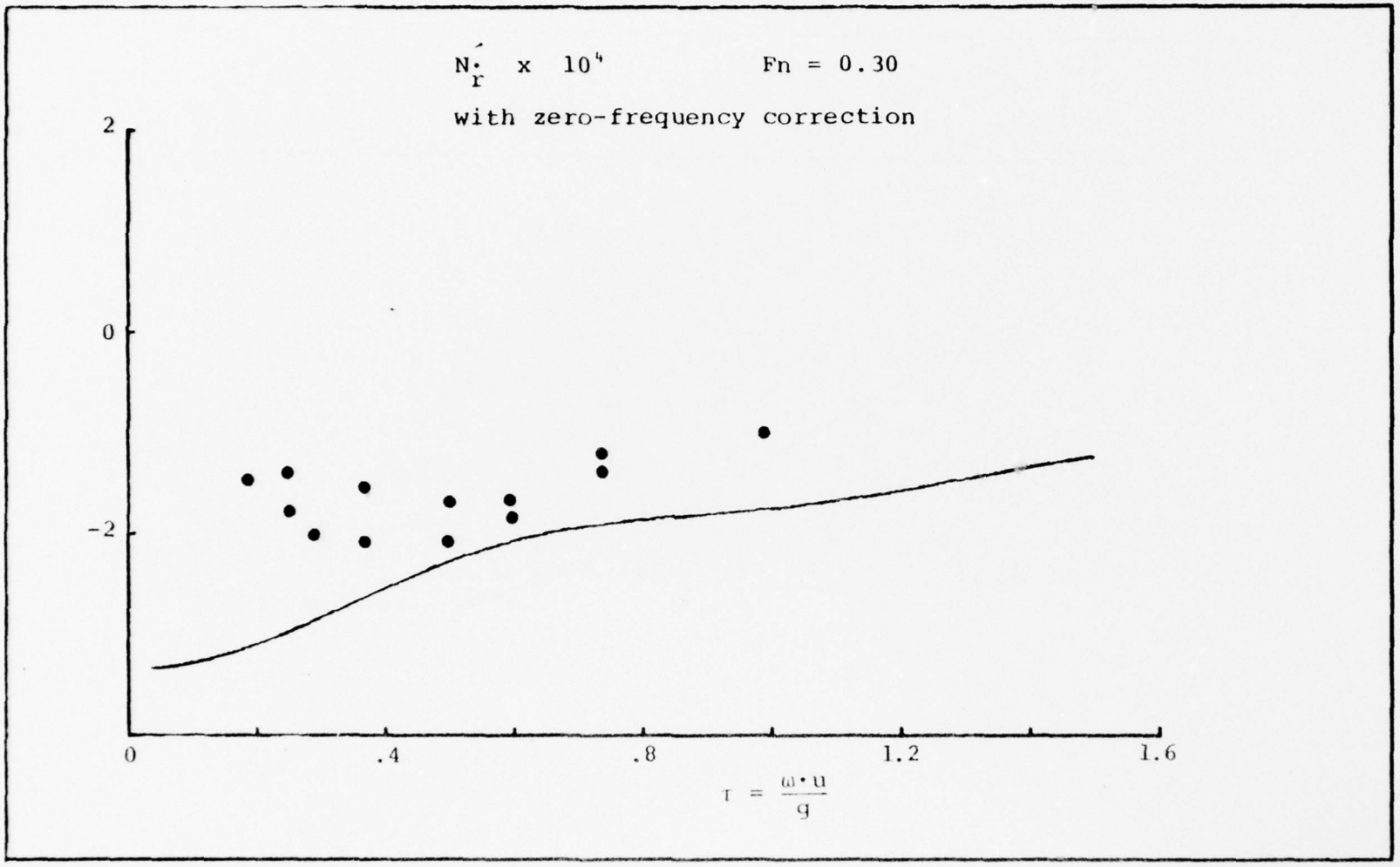

Figure 32: Zero-corrected results from 5 step-pulse runs.

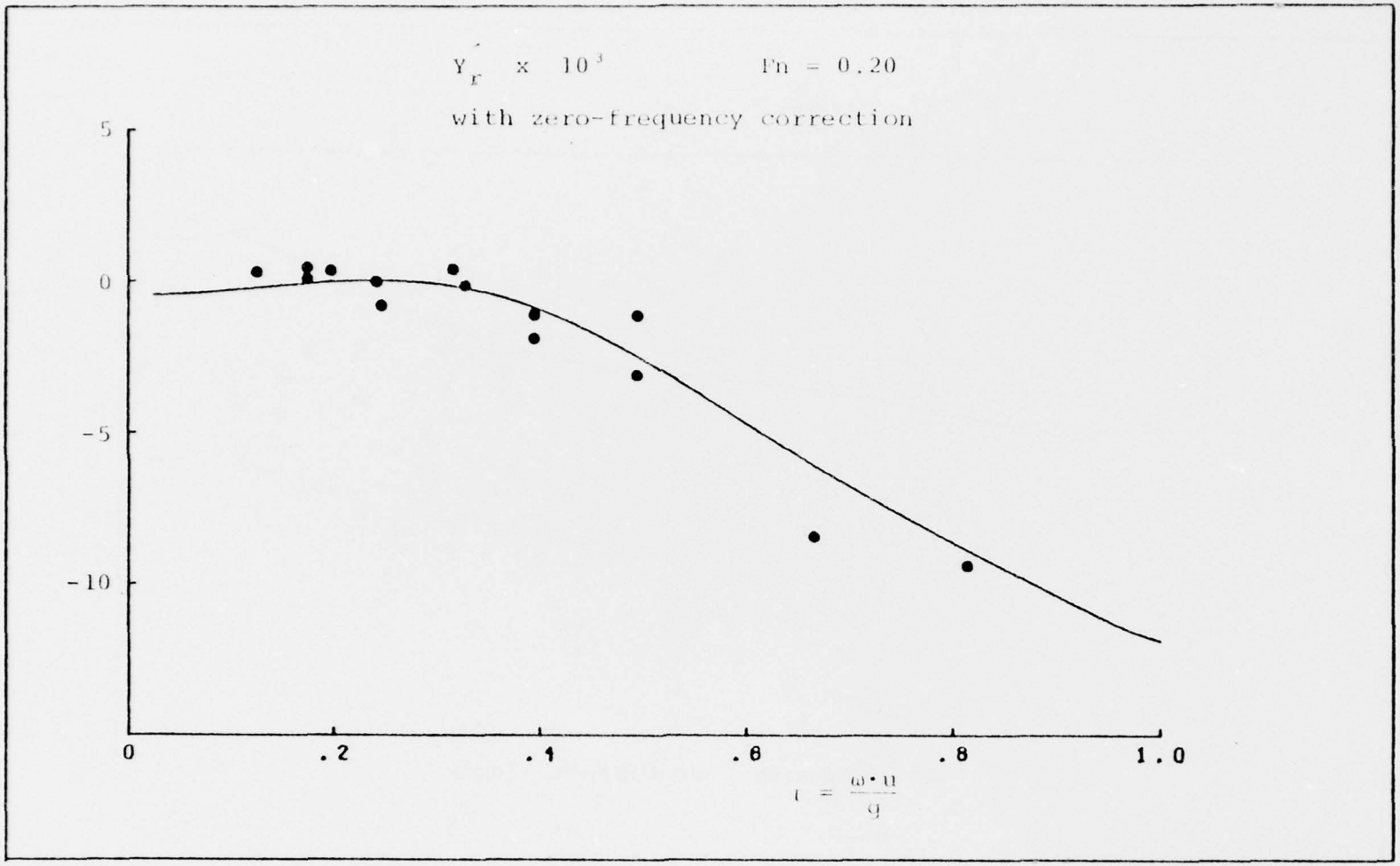

Figure 33: Zero-corrected results from 5 step-pulse runs.

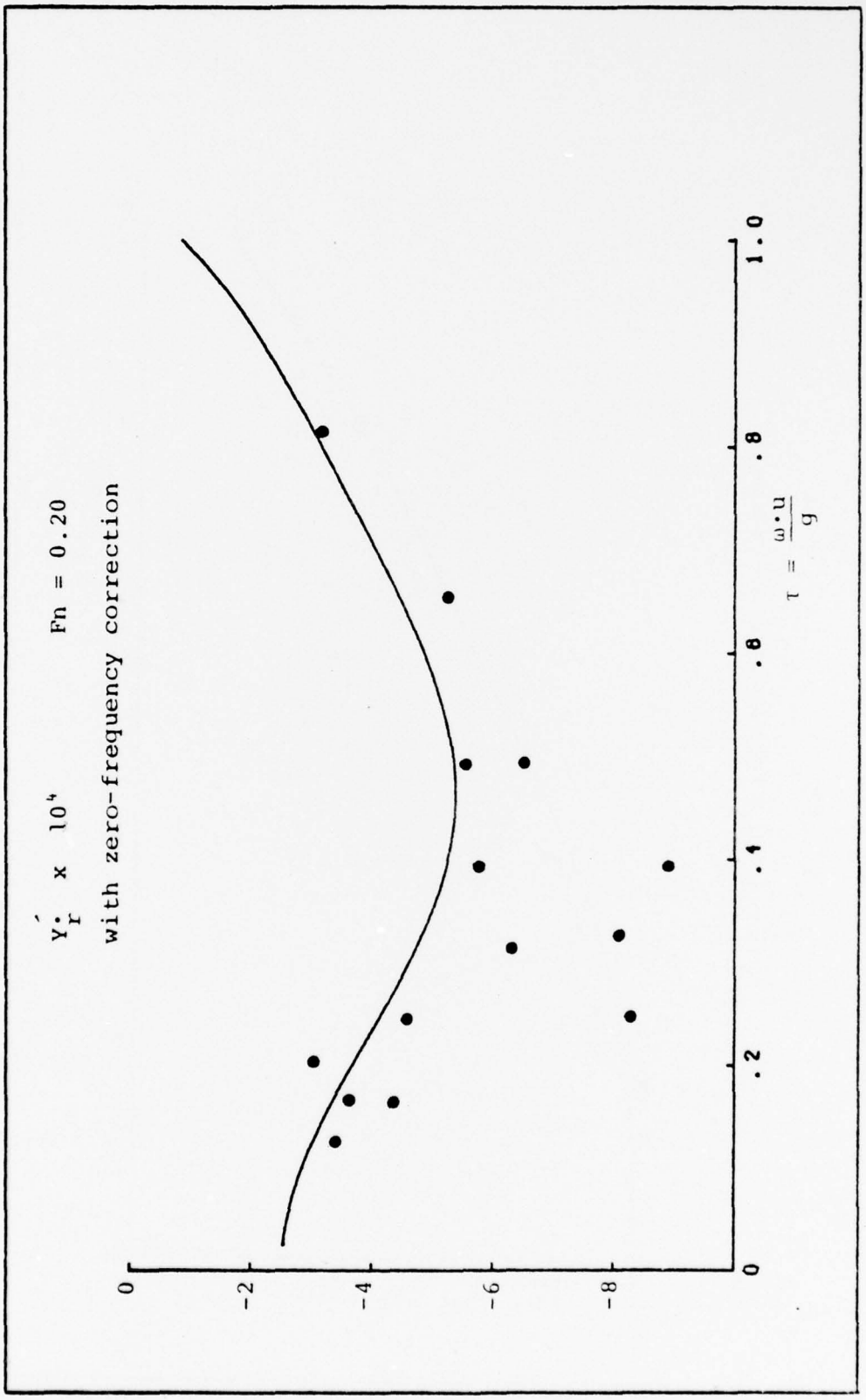

Figure 34: Zero-corrected results from 5 step-pulse runs.

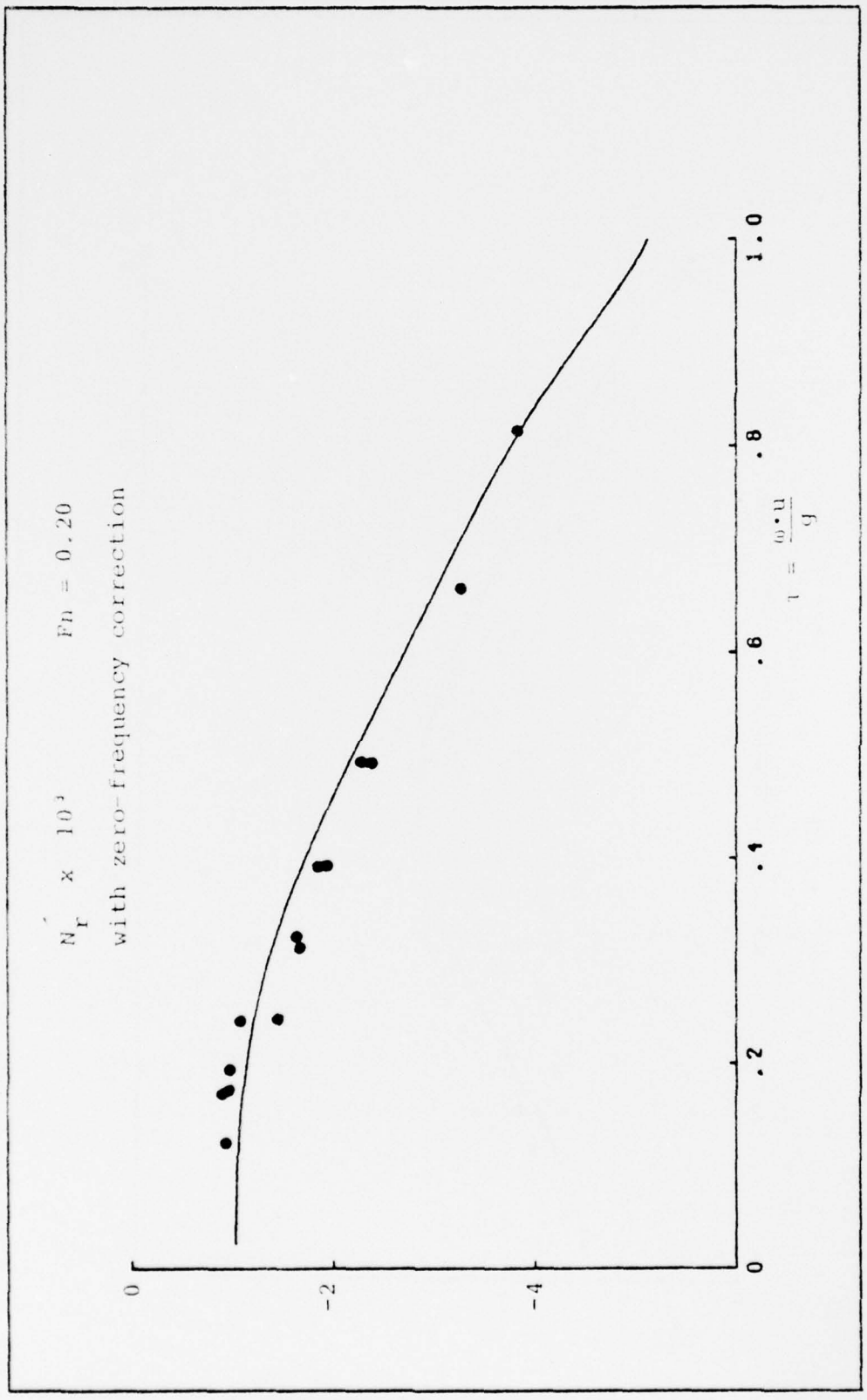

Figure 35: Results from 5 step-pulse runs, with zero-correction.

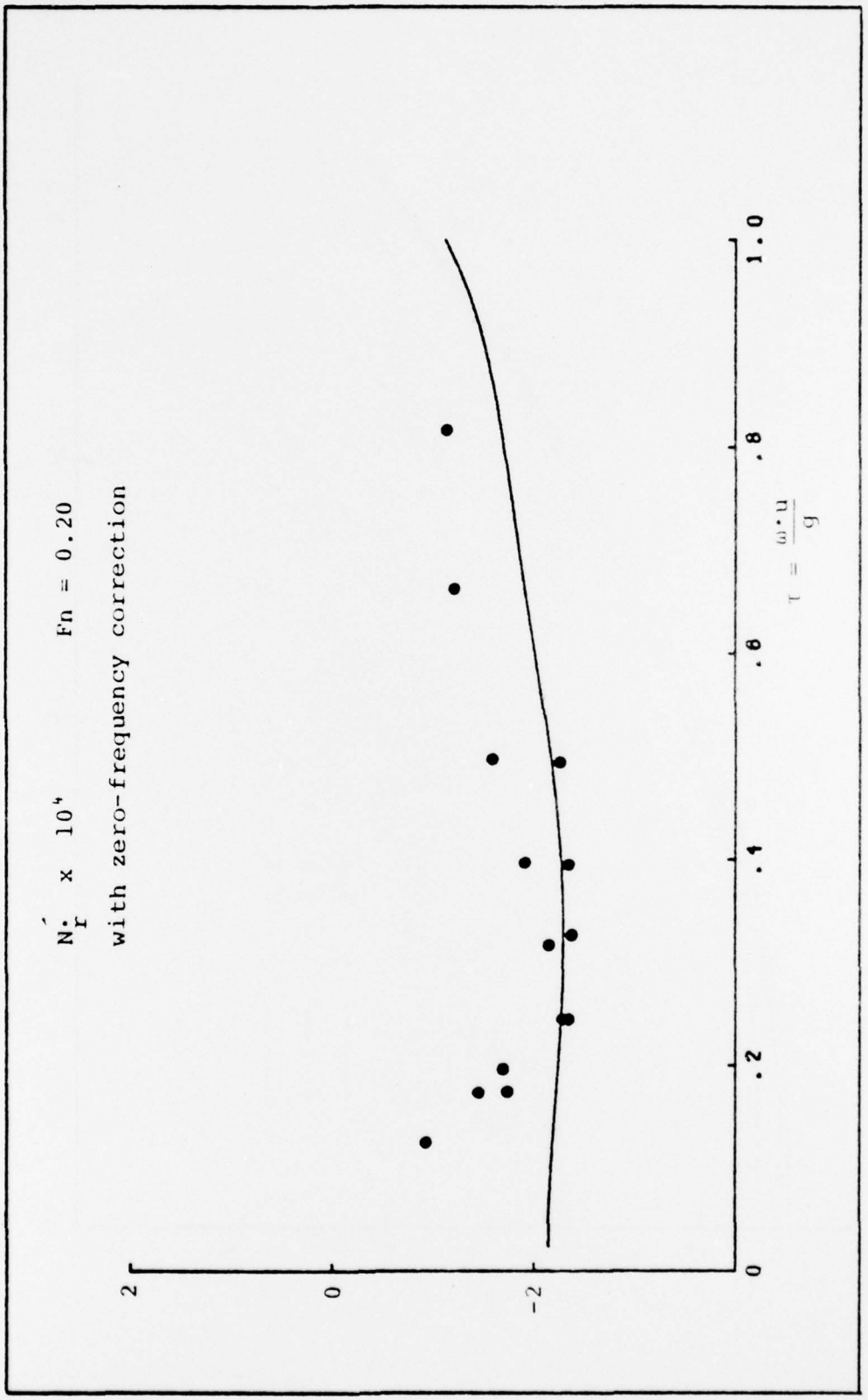

Figure 36: Zero-corrected results from 5 step-pulse runs.

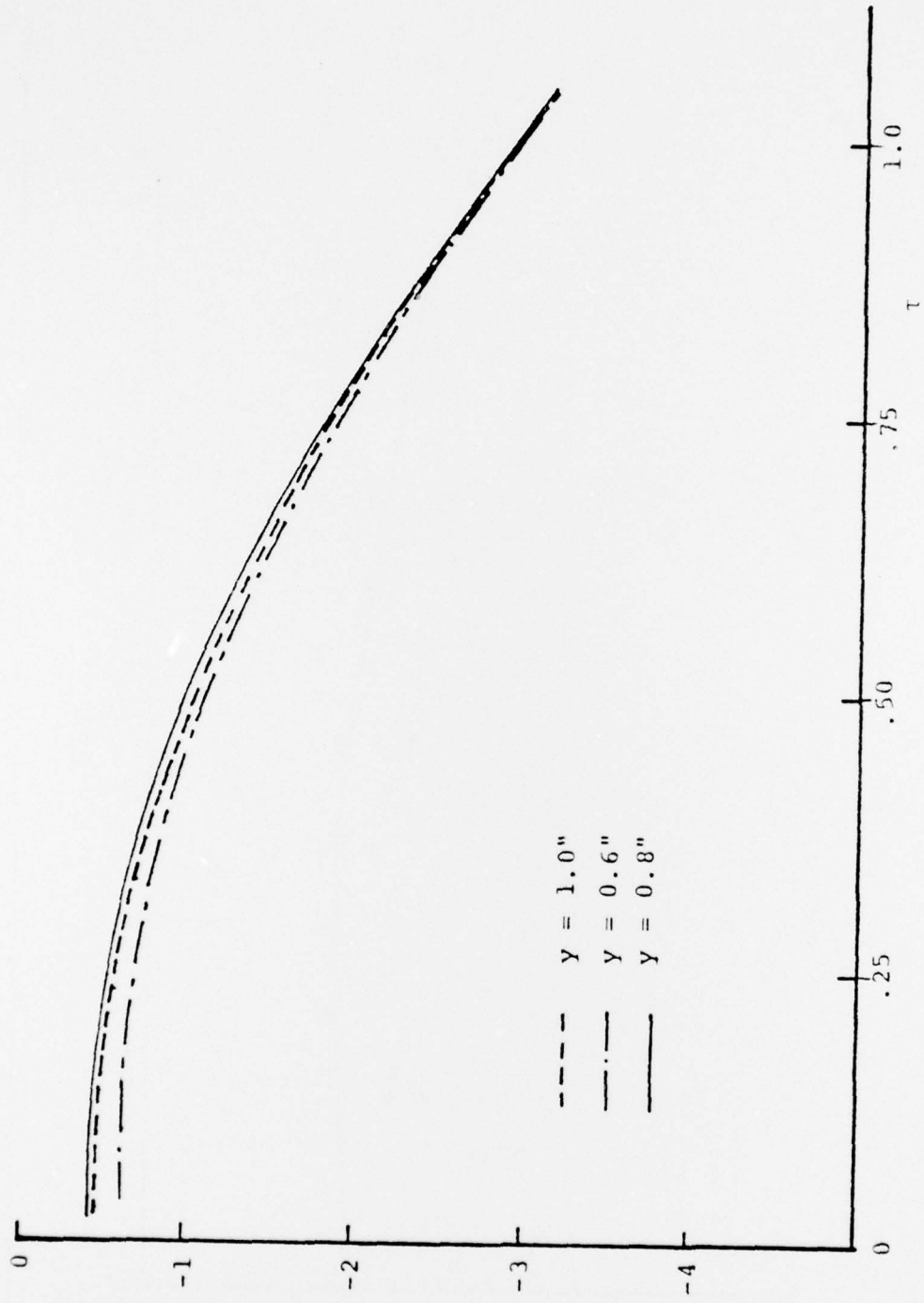

Figure 37: Results of various amplitude step-pulse runs.

Figure 38: Results of various amplitude step-pulse runs.

TURNING CIRCLE

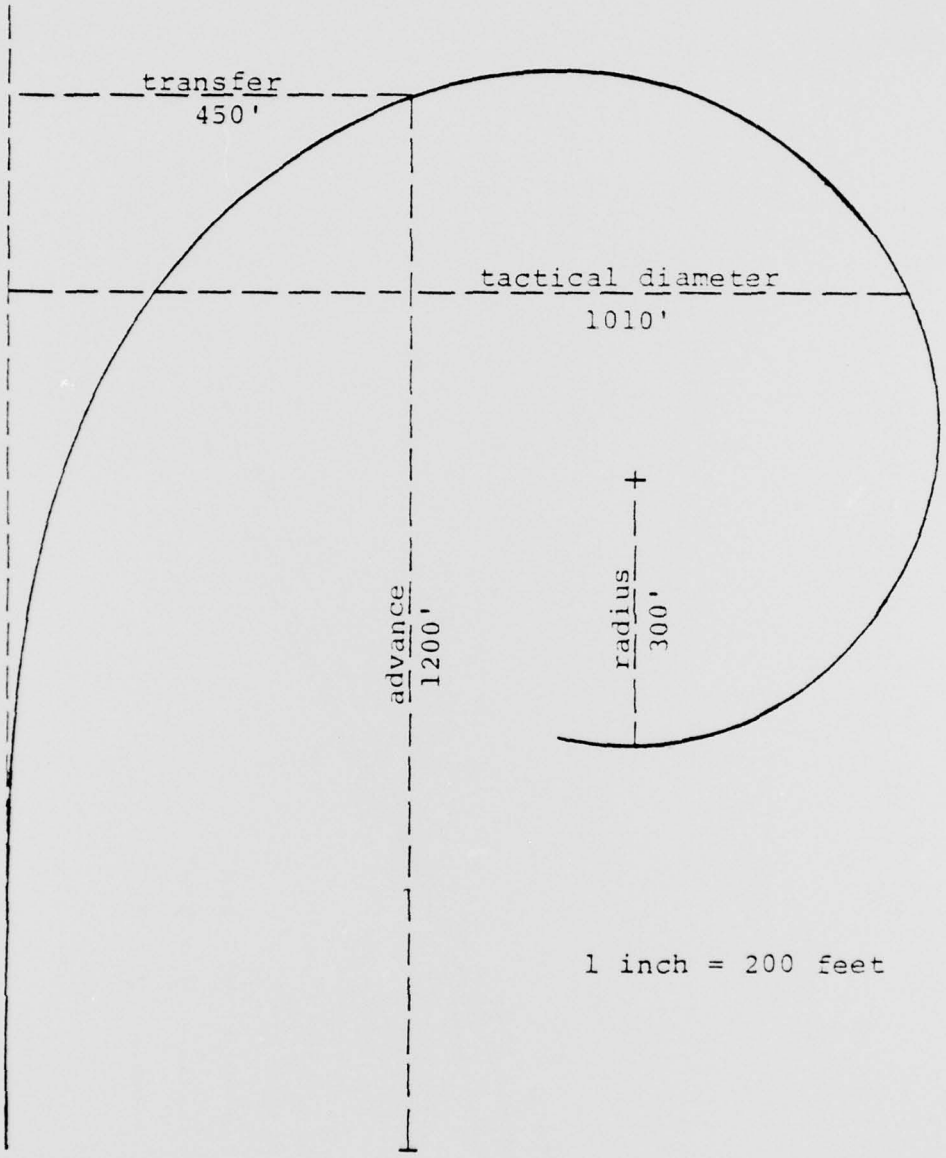

Figure 39: Path of a turning circle, $\delta_1(t)$, predicted from the transient-motion equations. Fn = 0.30.

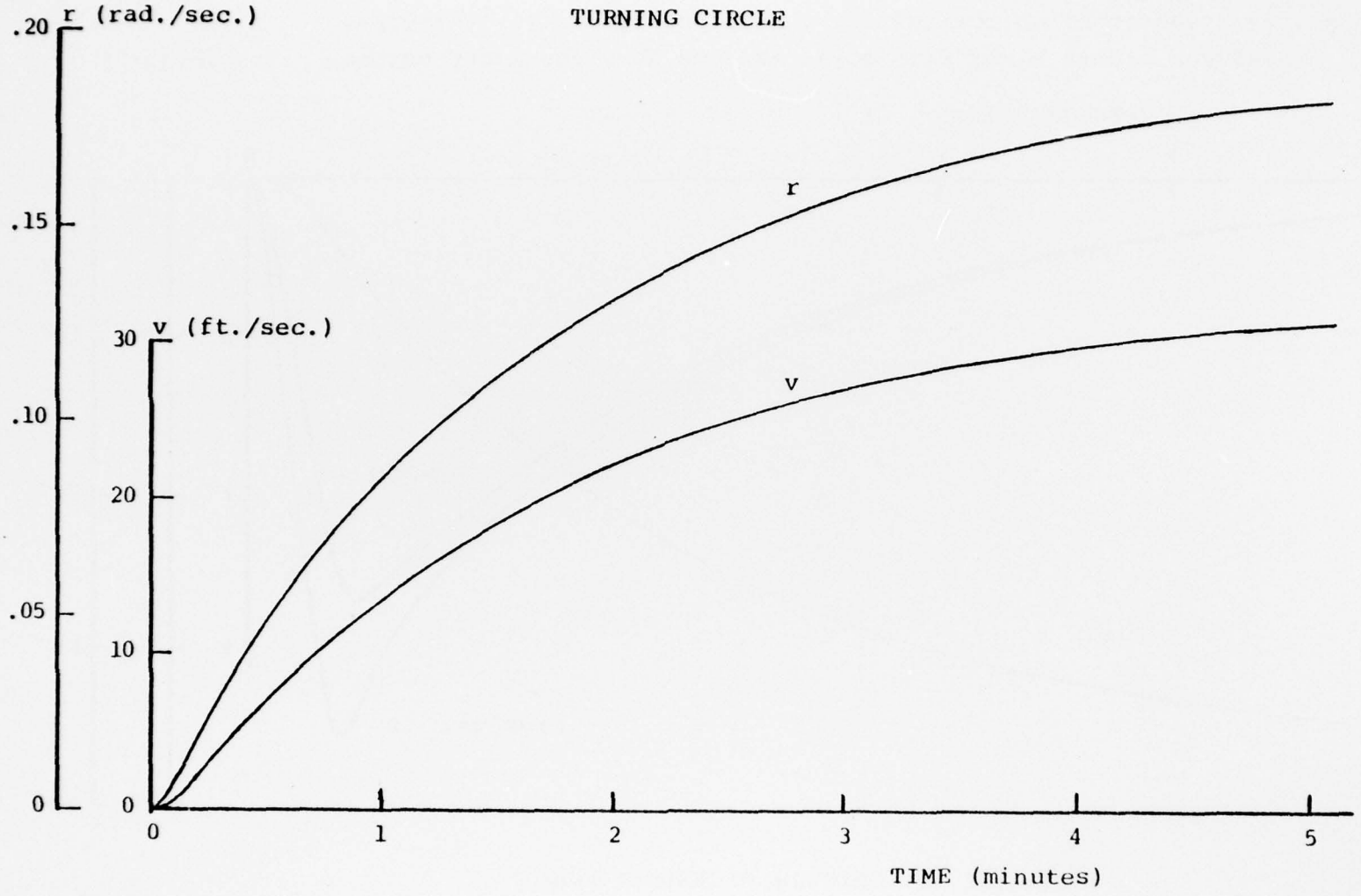

Figure 40: Sway and yaw velocities for turning circle, $\delta_1(t)$, predicted from transient-motion equations. Fn = 0.30.

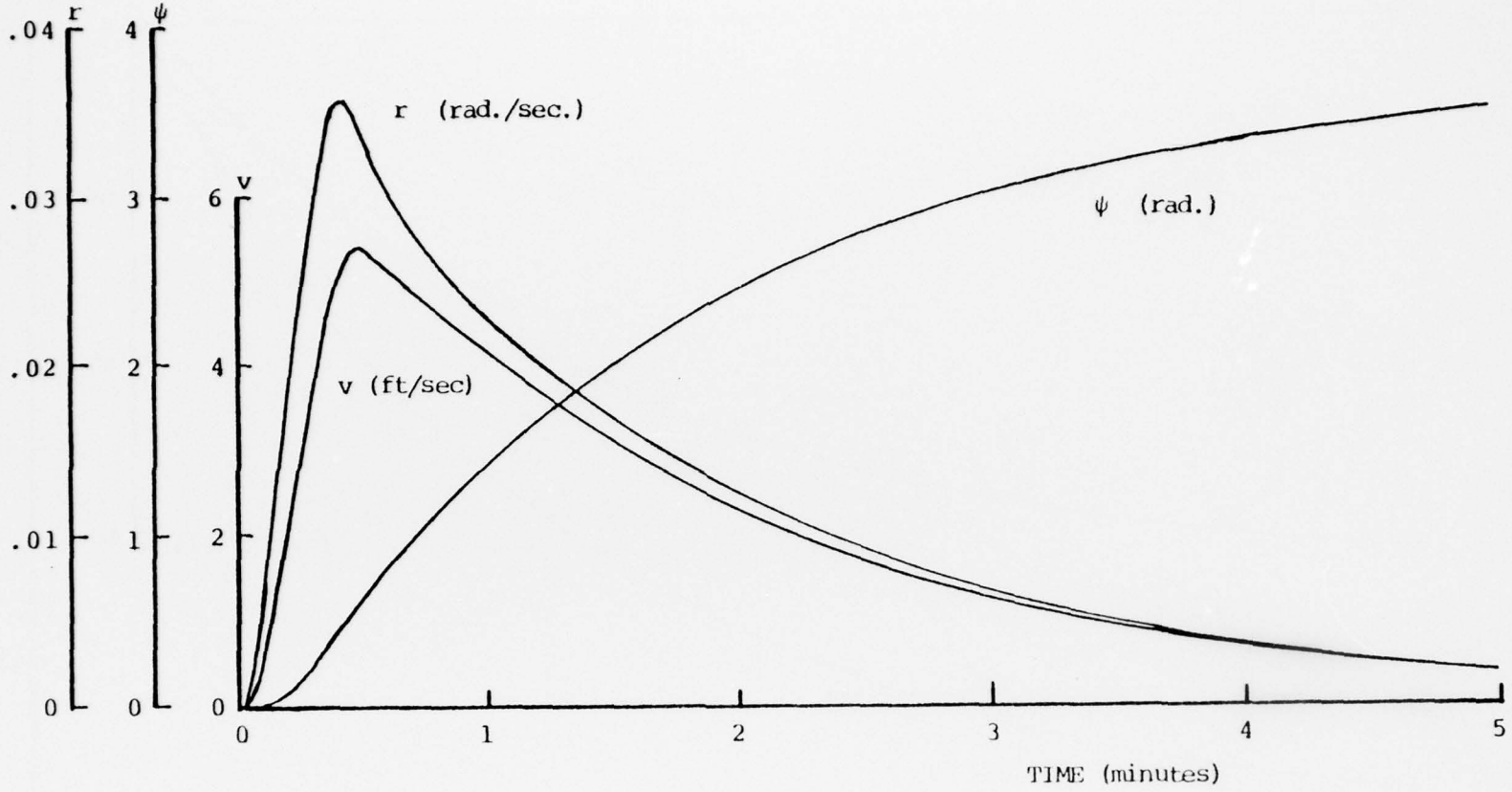

Figure 41: Heading angle and sway and yaw velocities for a simple change of heading, $\delta_3(t)$, predicted from transient-motion equations. Fn = 0.3

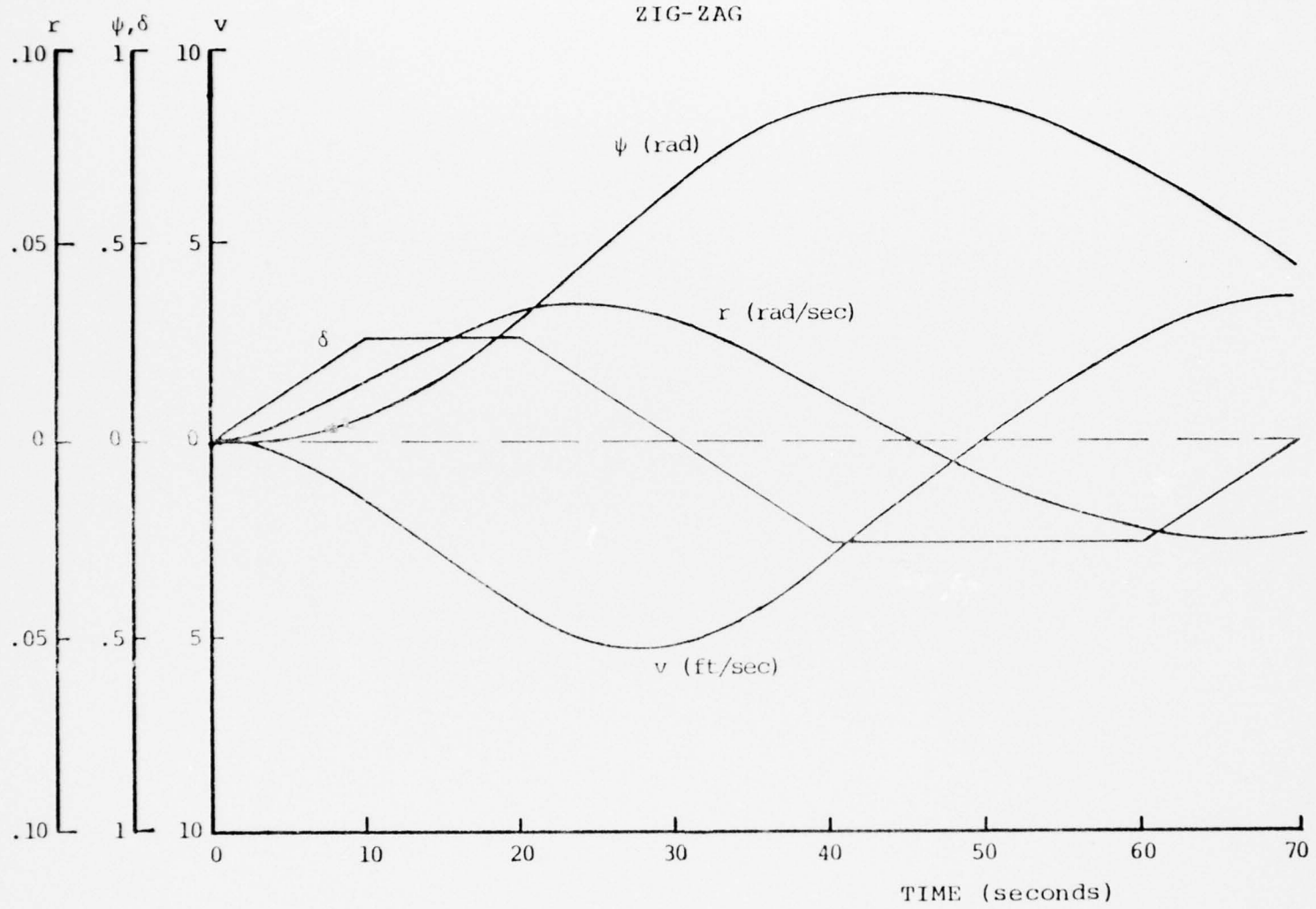

Figure 42: Initial phases of zig-zag maneuver, $\delta_4(t)$, predicted from the transient-motion equations. Fn = 0.30

DISTRIBUTION LIST FOR REPORTS PREPARED UNDER THE
GENERAL HYDROMECHANICS RESEARCH PROGRAM

40 Commander
David W. Taylor Naval Ship
Research and Development Center
Bethesda, Md 20084
Attn: Code 1505 (1)
Code 5211.4 (39)#

1 Officer-in-Charge
Annapolis Laboratory
Naval Ship Research and
Development Center
Annapolis, Maryland 21402
Attn: Code 522.3 (Library)

7 Commander
Naval Sea Systems Command
Washington, D. C. 20360
Attn: SEA 09G32 (3 cys)
SEA 03512 (Peirce)
SEA 037 ---------- ADF+
SEA 0322
SEA 033

12* Director
Defense Documentation Center
5010 Duke Street
Alexandria, Virginia 22314

1 Office of Naval Research
800 N. Quincy Street
Arlington, Virginia 22217
Attn: Mr. R. D. Cooper (Code 438)

1 Office of Naval Research
Branch Office
492 Summer Street
Boston, Mass 02210

1 Office of Naval Research
Branch Office (493)
536 S. Clark Street
Chicago, Illinois 60605

1 Chief Scientist
Office of Naval Research
Branch Office
1030 E. Green Street
Pasadena, CA 91106

1 Office of Naval Research
Resident Representative
715 Broadway (5th Floor)
New York, New York 10003

1 Office of Naval Research
San Francisco Area Office
760 Market St., Rm 447
San Francisco, Calif 94102

2 Director
Naval Research Laboratory
Washington, D. C. 20390
Attn: Code 2027
Code 2629(ONRL)

1 Commander
Naval Facilities Engineering
Command(Code 032C)
Washington, D. C. 20390

1 Library of Congress
Science & Technology Division
Washington, D. C. 20540

If more than one copy of the report is to be forwarded to the attention of an addressee, the number will be designated in parenthesis following the name and/or code.

+ The letters (ABCDEF) are for use by this activity and are to be deleted from this list when published in the report.

* The DDC Form 50, "DDC Accession Notice" which is attached to this list must be forwarded with 12 copies of the report to the Defense Documentation Center.

ENCLOSURE (2)

Annapolis, Md - 21402

1 Commander BDEF
Naval Electronics Laboratory
Center (Library)
San Diego, CA 92152

1 Commander
Naval Ship Engineering Center
Center Building
Prince Georges Center
Hyattsville, Maryland 20782
Attn: SEC 6034B
SEC 6110
SEC 6114H
SEC 6120
SEC 6136
SEC 6144G

1 Naval Ship Engineering Center
Norfolk Division ABCE
Small Craft Engr Dept
Norfolk, Virginia 23511
Attn: D. Blount (6660.03)

1 Library (Code 1640)
Naval Oceanographic Office
Washington, D. C. 20390

1 Commander (ADL)
Naval Air Development Center
Warminster, Penna 18974

1 Naval Underwater Weapons Research
& Engineering Station (Library)
Newport, R.I. 02840

1 Commanding Officer (L31)
Naval Civil Engineering Laboratory
Port Hueneme, CA 93043

1 Library
Naval Underwater Systems Center
Newport, R. I. 02340

1 Research Center Library
Waterways Experiment Station
Corp of Engineers BCI
P.O. Box 631
Vicksburg, Mississippi 39180

1 AFOSR/NAM BDF
1400 Wilson Blvd
Arlington, Virginia 22209

1 Dept. of Transportation
Library TAD-491.1
400 - 7th Street S.W.
Washington, D. C. 20590

1 Charleston Naval Shipyard
Technical Library
Naval Base
Charleston, S. C. 29408

1 Norfolk Naval Shipyard
Technical Library
Portsmouth, Virginia 23709

1 Philadelphia Naval Shipyard
Philadelphia, Penna 19112
Attn: Code 240

1 Portsmouth Naval Shipyard
Technical Library
Portsmouth, N. H. 03801

1 Puget Sound Naval Shipyard
Engineering Library
Bremerton, Wash 98314

1 Long Beach Naval Shipyard
Technical Library (246L)
Long Beach, CA 90801

1 Hunters Point Naval Shipyard
Technical Library (Code 202.3)
San Francisco, CA 94135

1 Pearl Harbor Naval Shipyard
Code 202.32
Box 400, FPO
San Francisco, CA 96610

1 Mare Island Naval Shipyard
Shipyard Technical Library
Code 202.3
Vallejo, CA 94592

1 Assistant Chief Design Engineer
for Naval Architecture (Code 250)
Mare Island Naval Shipyard
Vallejo, CA 94592

3 U. S. Naval Academy
Annapolis, Maryland 21402
Attn: Technical Library
Dr. Bruce Johnson
Prof. P. Van Mater, Jr.

1 Naval Postgraduate School
Monterey, CA 93940
Attn: Library, Code 2124

1 Capt. L. S. McCready, USMS
Director, National Maritime
Research Center
U. S. Merchant Marine Academy
Kings Point, L.I., N.Y. 11204

1 U. S. Merchant Marine Academy
Kings Point, L.I., N.Y. 11204
Attn: Academy Library

1 Library
The Pennsylvania State University
Ordnance Research Laboratory
P. O. Box 30
State College, Penna 16801

1 Bolt, Beranek & Newman
50 Moulton Street
Cambridge, Mass 02138
Attn: Library

1 Bethlehem Steel Corporation
Center Technical Division
Sparrows Point Yard
Sparrows Point, Maryland 21219

1 Bethlehem Steel Corporation
25 Broadway
New York, New York 10004
Attn: Library (Shipbuilding)

1 Esso International
Design Division, Tanker Dept.
15 West 51st Street ABCD
New York, New York 10019

1 Mr. V. Boatwright, Jr.
R & D Manager ABCDF
Electric Boat Division
General Dynamics Corporation
Groton, Conn 06340

1 Gibbs & Cox, Inc.
21 West Street
New York, New York 10006
Attn: Technical Info. Control

2 Hydronautics, Inc.
Pindell School Road
Howard County
Laurel, Maryland 20810
Attn: Library
Mr. M. Gertler B

1 Lockheed Missiles & Space Co.
P.O. Box 504
Sunnyvale, CA 94088
Attn: Mr. R. L. Waid, Dept 57-74
Bldg. 150, Facility 1

1 Newport News Shipbuilding &
Dry Dock Company
4101 Washington Avenue
Newport News, Virginia 23607
Attn: Technical Library Dept.

1 North American Aviation, Inc.
Space & Information Systems Div.
12214 Lakewood Blvd BD
Downey, CA 90241
Attn: Mr. Ben Ujihara (SL-20)

1 Nielsen Engineering & Research Inc.
510 Clude Avenue
Mountain View, CA 94043 ABD
Attn: Mr. S. Spangler

1 Oceanics, Inc.
Technical Industrial Park
Plainview, L.I., N.Y. 11803

1 Society of Naval Architects
and Marine Engineers
74 Trinity Place
New York, New York 10006
Attn: Technical Library

1 Sun Shipbuilding & Dry Dock Co.
Chester, Penna 19000 ABC
Attn: Chief Naval Architect

1 Sperry Systems Management Division
Sperry Rand Corporation
Great Neck, N. Y. 11020
Attn: Technical Library

1 Stanford Research Institute
Menlo Park, CA 94025
Attn: Library G-021

2 Southwest Research Institute
P. O. Drawer 28510
San Antonio, Texas 78284
Attn: Applied Mechanics Review
Dr. H. Abramson

1 Tracor, Inc.
6500 Tracor Lane ABCD
Austin, Texas 78721

1 Mr. Robert Taggart
3930 Walnut Street
Fairfax, Virginia 22030

1 Ocean Engr Department
Woods Hole Oceanographic Inst.
Woods Hole, Mass 02543

[illegible]

1 Applied Physics Laboratory
University of Washington ABCDF
1013 N. E. 40th Street
Seattle, Washington 98105
Attn: Technical Library

1 University of Bridgeport ABDEF
Bridgeport, Conn 06602
Attn: Dr. E. Uram

1 Cornell University
Graduate School of Aerospace Engr
Ithaca, New York 14850 BDEF
Attn: Prof. W. R. Sears

4 University of California
Naval Architecture Department
College of Engineering
Berkeley, CA 94720
Attn: Library
Prof. W. Webster ABCD
Prof. J. Paulling ABCD
Prof. J. Wehausen ABCD

3 California Institute of Technology
Pasadena, CA 91109
Attn: Aeronautics Library
Dr. T. Y. Wu
Dr. A. J. Acosta ABDE

1 Docs/Repts/Trans Section
Scripps Institution of
Oceanography Library BCD
University of California, San Diego
P.O. Box 2367
La Jolla, CA 92037

1 Catholic University of America
Washington, D. C. 20017 ABI
Attn: Dr. S. Heller, Dept of
Civil & Mech Engr

1 Colorado State University
Foothills Campus BDI
Fort Collins, Colorado 80521
Attn: Reading Room, Engr Res Cente

[illegible]

Florida Atlantic University
Ocean Engineering Department
Boca Raton, Fla 33432
Attn: Technical Library
[illegible]

1 University of Hawaii
Department of Ocean Engineering
2565 The Mall
Honolulu, Hawaii 96822
Attn: Dr. C. Bretschneider

[illegible]

3 Institute of Hydraulic Research
The University of Iowa
Iowa City, Iowa 52240
Attn: Library
Dr. L. Landweber BD
Dr. J. Kennedy BD

[illegible]

4 Department of Ocean Engineering
Massachusetts Institute of Technology
Cambridge, Mass 02139
Attn: Department Library
Prof. P. Mandel
Prof. M. Abkowitz
Dr. J. Newman

5 St. Anthony Falls Hydraulic Laboratory
University of Minnesota
Mississippi River at 3rd Avenue S.E.
Minneapolis, Minnesota 55414
Attn: Prof. E. Silberman
Mr. J. Wetzel BDEF
Mr. F. Schiebe BDEF
Mr. J. Killen DEF
Dr. C. Song BCDE

3 Department of Naval Architecture
and Marine Engineering
University of Michigan
Ann Arbor, Michigan 48104
Attn: Library
Dr. T. F. Ogilvie
Prof. F. Hammitt

2 College of Engineering
University of Notre Dame
Notre Dame, Indiana 46556
Attn: Engineering Library ABCDE
Dr. A. Strandhagen BDE

3 Davidson Laboratory
Stevens Institute of Technology
711 Hudson Street
Hoboken, New Jersey 07030
Attn: Library
Mr. J. Breslin
Mr. S. Tsakonas

2 Stanford University
Stanford, CA 94305
Attn: Engineering Library ABDE
Dr. R. Street

3 Webb Institute of Naval Architecture
Crescent Beach Road
Glen Cover, L.I., N.Y. 11542
Attn: Library
Prof. E. V. Lewis
Prof. L. W. Ward

1 [illegible]

1 [illegible]

1 Applied Research Laboratory
P.O. Box 30
State College, Pa 16801
Attn: Dr. B. Parkin, Director
Garfield Thomas Water Tunnel

1 Dr. Michael E. McCormick
Naval Systems Engineering Department
U. S. Naval Academy
Annapolis, Maryland 21402

1 Dr. Douglas E. Humphreys (Code 712)
Naval Coastal Systems Laboratory
Panama City, Florida 32401 ABCDE